DEPARTMENT DE GENIE CIVIL
DEPARTMENT OF CIVIL ENGINEERING

DEPARTMENT OF CIVIL, ARCHITECTURAL
AND ENVIRONMENTAL ENGINEERING

FINITE ELEMENT ANALYSIS APPLIED TO THE STUDY OF THE STRESS TRANSMISSION IN THE CORRUGATED SHEET SLAB

A thesis submitted in partial fulfilment of the requirements for obtention of the

Master of Engineering (MEng) degree in Civil Engineering

CURRICULUM: Structural Engineering

Presented by:
MBOH Helbert Shayeh

Student number: 15TP20948

Supervised by:
Prof. Carmelo MAJORANA

Co-supervised by:
Dr. Eng. POH'SIE Guillaume Hervé
Eng. CARDILLO Giuseppe

Examiner:
Dr. FEUMO Achille

Academic year: 2019/2020

DEDICATION

I dedicate my work

To

My parents

In gratitude for all the love with which you cover me and the support that you bring to me for the success in my studies and my accomplishment as a man

FEM analysis applied to the study of the stress transmission in the corrugated sheet slab
Master of Civil Engineering, defended by: MBOH HELBERT SHAYEH, NASPW, Yaoundé, 2019/2020

i

ACKNOWLEDGEMENTS

I would like to thank above all the GOD ALMIGHTY for his protection and his breath without which I wouldn't have achieved this work and for the blessings he keeps flooding me. My special thanks to:

- The President of the jury for the honour you give me in being the president of the jury in my thesis presentation;

- The Examiner for the honour you give me in being the examiner of this work and adding to it by criticizing to ameliorate;

- My supervisors Prof. **Carmelo MAJORANA**, Dr Eng. **POH'SIE Guillaume Hervé** and Eng**. Giuseppe CARDILLO** for their guidance and availability;

- Director of the National Advanced School of Public Works (NASPW) of Yaoundé Prof. **NKENG George ELAMBO**, and Prof. **Carmelo MAJORANA** of University of Padua in Italy for all their academic and administrative support during these five years spent at NASPW;

- Prof. **MBESSA Michel**, Head of Department of civil engineering for his availability, his advice and tutoring;

- **All the teaching staff** of NASPW and University of Padua for their good quality teaching and motivation they administrated us;

- **All my classmates** and my friends of the 6th batch of NASPW who were a source of motivation and joy especially to my friends at **Nolanga** and "**La Squadra**";

- My parents Mr **MICHAEL MBOH and** Mrs **ERNESTINE TATAH** for the trust, love, unconditional support, valuable advice and efforts invested in me for the obtaining of this degree;

- The families **MBOH** and **TATAH** families for their moral support during all these years;

- To all people who, from near or far have given me their heartfelt help in carrying out this work.

FEM analysis applied to the study of the stress transmission in the corrugated sheet slab
Master of Civil Engineering, defended by: MBOH HELBERT SHAYEH, NASPW, Yaoundé, 2019/2020

ii

GLOSSARY

NOTIONS AND SYMBOLS

ANSI	American National Standard Institute
AS	Australian Standards
ASCE	American Society of Civil Engineers
EC	Eurocode
EN	European Nations
FE	Finite Elements
FEA	Finite Element Analysis
FEM	Finite Element Method
NZS	New Zealand Standards
SLS	Serviceability Limit State
ULS	Ultimate Limit State
PSC	Partial Shear Connection

α	Relevant category of the sheet
A_p	Area of the sheet reinforcement
A_s	Area of the steel reinforcement section
b	Width of the design slab strip
b_m	Overall width of the slab
b'_m	Average width of one width
d	Deflection of the slab
d_p	Depth to the neutral axis of the corrugated sheet from the top of concrete
f_{bv}	Shear buckling strength of a composite sheet
f_{cd}	Design value of the concrete compressive strength
f_k	Characteristic value of compressive strength
G_1	Permanent structural actions
G_2	Permanent non-structural action

FEM analysis applied to the study of the stress transmission in the corrugated sheet slab
Master of Civil Engineering, defended by: MBOH HELBERT SHAYEH, NASPW, Yaoundé, 2019/2020

iii

γ_g	Partial factor of safety for actions
g_k	Permanent action
λ_p	Slenderness of steel plate
γvs	Partial safety factor for vertical shear.
h	Degree of shear connection
h_p	Total thickness of composite slab
I_{cc}	Second moment of areas for cracked section
I_{cu}	Second moment of areas for uncracked section
$k\sigma$	Buckling reduction factor
la	Effective bearing length of the sheeting
Lo	Slab overhang from beam ends
Ls	Shear span for linear loading of sheet
Med	Design moment solicitation
$M_{f,rd}$	Moment of resistance of a cross-section consisting of the effective area of flanges only
$M_{pl,rd}$	Plastic moment of the composite section
$M_{y,rd}$	Design moment resistance of the cross-section provided by the manufacturer
n	Modular ratio for composite section
Nc,f	Axial force in the concrete
Npa	Axial strength of the kidney
Q_1	Variable action
q_k	Variable action
r	Internal radius of the sheet corners
Rw,rd	Transverse resistance of a sheet web
sw	Slant height of the sheet web
t	Thickness of the composite sheet
tu	Maximum shear force in composite slab
Ved	Design shear solicitation
Vl,rd	Longitudinal shear resistance of composite slab
xc	Depth of neutral axis for cracked slab section

FEM analysis applied to the study of the stress transmission in the corrugated sheet slab
Master of Civil Engineering, defended by: MBOH HELBERT SHAYEH, NASPW, Yaoundé, 2019/2020

iv

x_{pl}	Depth to the plastic neutral axis
x_u	Depth of neutral axis for uncracked slab section
Ψ_m	Combination coefficients for variable actions
z	Distance between normal forces in the composite sheet
ψ	Stress ratio of steel plate
ϕ	Angle between flange and webs
$\bar{p}$	Effective hydrostatic pressure stress tensor
$\bar{\sigma}$	Effective stress tensor
$\tilde{\varepsilon}^{pl}$	Plastic strain in concrete
$\bar{\sigma}_{to}$	Ultimate uniaxial tensile yield stress
$\bar{\sigma}_{co}$	Ultimate uniaxial compressive yield stress
$\bar{\sigma}_{bo}$	Initial equibiaxial stress
Kc	Hydrostatic effective stress in the tensile meridian
dc	Compressive damage parameter
dt	Tensile damage parameter

FEM analysis applied to the study of the stress transmission in the corrugated sheet slab
Master of Civil Engineering, defended by: MBOH HELBERT SHAYEH, NASPW, Yaoundé, 2019/2020

v

ABSTRACT

This work aimed to extend the field of application of Finite Element Method (FEM) to the design of the corrugated sheet slab, simulating already existing methods. The typical actions and load for a four-storey steel office building were computed and used for the design of a composite slab according to Eurocode 4. The shape of the steel deck used in the analysis was the same as that used by Abdullah (2004) in earlier experimental tests for determining the shear bond behaviour. A nonlinear finite element analysis (FEA) of the composite slab under imposed loading in a similar fashion to the design tests, was performed, to investigate the applicability of FEM to the study of the mechanical behaviour of composite slabs. A 3D model of the designed slab was created, capable of adequately representing the nonlinear material behaviour such as concrete cracking, concrete crushing and steel yielding. The concrete damaged plasticity model (CDP) was applied to the numerical analysis to simulate the concrete nonlinear behaviour, and CONN3D2 connector elements were assigned between selected nodes of the steel sheet and the concrete slab in a quasi-static analysis using ABAQUS/CAE. The model was verified against already existing and verified experimental results, which showed that the model was a good approximation of the corrugated sheet slab behaviour. Nonlinear phenomena such as cracking in the concrete and buckling in the steel deck were then examined to see their degree of influence in the loss of strength for the loaded slab. The crack pattern was seen to be more influential in the loss of strength in the slab, as fewer buckles were present during the periods of high loss of strength, although the buckles in the sheet were quite numerous at the slab failure.

Keywords: Finite Element Method, Corrugated sheets, Shear bond, Composite structures

FEM analysis applied to the study of the stress transmission in the corrugated sheet slab
Master of Civil Engineering, defended by: MBOH HELBERT SHAYEH, NASPW, Yaoundé, 2019/2020

vi

RESUME

Le but de ce travail était d'étendre le champ d'application de la méthode des éléments finis à la conception des dalles en tôle nervuré, en simulant des méthodes déjà existantes. Les charges typiques pour un immeuble de bureaux en acier de quatre étages ont été calculées et utilisées pour la conception d'une dalle mixte selon les normes européens EC4. La forme de la tôle nervurée utilisé dans l'analyse était la même que celle utilisée dans les tests expérimentaux précédents pour le cisaillement. Une analyse par éléments finis non linéaire (FEA) de la dalle mixte sous chargement imposé de manière similaire aux essais de conception a été réalisée pour étudier l'applicabilité de la méthode des éléments finis à l'étude du comportement mécanique des dalles mixte. Un modèle 3D de la dalle conçue a été créé, capable de représenter de manière adéquate le comportement non linéaire du matériau tel que la fissuration du béton, l'écrasement du béton et la plastification de l'acier. Le modèle appelé « Concrete Damaged Plasticity » (CDP) a été appliqué à l'analyse numérique pour simuler le comportement non linéaire du béton, et des éléments de connecteur CONN3D ont été attribués entre des nœuds sélectionnés de la tôle d'acier et du béton dans une analyse quasi-statique utilisant ABAQUS/CAE. Le modèle a été vérifié par rapport à des résultats expérimentaux déjà existants et vérifiés, qui ont montré que le modèle était une bonne approximation du comportement de la dalle de tôle ondulée. Des phénomènes non linéaires tels que la fissuration du béton et le flambement du tablier métallique ont ensuite été examinés afin de voir leur degré d'influence sur la perte de résistance de la dalle chargée. La configuration des fissures s'est avérée plus influente sur la perte de résistance de la dalle, car moins de flambages étaient présents pendant les périodes de forte perte de résistance, bien que les flambages de la tôle aient été assez nombreux à la rupture de la dalle.

Mot clé : Méthode des éléments finis, Dalle mixte, Cisaillement longitudinal, Structures mixtes

FEM analysis applied to the study of the stress transmission in the corrugated sheet slab
Master of Civil Engineering, defended by: MBOH HELBERT SHAYEH, NASPW, Yaoundé, 2019/2020

vii

LIST OF FIGURES

FEM analysis applied to the study of the stress transmission in the corrugated sheet slab
Master of Civil Engineering, defended by: MBOH HELBERT SHAYEH, NASPW, Yaoundé, 2019/2020

viii

FEM analysis applied to the study of the stress transmission in the corrugated sheet slab
Master of Civil Engineering, defended by: MBOH HELBERT SHAYEH, NASPW, Yaoundé, 2019/2020

ix

FEM analysis applied to the study of the stress transmission in the corrugated sheet slab
Master of Civil Engineering, defended by: MBOH HELBERT SHAYEH, NASPW, Yaoundé, 2019/2020

x

LIST OF TABLES

FEM analysis applied to the study of the stress transmission in the corrugated sheet slab
Master of Civil Engineering, defended by: MBOH HELBERT SHAYEH, NASPW, Yaoundé, 2019/2020

xi

TABLE OF CONTENTS

FEM analysis applied to the study of the stress transmission in the corrugated sheet slab
Master of Civil Engineering, defended by: MBOH HELBERT SHAYEH, NASPW, Yaoundé, 2019/2020

xii

FEM analysis applied to the study of the stress transmission in the corrugated sheet slab
Master of Civil Engineering, defended by: MBOH HELBERT SHAYEH, NASPW, Yaoundé, 2019/2020

xiii

FEM analysis applied to the study of the stress transmission in the corrugated sheet slab
Master of Civil Engineering, defended by: MBOH HELBERT SHAYEH, NASPW, Yaoundé, 2019/2020

xiv

FEM analysis applied to the study of the stress transmission in the corrugated sheet slab
Master of Civil Engineering, defended by: MBOH HELBERT SHAYEH, NASPW, Yaoundé, 2019/2020

XV

GENERAL INTRODUCTION

The actions on buildings and bridges due to imposed loads by occupants, installed facilities and natural actions are usually resisted first by the slab, which distributes the effects of these actions to the beam alongside the actions due to the structural self-weight. The slab can also help to distribute seismic action on the building by acting as a diaphragm between the columns. Building designers are always thus tasked to design slabs that can properly bear and transfer these actions without reaching very high deformations unacceptable to the building integrity and function.

Aided by research work, different types of slabs are being invented to ensure that they are stiff enough for resisting the imposed loads, and also of small self-weight to reduce the dimensions of the beams, columns and foundation. The corrugated sheet slab has been amongst the leading slab typologies to incorporate a high stiffness with a relatively low self-weight and has since the 1970s enjoyed high applicability in steel building and bridge construction in Europe, America and in other parts of the world.

The design of composite slabs by experimental methods like the Partial Shear Connection method and m-k method is based on the discovery by Porter and Ekberg (1978) and Schuster (1970) that the most likely failure mode in composite slabs was by horizontal shear failure. These methods, although widely used by slab manufacturers and designers require many resources, time and effort. An (1993), Veljkovic (1996) and Abdullah (2004, 2007, 2009) developed semi-empirical FE models of composite slabs, in which the shear bond behaviour of the slab was obtained by small-scale bending tests and used in the model of a composite slab with ABAQUS. The accuracy of the method proposed by Abdullah was further confirmed by Degtyarev (2014) and Chen (2011) using ANSYS.

This work aims to further show the accuracy of the FE method in modelling design tests on composite slabs and to study the stress distribution in the composite slab. To attain this objective, the work is divided into 4 parts: the first chapter is on the state of the art and will permit the mastery of the basic concepts related to composite slabs and FEM.

The second and third chapters focus on establishing a nonlinear FE model for a slab test of a composite slab verified according to Eurocode 4 using ABAQUS software. The results of the analysis are then compared to see how the FE model attempts to simulate the experimental

FEM analysis applied to the study of the stress transmission in the corrugated sheet slab
Master of Civil Engineering, defended by: MBOH HELBERT SHAYEH, NASPW, Yaoundé, 2019/2020

1

observations and to study the stress distribution in the slab concrete, steel sheet and reinforcement.

FEM analysis applied to the study of the stress transmission in the corrugated sheet slab
Master of Civil Engineering, defended by: MBOH HELBERT SHAYEH, NASPW, Yaoundé, 2019/2020

2

CHAPTER 1: **LITERATURE REVIEW**

Introduction

Corrugated sheet slabs, or composite slabs, enjoy a fair share of the demand in the steel building construction industry. The accurate design of such sheets has thus gained in importance and is usually among the information presented by the manufacturer. The main challenge to modern methods of simulating the design of the composite slabs has been the accurate representation of the shear bond model of the slab. The finite element method being an approximate method by nature also encounters the issue of accurate representation of the slab horizontal shear behaviour, alongside the other accuracy elements. This section aims to explain the basis of the composite slab and the finite element method, to permit mastery of the current FEM of slab modelling. Corrugated sheet slabs were reviewed, to understand the basis of their functionality based on the influence of each slab component and research findings on the behaviour of the assembly. The basis of the finite element method was also presented in this section to easily emphasize its contribution to the study and design of composite slabs. Modern methods of composite slab design were reviewed, as well as proposed small-scale, analytical and numerical methods for accurately modelling the composite slab.

1.1. **Corrugated sheet slabs**

The corrugated sheet slab will be presented in this section in terms of its components, innovation, mechanical action and design.

1.1.1. Generalities on composite slabs

Composite slabs, like all composite members, are made of concrete and of structural or cold-formed steel, interconnected by a shear connection to limit the longitudinal slip between concrete and steel and the separation of one component from the other (EC4,2004). The most commonly implemented type of composite slab is the consist of profiled steel sheet (or corrugated sheet) overlaid with an in-situ reinforced concrete topping. The corrugated sheet is used initially as permanent shuttering and subsequently combines structurally with the hardened concrete and act as tensile reinforcement in the finished floor (EC4,2004). They are commonly used (with steel columns) in the commercial, industrial, leisure, health and residential building sectors due to the high speed of construction and general structural economy that can be achieved. Although most commonly used on steel-framed buildings,

FEM analysis applied to the study of the stress transmission in the corrugated sheet slab
Master of Civil Engineering, defended by: MBOH HELBERT SHAYEH, NASPW, Yaoundé, 2019/2020

3

composite slabs may also be supported off masonry or concrete components. A typical example of the decking layout for a composite floor is shown in Figure 1.1. The lines of shear connectors indicate the positions of the supporting beams (J W Rackham *et al.*, 2009).
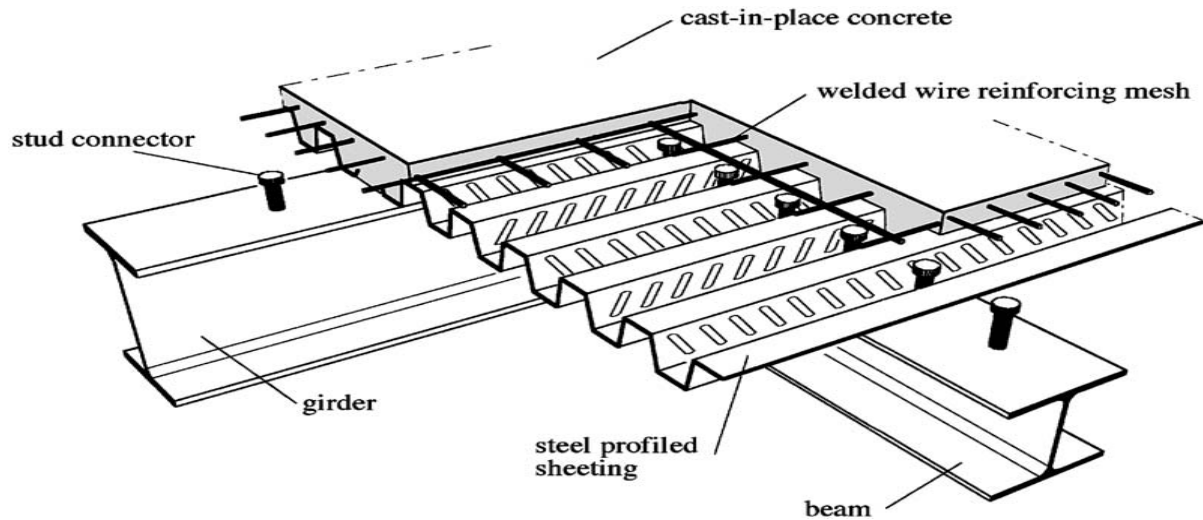
Figure 1.1. Layout of composite deck supported by a steel frame (Source: Crisinel et al, 2003)
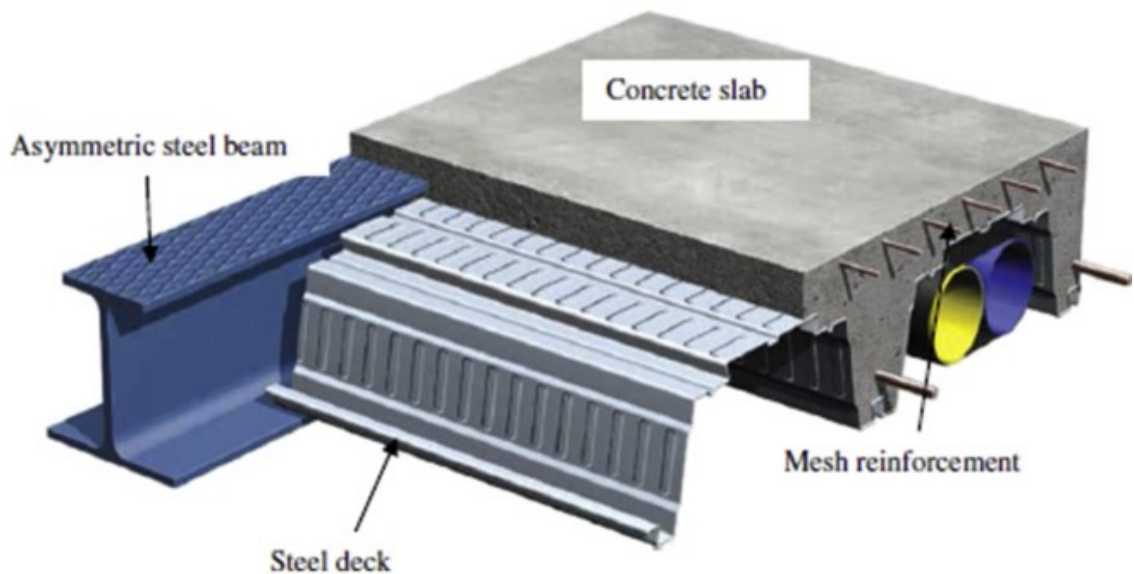
Figure 1.2. Composite slab components (Ahmed et al, 2019)

1.1.2. Composite action in corrugated sheet slabs

The shear connection between the concrete and the steel sheet is the interconnection between both members that has sufficient strength and stiffness to enable their design as parts of a single member. Although there exists a pure bond between the two materials as a result of

FEM analysis applied to the study of the stress transmission in the corrugated sheet slab
Master of Civil Engineering, defended by: MBOH HELBERT SHAYEH, NASPW, Yaoundé, 2019/2020

4

the hardening of the concrete on the sheet, this bond is week and is generally not considered responsible for the shear action. Eurocode 4 identifies several means by which a sufficiently stiff shear connection can be achieved in the corrugated sheet slab, illustrated in Figure 1.3:

- mechanical interlock provided by deformations in the profile (indentations or embossments);
- frictional interlock for profiles shaped in a re-entrant form;
- end anchorage provided by welded studs or another type of local connection between the concrete and the steel sheet, only in combination with the aforementioned means;
- end anchorage by deformation of the ribs at the end of the sheeting for the re-entrant profile shape.
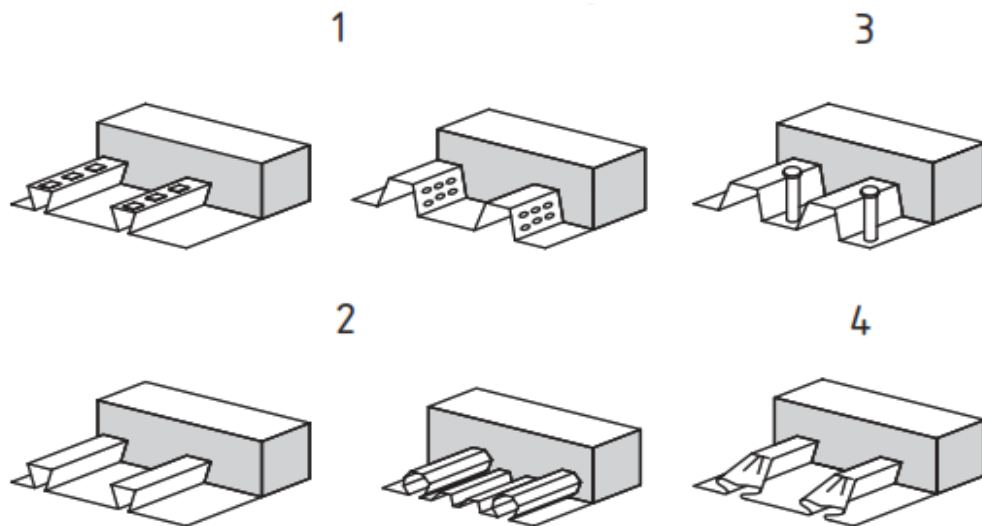
Figure 1.3. Types of shear connection in the composite slab (1) Mechanical interlock (2) Frictional interlock (3) End anchorage by shear studs (4) End anchorage by rib deformation (Eurocode 4,2004)

For slabs on steel frames, the composite interaction for the supporting steel beam is achieved by the attachment of shear connectors to the top flange of the beam into the concrete. These connectors generally take the form of headed studs. It is standard practice in the UK for the studs to be welded to the beam through the decking (known as 'thru-deck' welding) before placing the concrete. The shear connectors provide sufficient longitudinal shear connection between the beam and the concrete so that they act together structurally (J. W. Rackham et al., 2009a)

1.1.3. Components of composite slabs

FEM analysis applied to the study of the stress transmission in the corrugated sheet slab
Master of Civil Engineering, defended by: MBOH HELBERT SHAYEH, NASPW, Yaoundé, 2019/2020

5

Although there are many minute differences in the manufactured steel-concrete composite slabs between countries, the main components are much less the same. Every composite slab contains a steel profiled deck (or corrugated sheet), a reinforced concrete slab laid on the deck, and shear connectors to connect the deck to the supporting beam.

1.1.3.1 Corrugated profiled sheet

The profiled sheets for composite slabs are cold-formed by mechanically deforming and reshaping a steel sheet in roll-forming machines such or by press brakes and bending brakes, with no heat application (Yu and LaBoube, 2010). They are one of the oldest types of cold-formed steel products and have been used in building construction since about 1784. At present, numerous types of sheets with different coatings are being produced by many manufacturers with several standard sheet shapes available for building construction and other usages. The sheets mostly serve as panels for building roofs and walls for industries and warehouses as well as in the floors of buildings and bridges. In composite slabs, the cold-formed steel deck serves in four ways:

- as permanent formwork for the concrete;
- as the concrete reinforcement for positive bending;
- as a working platform for the various trades during construction;
- as bracing for the steel frame by acting as a diaphragm.

The placement of the steel deck is done in a fraction of the time required for wood forming in reinforced concrete slabs, so it is no surprise that wood has been replaced in steel-framed building construction. The steel deck achieves its composite bonding with the concrete through its shape and by embossments or indentations formed in the deck webs. In the past, successful composite decks were made by welding transverse wires across the deck ribs or by punching holes in the deck to allow concrete to fill the ribs. Research sponsored by the Steel Deck Institute and by the American Iron and Steel Institute has shown that the shear studs used to make the beams composite also greatly enhance the composite behaviour of the steel deck (Yu and LaBoube, 2010).

Shapes for corrugated sheets in composite slabs differ widely, depending on the manufacturer. The main types of profiles are trapezoidal and re-entrant (dovetail) profiles. Re-entrant profiles are characterized by a closed trough and are common in the UK, while

FEM analysis applied to the study of the stress transmission in the corrugated sheet slab
Master of Civil Engineering, defended by: MBOH HELBERT SHAYEH, NASPW, Yaoundé, 2019/2020

6

trapezoidal profiles have open troughs and are common in the US as shown in Figure 1.7. Recent profiles contain embossments and indentations on the webs to increase the shear bond with the concrete slab. The flanges usually contain stiffened ribs to increase the resistance of the section to bending forces. The thickness of the sheets is usually between 0.38 to 2.0mm with a steel grade of 350MPa.

Figure 1.4. Production of a steel sheet in a rolling mill

a) Trapezoidal type   b) Re-entrant type   c) Clip-pan ou L type
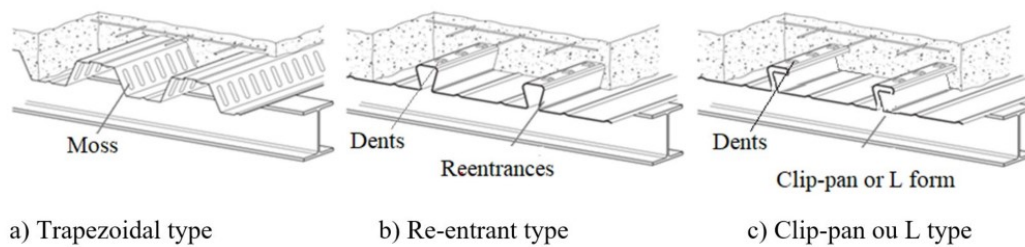
Figure 1.5. Steel decking types for composite slabs

FEM analysis applied to the study of the stress transmission in the corrugated sheet slab
Master of Civil Engineering, defended by: MBOH HELBERT SHAYEH, NASPW, Yaoundé, 2019/2020

7
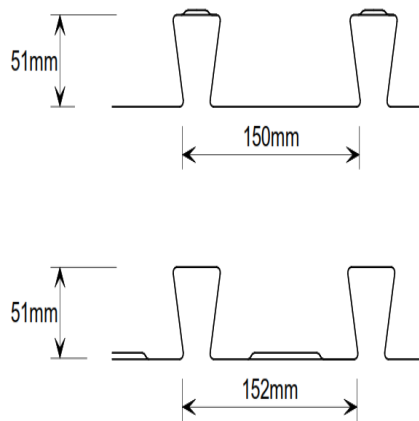
Figure 1.7a. Re-entrant profiles
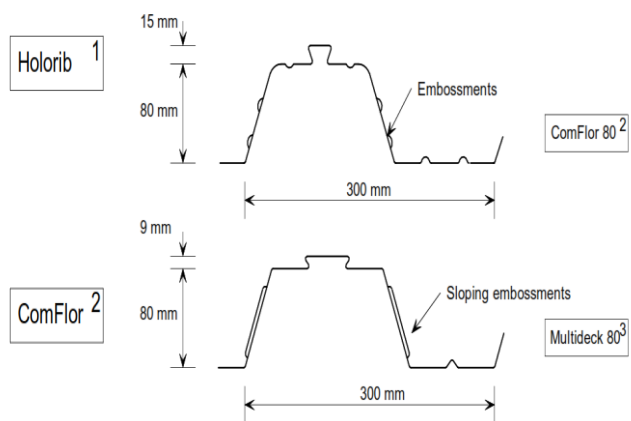
Figure 1.7b. Trapezoidal profiles
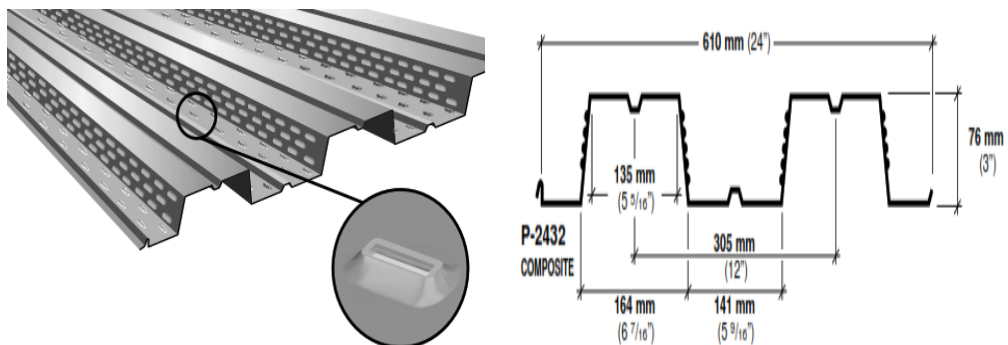
Figure 1.8. Indentations and embossments in the profiled sheet for increased mechanical interlock

1.1.3.2 Concrete slab

The concrete slab which overlays the steel deck is poured as wet concrete and allowed to harden over the curing period allowing the shear bond to be formed between the two layers.

a. Concrete

Both normal-weight concrete and lightweight concrete can be used in composite slabs. Normal concrete is made using dense aggregates from natural sources while lightweight aggregate concrete contains artificially produced aggregates such as expanded pulverized fuel ash pellets. The cement and water contents are higher in lightweight concrete because of the absorption of water by the aggregate. For normal-weight concrete, strength classes C25/30, C28/35 or C32/40 are normally chosen in composite slab construction while strength classes LC25/28, LC28/31 or LC32/35 are typical lightweight concrete.

FEM analysis applied to the study of the stress transmission in the corrugated sheet slab
Master of Civil Engineering, defended by: MBOH HELBERT SHAYEH, NASPW, Yaoundé, 2019/2020

8

Lightweight concrete is commonly used because the obvious advantage of (typically) 25% weight saving can provide economic benefit for the overall design of the structure and its foundations. It also has better fire insulating qualities than normal-weight concrete, and so thinner slabs may be possible when the 'fire condition' governs the slab design. Unfortunately, lightweight concrete is not always readily obtainable in all areas and it may not be appropriate if it is to be used in trafficked areas; to achieve a good wearing surface, the finishing process must cover the particles of lightweight coarse aggregate with an adequate, well-trowelled dense surface mortar layer. It also has poorer sound insulation properties than normal-weight concrete (J. W. Rackham et al., 2009a).

Usually, the resistance of the composite slab is sufficient for the conditions of use. However, reinforcement is usually added to the concrete to increase its strength and to help resist tensile forces at the top of the concrete in support regions. Two types of concrete reinforcement are usually used: bar reinforcement and fibre reinforcement.

b. Bar Reinforcement

The bar reinforcement in concrete for composite slabs is usually a welded fabric, supplemented by a bar in the slab ribs. At the slab supports the welded fabric reduces concrete cracking and increases bending resistance of the slab in case of a fire. They also help to distribute the effects of localised point and line loads and help strengthen the edges of openings. They also assist in shear resistance for the composite beams.

The bars for the fabric are usually of 2 types: Type A fabrics are equally spaced in both directions, while type B fabrics have a 100mm longitudinal bar spacing and a 200mm transverse bar spacing. A third fabric type exists, which is used only for highways (J. W. Rackham et al., 2009a). Figure 1.9 shows a typical reinforcement disposition in a composite slab.

FEM analysis applied to the study of the stress transmission in the corrugated sheet slab
Master of Civil Engineering, defended by: MBOH HELBERT SHAYEH, NASPW, Yaoundé, 2019/2020

9
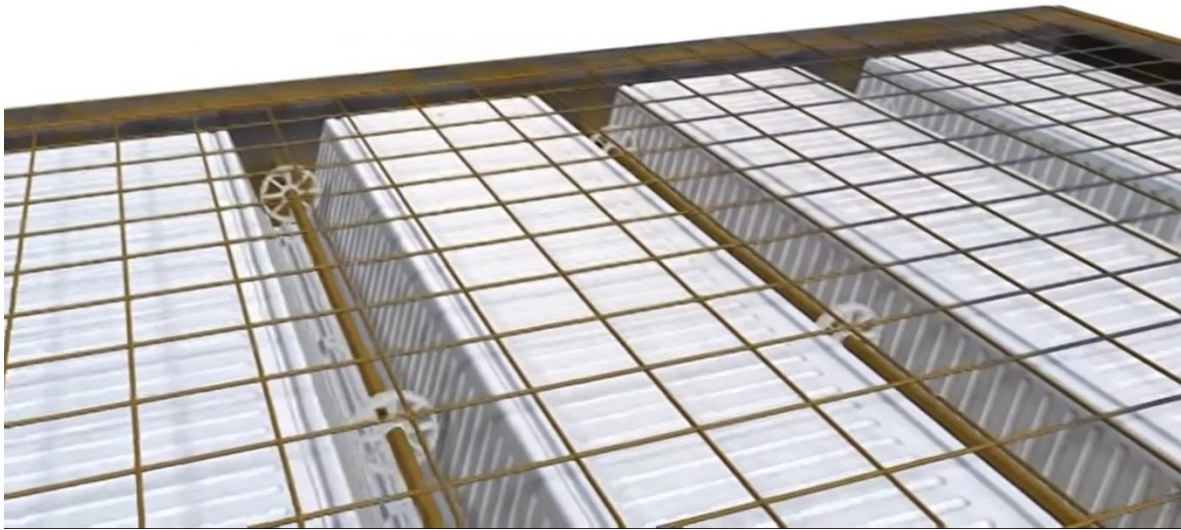
Figure 1.9. Fabric reinforcement and bar reinforcement in Composite slabs (Comflor product overview)

c. Fibre reinforcement

Fibre reinforcement consists of short fibres made from steel, polypropylene or a combination of both, which are mixed into the concrete before placement. Under controlled circumstances, fibres may be substituted for some or all of the fabric reinforcement. Use of fibre reinforcement results in a three-dimensional reinforced concrete composite slab. The performance of fibre reinforcement is verified empirically, specifically for fire resistance and for longitudinal shear transfer, using the same testing regimes that are used to validate the use of traditional reinforcement within steel deck composite floors.

Considerable benefits can be achieved using fibre reinforcement, including a reduction in labour costs and a saving on the construction programme. The requirement for longitudinal shear reinforcement, in the form of bars or fabric, can be dramatically reduced and only a minimal amount of fabric reinforcement need to be purchased, transported and stored. There is less usage of the crane as there are fewer lifting operations. The installation of the floor is easier and safer because there is less reinforcement to obstruct the floor working area and to handle, fix and check, and this can reduce installation times by up to 20%. Independent testing has shown that fibre reinforcement systems can provide an equivalent or superior performance to traditional welded wire fabric solutions, although local reinforcement may be necessary in locations of concentrated loads. Fibre reinforcement provides resistance to plastic shrinkage,

FEM analysis applied to the study of the stress transmission in the corrugated sheet slab
Master of Civil Engineering, defended by: MBOH HELBERT SHAYEH, NASPW, Yaoundé, 2019/2020

10

settlement cracking and toughness, but the performance is related to the specific fibre. Studies on the strength of fibre reinforced concrete have been done by Ackermann and Schnell (2011), Ryu *et al.* (2013) and Radik, Erdogmus and Schafer (2011)

Figure 1.10. Polymer-reinforced concrete mould (Radik, Erdogmus and Schafer, 2011)

1.1.3.3 Shear connector

Shear connectors can resist the horizontal shear and provide vertical interlocking between the concrete slab and steel beams to produce a composite section that acts as a single unit. Types of shear connectors include studs, channels, stiffened angles, and flat bars, as shown in Figure 1.11. The most often used connectors are the shear studs. In building construction, the studs are welded through the steel deck into the structural steel framing; in bridge construction, the studs are welded directly to the framing members. They are usually welded through the deck unto the top flange of the primary or secondary steel beams supporting the floor (Figure 1.12)
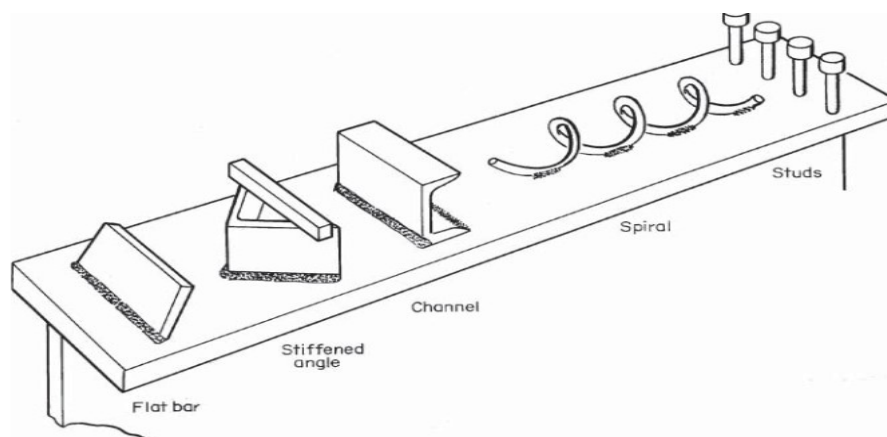
Figure 1.11. Types of shear connectors used over the years(J. W. Rackham et al., 2009a)**.**

FEM analysis applied to the study of the stress transmission in the corrugated sheet slab
Master of Civil Engineering, defended by: MBOH HELBERT SHAYEH, NASPW, Yaoundé, 2019/2020

11

Assisted by the reinforcement, the shear studs transfer forces from the deflecting steel beam to the concrete flange of the resulting composite beam. The functionality of the shear connection usually depends on the geometry of corrugated sheet, the thickness of the sheet and material strengths for the steel and the concrete.
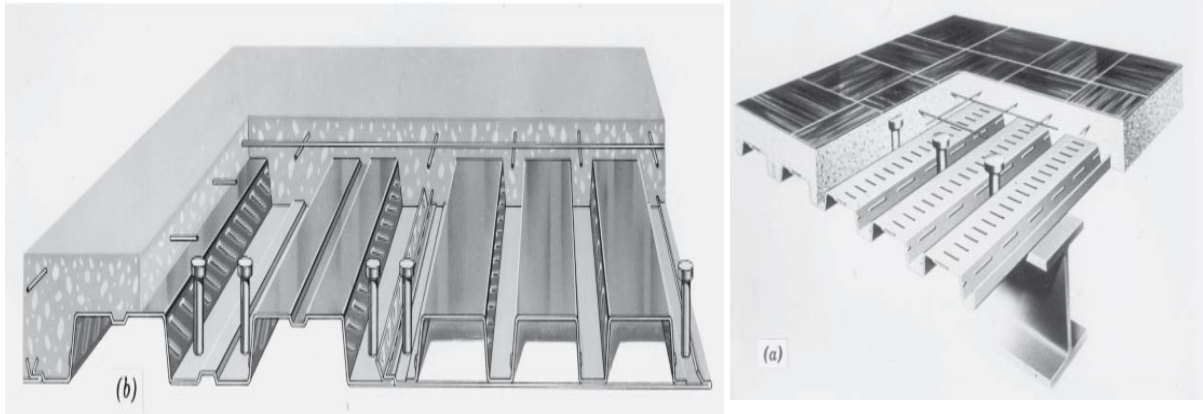
Figure 1.12. Shear connectors connected to secondary beams (a) and to primary beams(b)

The shear connections are liable to failure when fewer shear connectors are used than prescribed-a state known as partial shear connection- or when the concrete cracks to a large diameter. Deformation of the shear connectors allows slip between the concrete and the steel section. This slip is zero at the point of maximum bending moment (often at mid-span) and increases towards the supports; the longer the beam span, the greater the slip at the supports. For partial shear connection, because there are fewer shear connectors, there will be more slip for a given load than with full shear connection. To avoid any adverse effects arising from excessive slip, a minimum limit to the degree of shear connection is specified in national codes. Figure 1.13 shows the distribution of stresses around the shear connector on the primary beams (parallel to the slab ribs) and for the shear connector in the secondary beams. In the latter, the concrete area is much reduced and hence the risk of failure is higher.

1.1.4.Innovations to corrugated sheet slabs

The principal innovations to the corrugated sheet slabs have been on each member to ensure a much firmer shear bond between the concrete slab and the steel sheet and also to ensure a stronger shear connection. The overall slab thickness has also been greatly reduced due to newer methods of supporting the steel deck on the beams.

FEM analysis applied to the study of the stress transmission in the corrugated sheet slab
Master of Civil Engineering, defended by: MBOH HELBERT SHAYEH, NASPW, Yaoundé, 2019/2020

12
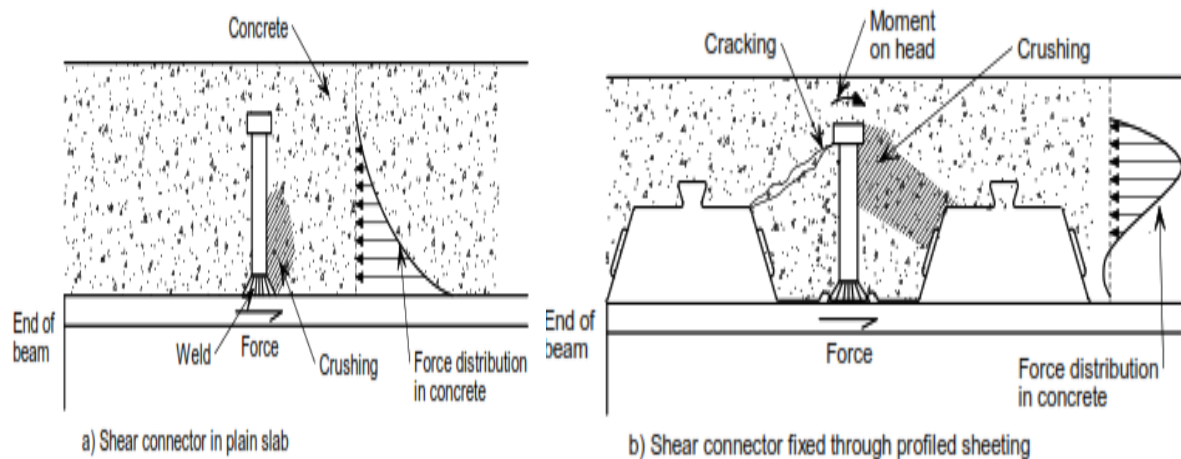
Figure 1.13. Shear connector forces in composite slabs(Rackham et al., 2009)

1.1.4.1 Innovations for stronger mechanical interlock.

Manufacturers have sought to experimentation to test how to innovate the section of the corrugated sheet so as to ensure a greater mechanical interlock with the concrete slab. This led to the rapid development in steel decks with embossments and indentations on the sheets. In the past, successful composite deck was made by welding transverse wires across the deck ribs or by punching holes in the deck to allow concrete to fill the ribs. Research sponsored by the Steel Deck Institute and by the American Iron and Steel Institute has shown that the shear studs used to make the beams composite also greatly enhance the composite behaviour of the steel deck (Yu and LaBoube, 2010).

Steel decks were also created containing stiffeners on the flanges so as to ensure that the whole section works. The bottom flange stiffeners could be multiple to increase the stiffness of the section.

1.1.4.2 Innovations for stronger shear connection

For steel decks with a single stiffener in the trough, numerous research such as Qureshi et al (2011) has pointed to the weakness of the shear connection when the stud is welded on the side of the stiffener that faces the midspan of the composite beam. This side has become known as the 'unfavourable position' and is not recommended to achieve good shear connection. It is advised that the shear connectors be positioned on the side away from the beam mid-span, known as the favourable position, illustrated in Figure 1.14 below.

FEM analysis applied to the study of the stress transmission in the corrugated sheet slab
Master of Civil Engineering, defended by: MBOH HELBERT SHAYEH, NASPW, Yaoundé, 2019/2020

13

1.1.4.3 Slab thickness reductions

The development of 'Slimflor' and 'Slimdek' in the 1990s (Lawson *et al.*, 1999) have led to the use of very thin composite slabs in buildings. The steel deck in such floors, is fixed to a steel shelf angle which is connected to the web or the flange of the steel beam. This has led to much thinner yet equally resistant slabs, permitting a general reduction in the overall structural height without loss in functionality. The different deck support possibilities for these new decks are shown in Figure 1.15.
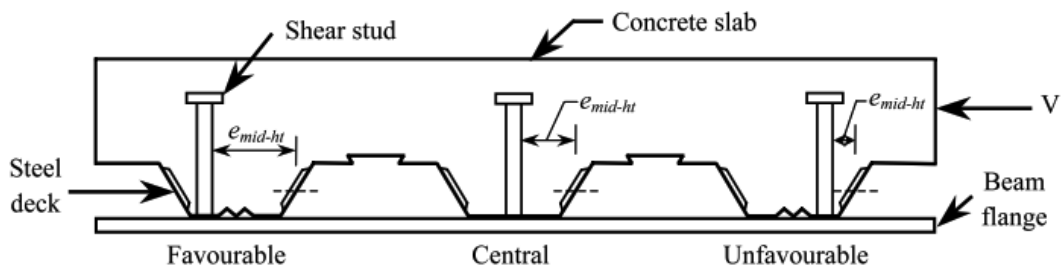
Figure 1.14. The different shear connector positions in a composite deck (Qureshi et al,2011)
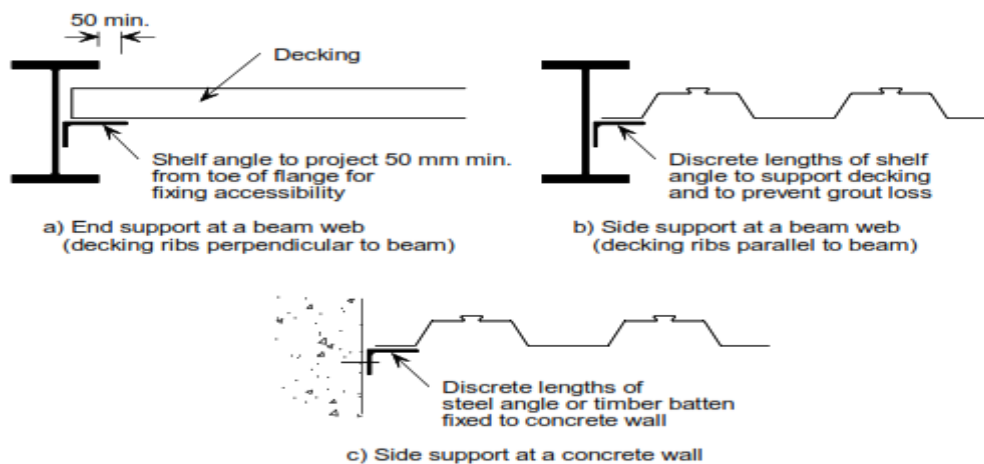
Figure 1.15. Decking support details at a beam web and at a concrete wall for slim floor construction (J. W. Rackham et al., 2009)**.**

1.2. **Design of corrugated sheet slabs**

Although composite slabs are an increasingly popular slab choice for most construction companies, their design is very complex because the slab behaviour is not very easy to predict due to several secondary effects in the slab. Examples of these effects include local buckling

FEM analysis applied to the study of the stress transmission in the corrugated sheet slab
Master of Civil Engineering, defended by: MBOH HELBERT SHAYEH, NASPW, Yaoundé, 2019/2020

14

of the thin steel sheeting, partial connection between the steel and concrete, punching shear due to concentrated loads, dynamic effects, and anisotropy (Crisinel and Marimon, 2004). The orthotropic structural properties and the staged construction of the composite slabs also cause them to have very complex rules for their design. Manufacturer companies have developed several methods over the past years to better observe these effects. However, the most used and promising are experiments performed with multiple units of full-scale slabs.

1.2.1.1 Failure mechanisms of corrugated sheet slabs

It has been recognized that composite slabs under bending can exhibit three major modes of failure: flexure failure at section 1-1, vertical shear failure at section 2-2 and horizontal shear failure at section 3-3 as shown in Figure 1.16 (Johnson, 2008)
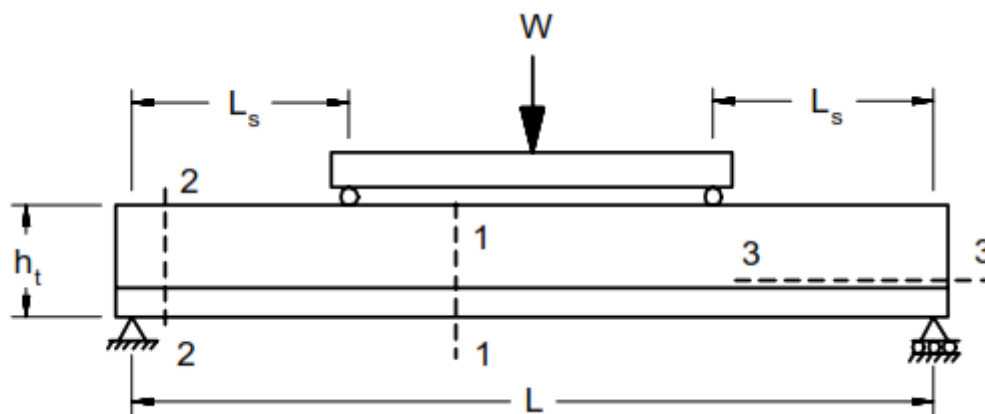
Figure 1.16. Modes of failure of composite slab (Johnson,1994)

The flexural failure (mode 1) occurs when complete interaction at the interface between concrete and steel is achieved. This type of failure usually occurs in long thin slabs. Analysis for this type of failure is quite easy, in which case ordinary reinforced concrete procedures can be followed (Samuel Easterling and Young, 1992; ASCE, 1994) The flexural failure however is not a dominant design criterion because the steel and concrete interaction is usually incomplete and the slab length is always limited by the serviceability (deflection) limit.

The characteristic of the second mode, which is the vertical shear failure, has been studied by Patrick and Bridge (1992). The slab has to be very short and thick with a high concentrated load near the supports for the mode 2 failure to be dominant. This is not common in

FEM analysis applied to the study of the stress transmission in the corrugated sheet slab
Master of Civil Engineering, defended by: MBOH HELBERT SHAYEH, NASPW, Yaoundé, 2019/2020

15

construction practice therefore it has not been the subject of much research. The effect is typically ignored in design.

Failure mode 3, which is a horizontal shear failure or shear bond failure as it is commonly referred to, is the mode more likely to occur for most composite slab systems subjected to vertical loads (Schuster, 1970; Porter *et al.*, 1976). This is characterized by the development of an approximate diagonal crack under or near one of the concentrated loads just before failure, followed by an observable end-slip between the steel deck and the concrete, within the concrete shear span, Ls, as illustrated in Figure 1.17 (Abdullah, 2004).
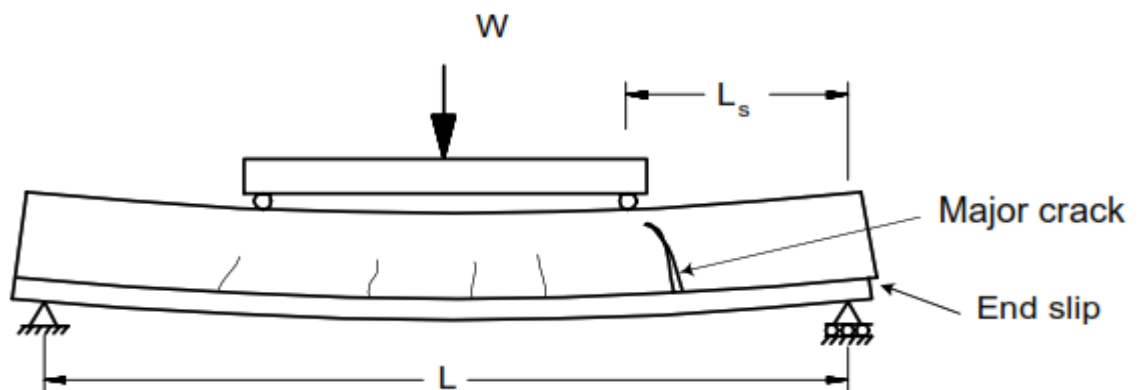
Figure 1.17. Horizontal shear failure (Abdullah,2004)

Several design methods have been developed over the past decades to better predict the horizontal shear strength of the composite slab among which are the m-k method and the partial shear connection method.

1.2.1.2 The m-k method of slab design

The semi-empirical based m-k method was developed by Schuster (1972), Porter and Ekberg (1976), and is adopted in ASCE and Eurocode 4. It is based on a test program of 2 sets of full-scale slabs, each of 3 slabs of equal geometry. The experiment is usually preceded with the application of a cyclic load of a certain magnitude to eradicate the shear bond in the slab. A line load is then applied to each slab symmetrically about the slab centre, in a simply supported configuration as shown in Figure 1.18. This step may be carried out as force-controlled or displacement-controlled. In the force-controlled test, a given load is incrementally applied and the displacement or other dependent variables are calculated from the system, while the displacement is being varied in the displacement-controlled test. Certain experiments

FEM analysis applied to the study of the stress transmission in the corrugated sheet slab
Master of Civil Engineering, defended by: MBOH HELBERT SHAYEH, NASPW, Yaoundé, 2019/2020

16

begin with force-controlled, until significant deflections are reached, after which displacement-control is adopted.

The reaction maximum reaction force for each specimen is measured, and the two sets of values are plotted, normalized against the slab geometry as shown in Figure 1.18. The values for m and k are obtained by using linear regression but are only applicable to specific slab configurations as shown in Figure 1.19. The slab longitudinal resistance can then be calculated by the relation in equation (1.1).

$$V_{l,rd} = \frac{b * d_p}{\gamma_{vs}} \left(\frac{m * A_p}{b * L_s} + k \right)$$

(1.1)

where,

$V_{l,rd}$ Longitudinal shear resistance;
γ_{vs} safety factor;
A_p sheet area;
l_s shear span;
b slab width;
d_p effective depth of sheet.

The load deflection curves for the slabs are also gotten from this test, and are used to judge whether the slabs are ductile or non-ductile in their behaviour.
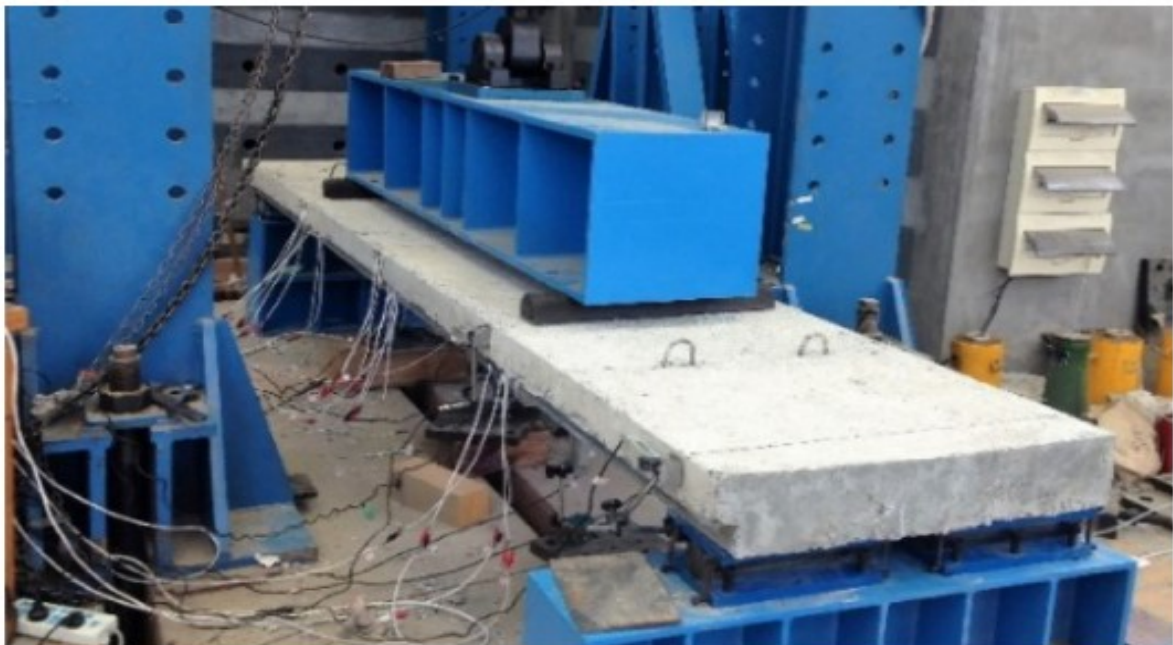
Figure 1.18. An m-k test experimental setup

FEM analysis applied to the study of the stress transmission in the corrugated sheet slab
Master of Civil Engineering, defended by: MBOH HELBERT SHAYEH, NASPW, Yaoundé, 2019/2020

17

Note: b, d_p and L_s are in mm, A_p is in mm², V_t is in N.
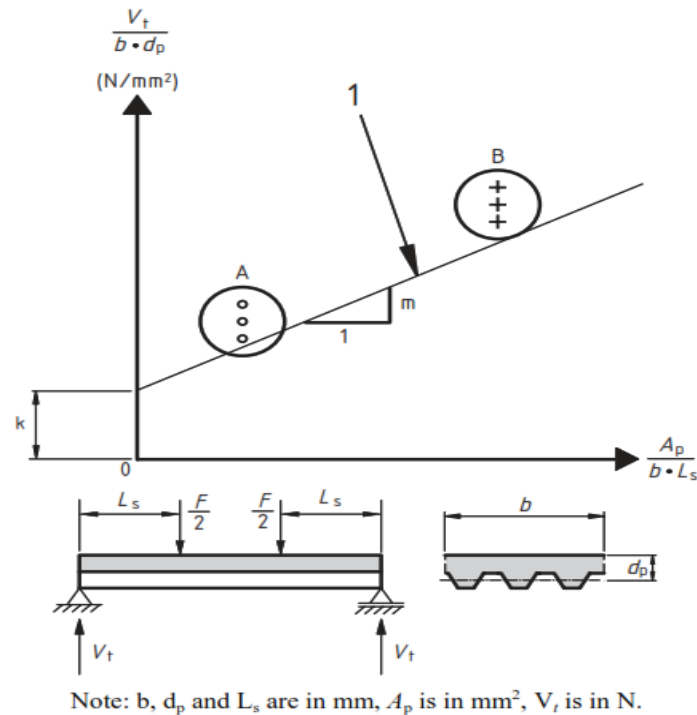
Figure 1.19. Evaluation of m-k test results (Eurocode 4,2004)

1.2.1.3 The partial shear connection (PSC) method of slab design

This method was developed by Bode (1992) and is adopted in Eurocode 4 with permission of use on slabs that show ductile shear behaviour only. The slab specimens are allowed to overhang from the supports by a distance Lo, and the loads are applied just like in the m-k design test. The maximum moment and support reaction in the slab are measured from the experiment for the slab specimens. The moment from the test is then normalized against the sheet resistant moment and is used in a standard curve to find the degree of shear connection in the slab. The ultimate shear stress in the slab is then calculated according to equation (1.2);

$$\tau_u = \frac{\eta N_{cf} - \mu V_t}{b(L_s + L_o)} \qquad (1.2)$$

where,

τ_u is the design shear stress;

η is the degree of shear connection;

μV_t is the contribution from the reaction force;

b   is the beam width;

N_{cf} is the axial force in the concrete;

L_s is the shear span;

FEM analysis applied to the study of the stress transmission in the corrugated sheet slab
Master of Civil Engineering, defended by: MBOH HELBERT SHAYEH, NASPW, Yaoundé, 2019/2020

18

L_o is the overhang.
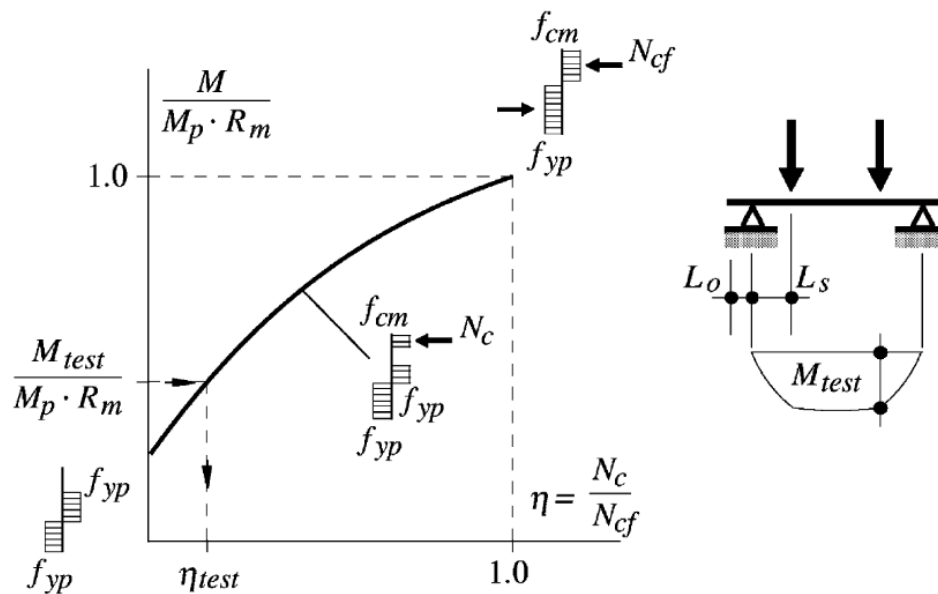
Figure 1.20. Partial connection design method

1.3. **National codes for detailing, design and verifications of composite slabs**

Mathematical models for system structural behaviour are developed into design rules, as found in codes of practice, by simplifying them wherever possible, defining their scope and introducing partial factors (R.P Johnson, 2010). The national and international norms existing to regulate composite slab design are studied in this section.

1.3.1. European norms

The European norms exist for numerous construction technologies or circumstances, usually divided into many parts. The part which is concerned with the design of composite slabs is Eurocode 4.

1.3.1.1 Eurocode 4

Eurocode 4 has several parts for all the fields of composite construction. EN 1994-1-1 describes the Principles and requirements for safety, serviceability and durability of composite steel and concrete structures, together with specific provisions for buildings. It is based on the limit state concept used in conjunction with a partial factor method (Eurocode 4, 2004) It is intended to be used in conjunction with the following codes (Eurocode 4, 2004):

- EN 1990 Eurocode: Basis of structural design

FEM analysis applied to the study of the stress transmission in the corrugated sheet slab
Master of Civil Engineering, defended by: MBOH HELBERT SHAYEH, NASPW, Yaoundé, 2019/2020

19

- EN 1991 Eurocode 1: Actions on structures
- ENs, hENs, ETAGs and ETAs for construction products relevant for composite structures
- EN 1090 Execution of steel structures and aluminium structures
- EN 13670 Execution of concrete structures
- EN 1992 Eurocode 2: Design of concrete structures
- EN 1993 Eurocode 3: Design of steel structures
- EN 1997 Eurocode 7: Geotechnical design
- EN 1998 Eurocode 8: Design of structures for earthquake resistance, when composite structures are built in seismic regions.

The design and detailing rules for composite slabs for buildings according to these codes will be discussed in this section.

1.3.1.2 Design according to EC4

Eurocode 4 adopts but the m-k and partial connection experimental methods for the design of the shear bond in composite slabs. The testing procedure for both methods is as follows:

- The test loading procedure is intended to represent loading applied over a period of time. It is in two parts consisting of an initial test, where the slab is subjected to cyclic loading; this is followed by a subsequent test, where the slab is loaded to failure under an increasing load.
- If two groups of three tests are used, one of the three test specimens in each group may be subjected to just the static test without cyclic loading in order to determine the level of the cyclic load for the other two.
- Initial test: the slab should be subjected to an imposed cyclic load, which varies between a lower value not greater than $0,2W_t$ and an upper value not less than $0,6W_t$, where W_t is the measured failure load of the preliminary static test according.
- The loading should be applied for 5000 cycles in a time not less than 3 hours.
- Subsequent test: on completion of the initial test, the slab should be subjected to a static test where the imposed load is increased progressively, such that failure does not occur

FEM analysis applied to the study of the stress transmission in the corrugated sheet slab
Master of Civil Engineering, defended by: MBOH HELBERT SHAYEH, NASPW, Yaoundé, 2019/2020

20

in less than 1 hour. The failure load W_t is the maximum load imposed on the slab at failure plus the weight of the composite slab and spreader beams.

- In the subsequent test the load may be applied either as force-controlled or deflection-controlled

If the behaviour is ductile, the representative experimental shear force V_t should be taken as 0,5 times the value of the failure load W_t. If the behaviour is brittle this value shall be reduced, using a factor 0,8. The graph of Figure 1.19 is then plotted for the different specimens and the m and k values obtained, after which the longitudinal shear resistance is calculated according to equation (1.1).

For the PSC method, the moment at failure is calculated by considering the slab being simply supported under the combined action of the maximum load at failure and the self-weight of the slab and spreader beams. The corresponding moment (M_{test}) is entered into the graph of Figure 1.20 to calculate the degree of shear connection. The characteristic shear stress in the slab is then calculated according to equation (1.2). A reduced shear stress is usually derived, after which a design curve or moment envelop is plotted for the slab resistant moment in terms of different coefficients, explained in Equation (1.3) to (1.7)and illustrated in Figure 1.21.

$$M_{rd} = N_c z + M_{pr} \qquad (1.3)$$

$$N_c = bL_x \tau_{u,Rd} \quad L_x < L_{sf} \qquad (1.4)$$

$$\tau_{u,Rd} = \tau_{u,Rk}/\gamma_v \qquad (1.5)$$

$$L_{sf} = N_{cf}/(b\,\tau_{u,Rd}) \qquad (1.6)$$

$$N_{cf} = A_p \cdot f_{yp}/\gamma_{ap} \qquad (1.7)$$

where,

$\tau_{u,Rd}$ is the design shear stress;

M_{rd} design value of resisting bending moment in partial interaction mode (ie. moment envelope);

$M_{p,Rd}$ maximum resisting moment for the particular profile at full interaction;

L_x distance from the support representing beam length;
L_s shear span length required.

FEM analysis applied to the study of the stress transmission in the corrugated sheet slab
Master of Civil Engineering, defended by: MBOH HELBERT SHAYEH, NASPW, Yaoundé, 2019/2020

21
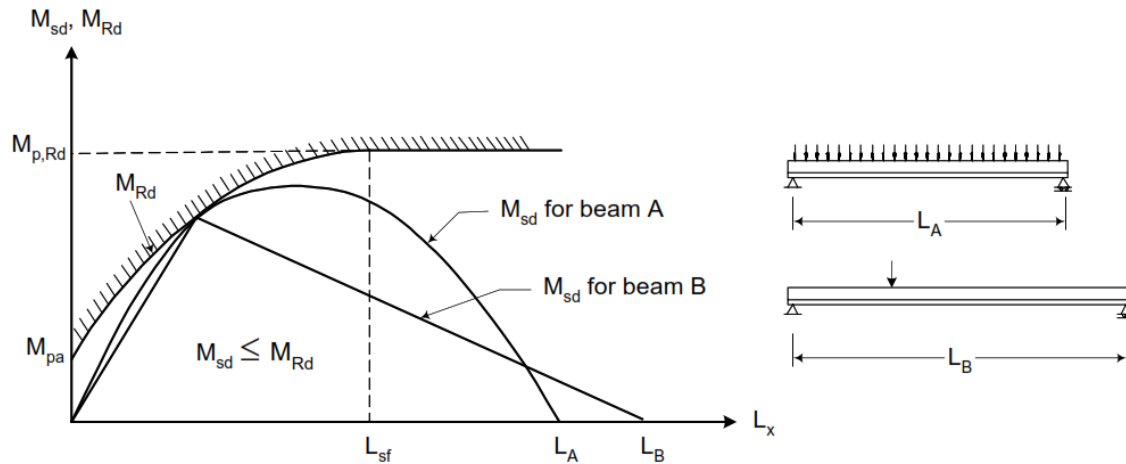
Figure 1.21. Demonstration of moment envelop and slab design (EC4.2004).

For a slab of the same profile to be loaded for a particular span, the calculated moment for the load configuration has to stay within the load envelope for the slab.

1.3.2. American norms

The American norms adopt the m-k test method only for the slab design. Two sets of slabs are as well used in the test: one set of slender long slabs, and a set of compact slabs. The m and k coefficients are calculated as slope an intercept of the line generated by linear regression of plotted curve for the equation(1.8) (ASCE, 1994);

$$\frac{V_e}{bd\sqrt{f'_{cl}}} = \frac{m\rho d}{L_s\sqrt{f'_{cl}}} + k \qquad (1.8)$$

where,

V_e maximum experimental shear at failure obtained from full-scale slab tests (not including the weight of slab);

b   unit width of the slab;

d   effective slab depth measured from extreme concrete compression fibre to the centroidal axis of the full cross-section of steel deck;

f'_{cl} compressive test cylinder strength of concrete at the time of slab testing;

ρ ratio of steel deck area to effective concrete area, $\frac{A_s}{bd}$;

L_s shear span.

FEM analysis applied to the study of the stress transmission in the corrugated sheet slab
Master of Civil Engineering, defended by: MBOH HELBERT SHAYEH, NASPW, Yaoundé, 2019/2020

22

The m and k values calculated from the regression of $\dfrac{V_e}{bd\sqrt{f'_{cl}}}$ against $\dfrac{\rho d}{L_s\sqrt{f'_{cl}}}$ points for both

sets of slabs are reduced by 10 to 15% to account for specimen behaviour variations and to be in the lower bound of slab resistance. For slabs of intermediate length and thickness, the m and k values are applied into equation(1.9);

$$\emptyset V_n = \emptyset \left[bd \left(\frac{mpd}{l'_i} + k\sqrt{f'_{cl}} \right) + \frac{\gamma W_s l_f}{2} \right] \qquad (1.9)$$

where,

> $\emptyset$ strength reduction factor;
>
> V_n nominal shear bond strength, lbs per ft of width;
>
> γ coefficient for the proportion of dead load added upon removal of shore;
>
> W_s Weight of slab;
>
> l_f length of span or length of shored span.

1.3.3. Commentary on both norms

Over the years, several general analyses have been given on the European and American methods for designing in the m-k and partial connection method. Generally, the m-k method has been signalled for its semi-empirical nature; lacking any clear mechanical model that shows factors contributing to slab performance.

The cyclic load applied to the slab specimens in the Eurocodes before static load has been shown to have a negligible effect on the slab resistance. The ASCE (1992) specification also does not specify the need for cyclic loading.

Eurocode 4 omits the concrete strength from the equations because it may give unsatisfactory values for m and k if the concrete strength varies widely within a series of tests (Johnson, 1994). Many researchers have reported that the concrete strength does not have a significant effect on the slab capacity (Seleim and Schuster, 1985; Luttrell, 1987; Daniels, 1988; Bode and Sauerborn, 1992; Veljkovic, 1994)

FEM analysis applied to the study of the stress transmission in the corrugated sheet slab
Master of Civil Engineering, defended by: MBOH HELBERT SHAYEH, NASPW, Yaoundé, 2019/2020

23

1.4. **Finite element method**

The finite element method, commonly called FEM, is amongst the frequently used numerical procedures to solve the partial differential equations that express certain phenomena in Engineering and Science. From an engineering standpoint, FEM is a method for solving engineering problems such as stress analysis, heat transfer, fluid flow and electromagnetics by computer simulation. Millions of engineers and scientists worldwide use the FEM to predict the behaviour of structural, mechanical, thermal, electrical and chemical systems for both design and performance analyses (Fish et al,2007). It is also largely used in other fields of science such as in the auto industry for car crash analysis, analysis of plastic surgeries or jaw reconstructions in medicine and seismic analysis of dams, amongst others. Its popularity can be gleaned by the fact that over \$1 billion is spent annually in the United States on FEM software and computer time. A 1991 bibliography (Noor and Peters, 1991) lists nearly 400 finite element books in English and other languages.

FEM basically divides the body (the domain of interest) into finite elements, connected by nodes, through which approximate solutions are calculated. The mesh of elements is then solved by considering the assembly of matrices that embody the properties of each element into a global matrix for the entire domain. The mathematical equations may be linear or non-linear equations which will require more work to be done.

Finite element analysis (or FEA), based on FEM is a simulation, applying a mathematical model. This model idealizes geometry, material properties, loads and/or boundary conditions based on an analytic understanding of important features for a physical phenomenon. Such representation of the physical phenomenon with mathematical equations entails several errors incurrent in the FEM:

- Modelling error in which approximations are made to the real problem. These approximations to the real world, do not take into in account the real behaviour.
- Discretization error where in the size and the shape of the finite elements are the parameters considered.
- Numerical error which is based on the algorithm used and finite precision of numbers used to represent the mathematical used to represent data in the computer.

FEM analysis applied to the study of the stress transmission in the corrugated sheet slab
Master of Civil Engineering, defended by: MBOH HELBERT SHAYEH, NASPW, Yaoundé, 2019/2020

24

To better understand FEM, its principle and chronological evolution must be known as well as its main applications. This section will also explain the complexity of FEM solutions to 3D problems and compare its accuracy to analytical models.

1.4.1. The principle of FEM

Zienkiewicz et al (1967) define FEM as a method of approximation to continuum problems such that

a) the continuum is divided into a finite number of parts (elements), the behaviour of which is specified by a finite number of parameters, and

b) the solution of the complete system as an assembly of its elements follows precisely the same rules as those applicable to standard discrete problems. (Zienkiewicz, Taylor and Zhu, 2005)

As already mentioned above, the physical/natural phenomenon is represented by a mathematical model, which will give several approximations to geometry, material behaviour, load and/or boundary conditions to understand the behaviour of the system.

The Finite element method then chooses the correct finite elements in the system (2D, 3D, wire, shell or solid elements) and a density for the mesh of elements. The loads and boundary conditions at the nodes are as well represented. This results in the development of matrices in which unknown variables for elements are expressed in terms of the known variables in the nodes.

With an accuracy assessment, the Finite element solution is tested, the mesh is refined and the analysis is repeated. This loop of refinement- recalculation continues until the FEM solution is within the tolerated limits according to the system as illustrated in Figure 2.6.1-1. The results of the FEM solution are then interpreted. Their correctness or incoherency may result in confirmation or in a refinement of the mathematical model or an optimization of the physical problem.

FEM analysis applied to the study of the stress transmission in the corrugated sheet slab
Master of Civil Engineering, defended by: MBOH HELBERT SHAYEH, NASPW, Yaoundé, 2019/2020

25
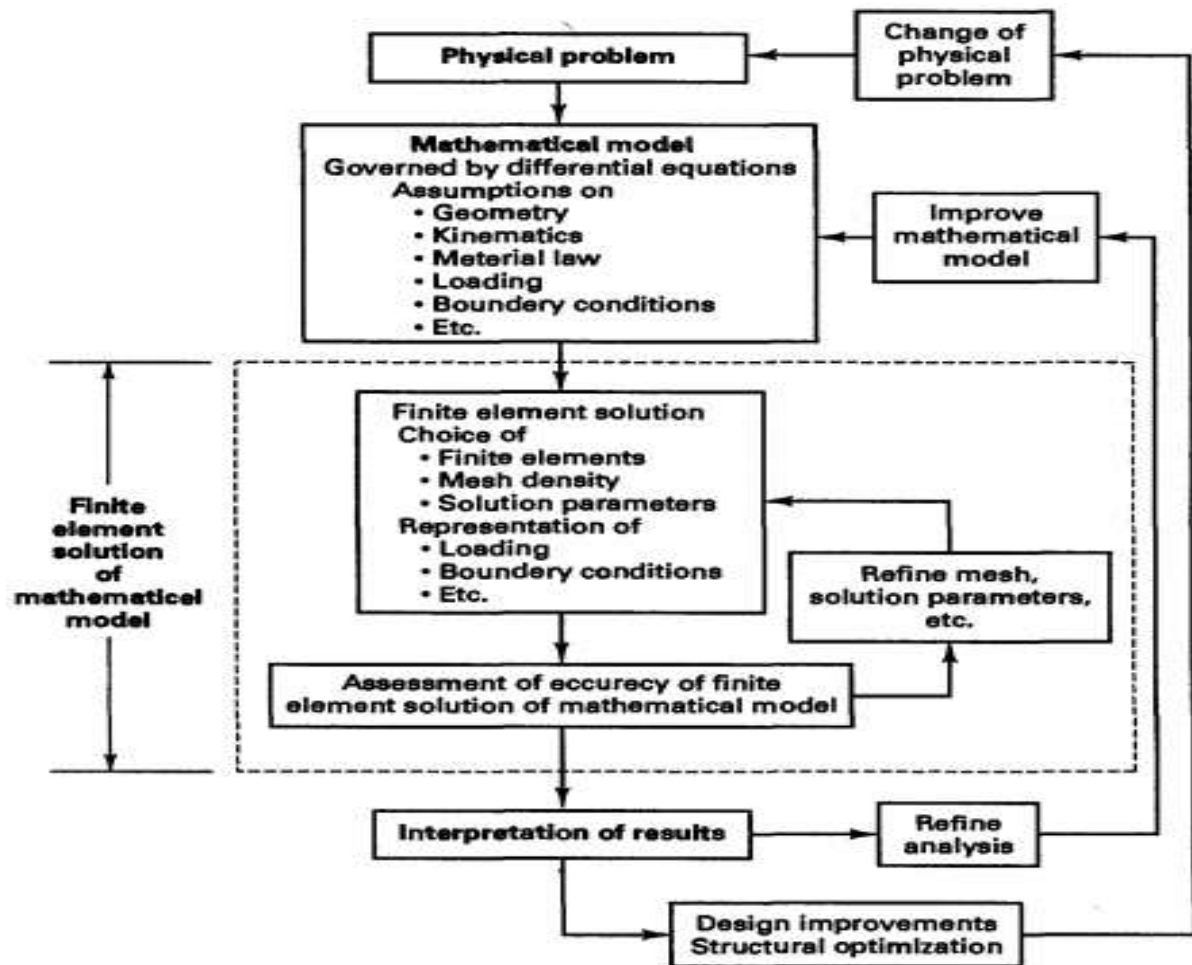
Figure 1.22. The process of finite element analysis (Bathe, 2006)

1.4.2. A brief history of FEM

The FEM was developed in the 1950s in the aerospace industry. The major players were Boeing and Bell Aerospace (long vanished) in the United States and Rolls Royce in the United Kingdom. M.J. Turner, R.W.Clough, H.C. Martin and L.J. Topp published one of the first papers that laid out the major ideas in 1956 (Turner et al., 1956). It established the procedures of element matrix assembly and element formulations. The second author of this paper, Ray Clough, who was a professor at University of California Berkeley, wrote a paper that first used the term 'finite elements. Other professors at Berkeley like E. Wilson and R.L. Taylor and graduate students such as T.J.R. Hughes, C. Felippa and K.J. Bathe. E. Wilson developed one of the first FEM programs which at the time was non-commercial.

FEM analysis applied to the study of the stress transmission in the corrugated sheet slab
Master of Civil Engineering, defended by: MBOH HELBERT SHAYEH, NASPW, Yaoundé, 2019/2020

26

Most of these methods could only solve linear problems. O.C. Zienkiewicz B. Irons and R. Owen from Wales pioneered concepts like the isoparametric element and nonlinear analysis methods. Zienkiewicz also discovered the serendipity elements: a way to reduce nodes in elements so as to save computational time.

More developments in the field of computational plasticity were largely fuelled by increase in computing power at the time. In 1965, NASA funded the development of NASTRAN, a FEM program with capabilities in two- and three-dimensional stress analyses, beam and shell elements, for analysing complex structures, such as airframes, and analysis of vibrations and time-dependent response to dynamic loads. John Swanson in 1969 then developed the ANSYS, which had both linear and non-linear capabilities and became widely used.

In 1978, a company called HKS went on to develop the program ABAQUS which solves both linear and non-linear problems, and also allowed users to add new material models and elements. ABAQUS and ANSYS are widely used among researchers in the fields of fluid dynamics and Stress analysis. Modern FEM software, which are mostly commercial, have Computer Aided Design databases to assist the users to create the material geometry. With the help of translators, Finite element meshes can be generated from CAD databases in these applications. These translators can also generate finite element meshes from digitisations of surface data. A typical view of a modern day Abaqus interface incorporating a CAD database is shown in Figure 1.23.

FEM was developed as a result of pre-existing numerical methods such as the Finite Difference method and the matrix method of solving continuum and discrete systems respectively. Such methods were much developed thanks to contributions from engineers and mathematicians. Understanding and innovations in continuum mechanics also prepared an adequate adaptability of FEM to the discretization of continua. A summary of the developments taken from Zienkiewicz,1969 is shown in Figure 1.24.

FEM analysis applied to the study of the stress transmission in the corrugated sheet slab
Master of Civil Engineering, defended by: MBOH HELBERT SHAYEH, NASPW, Yaoundé, 2019/2020

27
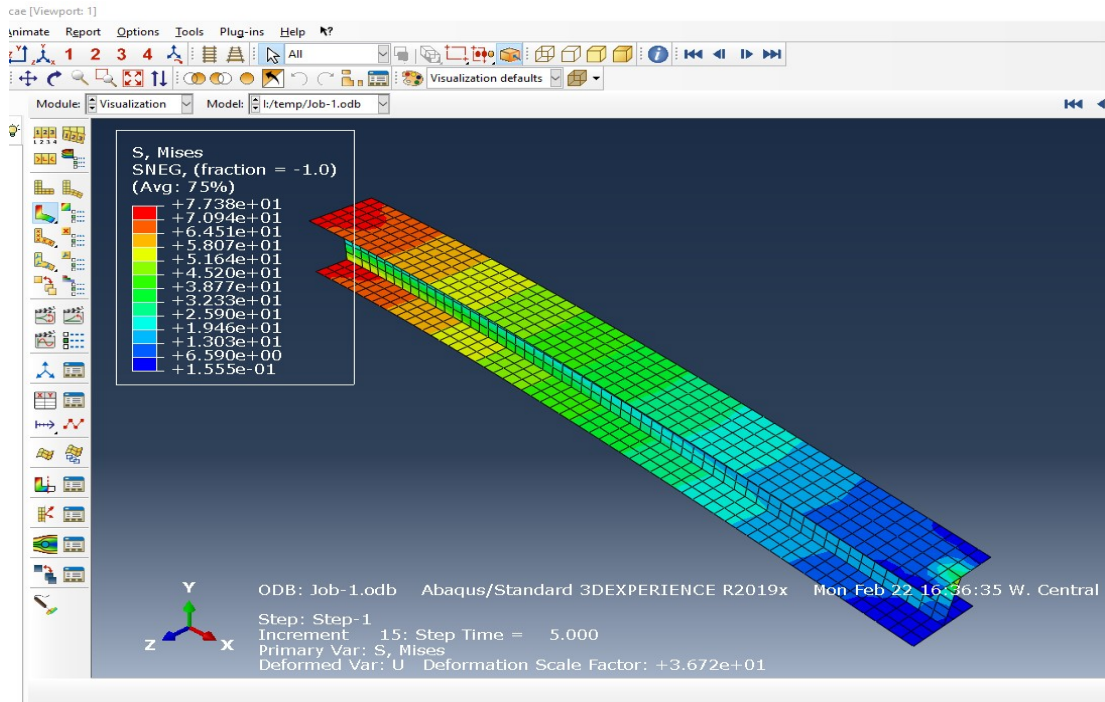
Figure 1.23. Typical view of a modern day Abaqus interface incorporating a CAD database (Abaqus/CAE)
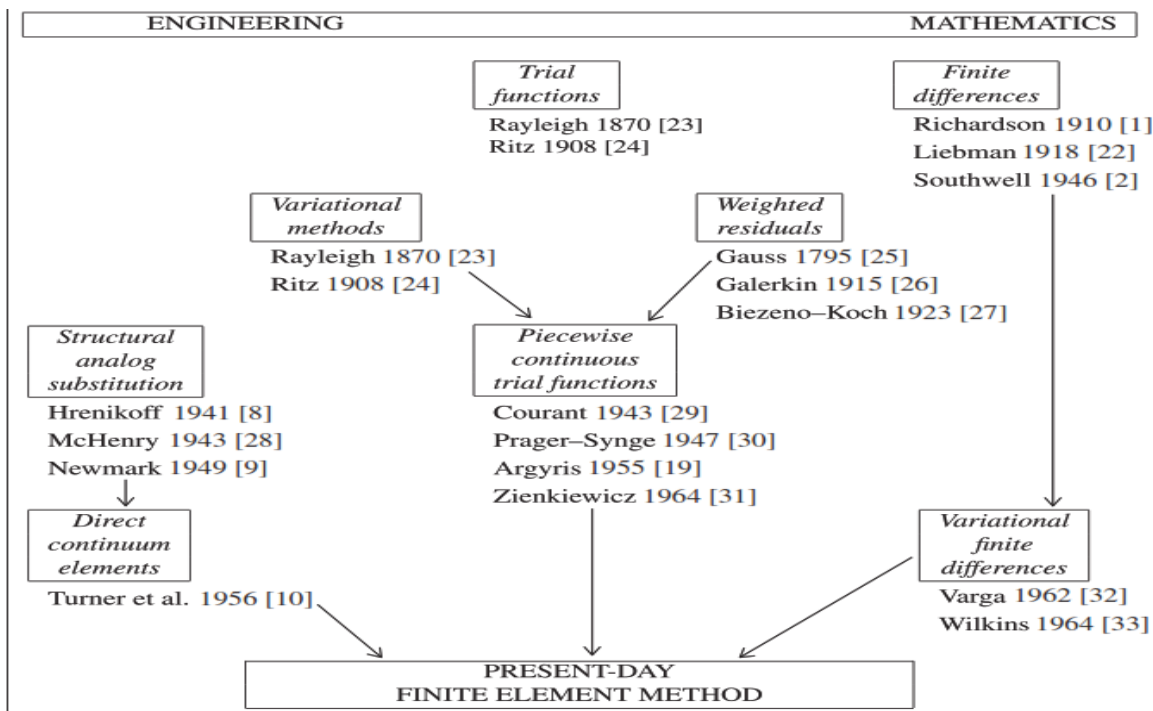
Figure 1.24. A history of approximate methods for FEM (Zienkiewicz,1969)

FEM analysis applied to the study of the stress transmission in the corrugated sheet slab
Master of Civil Engineering, defended by: MBOH HELBERT SHAYEH, NASPW, Yaoundé, 2019/2020

28

1.4.3. Finite Element in 3D Structural problems

Engineering problems are usually large and complex and require full three-dimensional representations of material behaviour and element geometries. The finite element method provides possibilities to solve such numerical problems by first allowing correct mathematical interpretations to be made of the problem. The appropriate 3 – dimensional elements are then conferred to the system, depending on the desired stress analysis the user wishes to perform.

Reinforced concrete structures are commonly designed to satisfy criteria of serviceability and safety. In order to ensure the serviceability requirement, it is necessary to predict the cracking and the deflections of RC structures, in our case the concrete slab of the composite floor. In order to assess the margin of safety of RC structures against failure an accurate estimation of the ultimate load is essential and the prediction of the load-deformation behaviour of the structure throughout the range of elastic and inelastic response is desirable.

For the analysis of Composite beams, the Timoshenko beam theory is used in the present study (Filip C. Filippou, 2015). Since this theory is well established and widely used in the analysis of beams, attention is focused below on some theoretical aspects of the plate bending problem followed by the finite element implementation of the material models in the analysis of RC beams. Columns likewise beams, are usually modelled as beam elements due to the fact that one dimension is very high compared to the two others. Each end node has six degrees of freedom (three translations and three rotations) in the spatial case and three degrees of freedom (two translation and one rotation) in the planar case. In the analysis of the composite slabs, the Timoshenko plate theory is used, in which it is assumed that the plate thickness is small relative to the dimensions in the x-y plane, which is the plane of the plate. When plates are subjected to in-plane loads the resulting stresses are assumed to be constant through the thickness of the plate and stresses σ_z, τ_{xz} and τ_{yz} are ignored.

The main assumptions of the theory are:

- Transverse displacements are small relative to the plate thickness,
- The stress normal to the mid-surface of the plate is negligible, and
- Normals to the mid-surface of the slab before deformation remain straight, but not necessarily normal to the mid-surface after deformation.

FEM analysis applied to the study of the stress transmission in the corrugated sheet slab
Master of Civil Engineering, defended by: MBOH HELBERT SHAYEH, NASPW, Yaoundé, 2019/2020

29

The deformation field of the problem consists of three components:

$$\{d\} = \{x \quad \vartheta x \quad \vartheta y\}^T \tag{1.10}$$

Where w is the transverse plate displacement normal to the xy plane and x and y are the rotations about the y-and the x-axis, respectively. Expressions for ϑ_x and ϑ_y are not given, as they are out of the scope of this work. The above assumptions are illustrated in Figure 1.25 and Figure 1.26
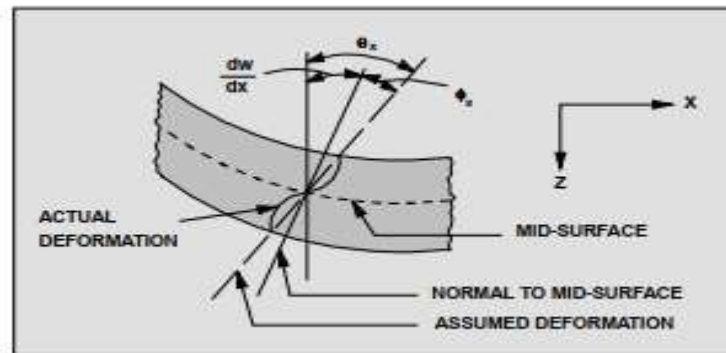
Figure 1.25. Assumed deformation of midline plate theory(F. C. Filippou, 2015)
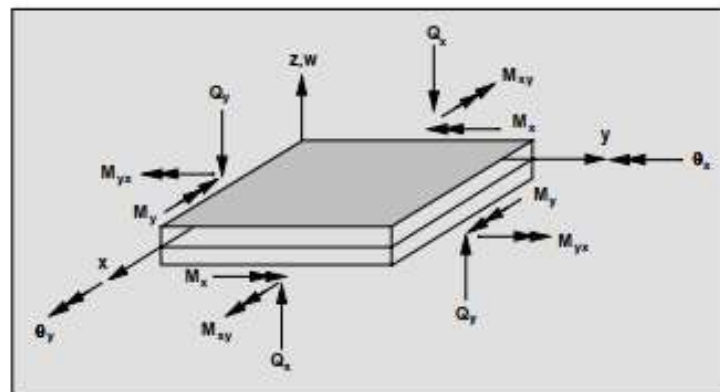
Figure 1.26. Typical Midline plate (F. C. Filippou, 2015)

1.4.4. Common Structural models and the FEM formulation for Multidimensional problems

Analytical solution to physical problems uses weight functions and trial solutions to adopt proper approximations to the system. The trial solutions are values that are true for several points in the domain, while the weight functions are several polynomials that allow for interpolation of the trial solutions to other points in the system. In 1D systems, solving these interpolative partial differential equations is very possible. However, the exact solution to the

FEM analysis applied to the study of the stress transmission in the corrugated sheet slab
Master of Civil Engineering, defended by: MBOH HELBERT SHAYEH, NASPW, Yaoundé, 2019/2020

30

partial differential equations in multidimensional problems is only feasible if the problem has a simple domain with simple boundary conditions. The finite element comes then to solve even problems with complex geometry (domain) that have multiple forms of support or loading (aerodynamic, uniform area loads, concentrated loads).

The trial solutions for FEM calculation are the nodal displacements (for the displacement method of FEM), while several types of approximative polynomials (linear, quadratic, cubic) can be constructed to properly represent the interpolations. These polynomials are usually built from the Pascal's 2D or 3D triangles (fig). The condition for a correctness of the polynomial are completeness and continuity. The blend of both results in the existence of shape functions. For each type of element, the corresponding shape functions have two basic properties that ensure C^0 continuity and completeness:

-   They have the Kronecker delta property. Each shape function is 1 at the corresponding node and zero at the other nodes

-   They are themselves C^0 continuous. This ensure convergence.
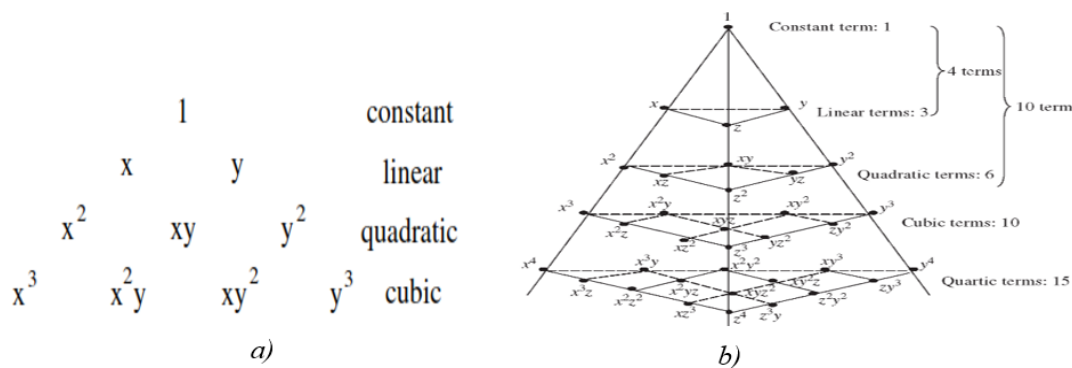
Figure 1.27. Pascal's triangle (a) and Pascal's tetrahedron for approximations of trial solutions for 2D and 3D elements

These two properties ensure that shape functions can be used as interpolants to find displacements at other points in the system, according to equation(1.11);

$$u(x, y, z) = \boldsymbol{N}^e \cdot \boldsymbol{u}^e = \sum_{i=1}^{n_{nodes}} N(x, y, z)_i u_i \qquad (1.11)$$

Where $\mathbf{N^e}$ is the matrix of the element shape functions, $\mathbf{u^e}$ is the nodal displacement matrix and n_{nodes} is the number of nodes in the element.

FEM analysis applied to the study of the stress transmission in the corrugated sheet slab
Master of Civil Engineering, defended by: MBOH HELBERT SHAYEH, NASPW, Yaoundé, 2019/2020

31

For the global system:

$$u(x, y, z) = \sum_{e=1}^{n_{ele}} N^e \cdot u^e = \left(\sum_{e=1}^{n_{ele}} N^e L^e \right) u = N \cdot u \qquad (1.12)$$

Where **N** is the global stiffness matrix, **L^e** is the gather matrix for each element assembly and **u** is the global displacement vector. The strain of the element is the gradient of the displacement as shown in equation (1.13).

$$\varepsilon(x, y, z) = \nabla^s u(x, y, z) = \nabla^s N(x, y, z) \cdot u = Bu \qquad (1.13)$$

where $B = \nabla^s N$ is the matrix of the scalar gradient of the shape function matrix in each direction of the system. Hence through calculation of strains is made possible through the shape functions and the nodal displacement.

As for a body that is constrained, with a global domain, Ω, the Principle of Virtual work says that the energy is conserved for a virtual displacement, η in the virtual domain, $\mathcal{M}$, when the body is subjected to real surface forces **t** on the surface domain, $\delta\Omega_t$, and real volume forces **b.** This principle can be explained in equation (1.14)

$$\int_\Omega [\sigma(\nabla^s u) : \nabla^s \eta - b.\eta] dv - \int_{\delta\Omega_t} t.\eta \, da = 0 \; \forall \eta \; \varepsilon \mathcal{M} \qquad (1.14)$$

The FE analysis of structures with this method depends on the linearity or nonlinearity of the stress-strain law. For elastic linear problems, the stress is solely dependent on the strain. This then makes the stress also related to the shape functions and the nodal displacements as shown in the equation above. The virtual displacement can be calculated from linear combinations of shape functions with nodal virtual displacements.

$$\sigma = D \cdot \varepsilon = DBu \qquad (1.15)$$

where D is the constitutive modulus matrix. The result of this reasoning is the final equation

$$\left\{ \int_\Omega [B^T \cdot \sigma - N^T \cdot b] dv - \int_{\delta\Omega_t} N^T \cdot t da \right\} \eta = 0 \; \forall \eta \; \varepsilon \mathcal{M}$$

$$=> \left[\int_\Omega B^T DB dv \right] u = \int_\Omega N^T \cdot b dv - \int_{\delta\Omega_t} N^T \cdot t da$$

FEM analysis applied to the study of the stress transmission in the corrugated sheet slab
Master of Civil Engineering, defended by: MBOH HELBERT SHAYEH, NASPW, Yaoundé, 2019/2020

32

$$\Rightarrow \qquad \boldsymbol{Ku} = \int_{\Omega} \boldsymbol{N^T} \cdot \mathbf{b} \mathrm{dv} - \int_{\delta\Omega_t} \boldsymbol{N^T} \cdot \boldsymbol{t} \mathbf{da} \qquad (1.16)$$

Where $\boldsymbol{K} = \left[\int_{\Omega} \boldsymbol{B^T} \cdot \boldsymbol{\sigma} \mathrm{dv} \right] = \left[\int_{\Omega} \boldsymbol{B^T DB} \mathrm{dv} \right]$, is the stiffness matrix for the element. The global stiffness matrix is obtainable by assembly of the element stiffness matrices using a gather matrix labelled L^e

For nonlinear analysis, the stress doesn't only depend on the strain. Hence more parameters are needed to predict the evolution of the stresses. Usually they are solved by linearization of the incremental stress updating procedure, as emphasized by Nagtegaal (1982).

1.4.5. FEM studies on stress transfer in corrugated sheets

Scientist aiming to understand slab behaviour or to simplify the design of composite slabs have produced much material to further develop the slab circumstances. A few of the important researches are reported in this section.

1.4.5.1 Daniels and Crisinel

Daniels and Crisinel developed a special purpose FE procedure using plane beam elements for analysing single and continuous span composite slabs. The procedure incorporated nonlinear behaviour of material properties, additional positive moment reinforcement, the load-slip property for shear studs (obtained from push tests commonly used for welded shear studs), and the shear interaction property between the concrete and the steel deck obtained from pull out test developed by the authors, see section 2.3.5. A ductile load-carrying mechanism was employed in the model, neglecting the brittle portion of the push test data. The compressive stress-strain behaviour of the deck was specified differently from the tensile behaviour where the relationship was estimated from flexural tests on bare deck. In their study, the maximum load capacities for models with different span lengths were shown to lie along the straight line if plotted on the m-k axes (see the m-k method in Sec. 4.4) but fell outside the same straight line if the steel thickness is changed(Crisinel and Marimon, 2004).

1.4.5.2 An (1993)

An was the first to propose the use of bending tests in the determination of the shear bond property of composite slabs. The parameters studied included the concrete type (normal and light weight concrete) and the shear span to depth ratio. The test results were used as input in

FEM analysis applied to the study of the stress transmission in the corrugated sheet slab
Master of Civil Engineering, defended by: MBOH HELBERT SHAYEH, NASPW, Yaoundé, 2019/2020

33

the finite element analysis. Two types of test setups were employed. The first shown in Figure 1.28(a) had the steel sheeting in direct contact with the support so that the effect of frictional force on the slip resistance could be studied. The second setup shown in Figure 1.28 (b) did not have the steel in direct contact with the support, thus was used to obtain the shear strength without support friction. The shear stress was determined by calculating tensile force in the sheeting using analytical methods. The results were verified with the strain in the sheeting whose values were measured during the test. The shear resistance of specimen with the sheeting extended into the support was found to be 20-30% higher than that without sheeting. This clearly indicated the presence of shear resistance at the support(Li An and Krister Cederwall, 1994).
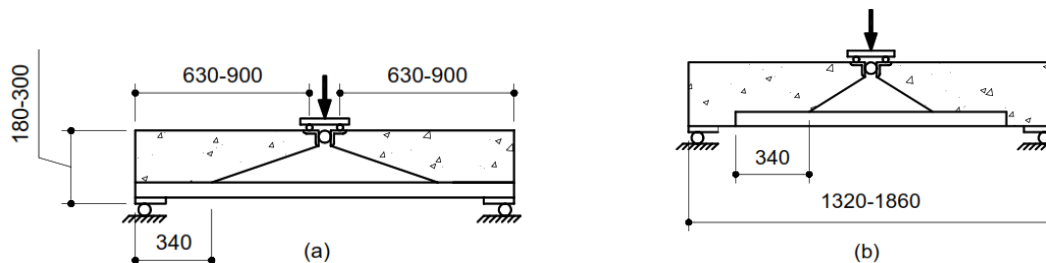
Figure 1.28. Block bending test by An (1993)

An later studied the behaviour of composite slabs with 2D nonlinear FE using the ABAQUS/Standard module. The steel sheeting and the concrete were modelled as 2-node Timoshenko beam elements. The interaction between the steel sheeting and the concrete slab was modelled with spring elements plus a set of imposed equations between degrees of freedom of concrete, spring and steel deck beam elements. The spring property was obtained from a block bending test. A smeared crack model was used for concrete cracking, while a nonlinear stress-strain curve was used for the steel deck and concrete in compression. The force slip relationship to simulate separation behaviour between concrete and steel deck in the vertical direction was assumed as linear elastic and was also modelled with spring elements. The FE results were found to be in good agreement with full-scale tests for long slabs but underestimated the capacity of the short slabs (An Li, 1993).

FEM analysis applied to the study of the stress transmission in the corrugated sheet slab
Master of Civil Engineering, defended by: MBOH HELBERT SHAYEH, NASPW, Yaoundé, 2019/2020

34

1.4.5.3 Veljkovic (1996)

Veljkovic (1996a, 2000) studied the behaviour of composite slabs using the finite element (FE) method. The parameters used in the FE model were mechanical interlocking (shear bond-slip) resistance, the friction coefficient and a reduction function. These parameters were obtained from three types of elemental tests, namely the push test (Figure 1.29a), slip block test, and tension-push test (Figure 1.29b). The push test was used to obtain the mechanical interlocking resistance. The slip block test was used to determine the friction coefficient at supports. The tension-push test was used to determine the reduction function of the shear bond strength. From the tension-push test, Veljkovic found that tensile strain could stretch and flatten the embossments which in turn would lower the shear bond resistance and increase the corresponding slip. Hence a reduction function was established to make a correction to the mechanical interlocking resistance obtained from the push test.

To achieve a correct simulation, a function was used to reduce the interfacial shear stress level during the analysis depending upon the strain level in steel sheeting. This modification is clear evidence regarding the need for variable shear interface properties when dealing with variable geometry models. If an automatic reduction function was not included in the FE package, the FE analysis conducted this way requires user intervention to modify the interface property several times along the analysis process. With so many tests to be conducted, the process of conducting FE analysis in this manner would require significant additional effort (Veljkovic, 1996).
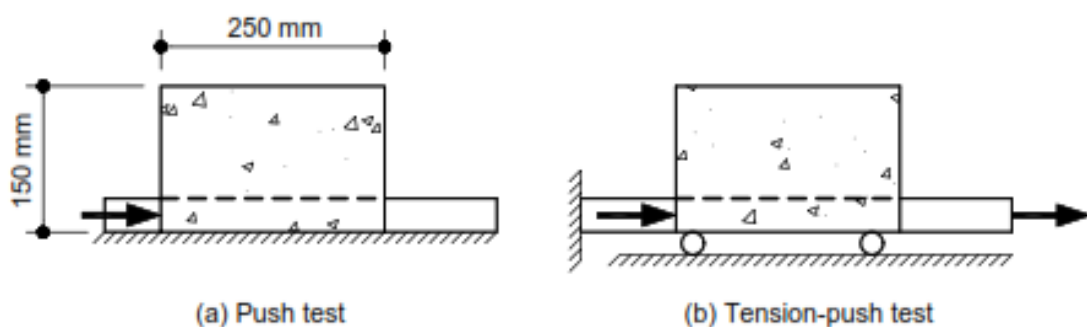
Figure 1.29. Push test and Tension-push test by Veljkovic (1995)

FEM analysis applied to the study of the stress transmission in the corrugated sheet slab
Master of Civil Engineering, defended by: MBOH HELBERT SHAYEH, NASPW, Yaoundé, 2019/2020

35

1.4.5.4 Jawed Qureshi, Dennis Lam and Jianqiao Ye

A three-dimensional finite element model is developed, validated and used in the parametric study to investigate the influence of shear stud's position and profiled sheeting thickness on the strength, ductility and failure modes of the headed shear stud welded to the modern profiled sheeting. A total of 240 push tests were analysed with different sheeting thicknesses, positions of the shear stud in the trough, concrete strengths and transverse spacings. The results showed that the sheeting thickness influenced the shear connector resistance of studs placed in the unfavourable position more than studs placed in favourable and central positions. The strength of the shear connector placed in the unfavourable position increased by as much as 30% when the sheeting thickness was increased. The shear connector resistance of the unfavourable stud was found to be primarily a function of the strength and the thickness of the profiled sheeting rather than the concrete strength. The strength prediction equations for unfavourable and central studs were also proposed. The results suggested that the strength of the shear connector increased as the distance of the shear stud increased from the mid-height of the deck rib in the load-bearing direction of the stud. The load–slip behaviour of the studs in the unfavourable position was more ductile than the studs in the favourable position, with the slip 2–4 times higher. It was found that the increase in sheeting thickness and transverse spacing improved the ductility of the stud in an unfavourable position, but had no effect on the stud in the favourable position. The failure modes suggested that the favourable and central studs failed by concrete cone failure and unfavourable studs failed by rib punching together with crushing of the narrow strip of the concrete in front of the stud (Qureshi, Lam and Ye, 2011).

1.4.5.5 Redzuan Abdullah

Abdullah obtained the shear stress - end slip curves of the slab experimentally by bending tests carried out on small-scale slab specimens and full-scale slab. Bending tests were preferred to push tests for the elemental tests because the effect of bending, end support and curvature are important to the shear behavior of the interfacial layer. The small-scale bending tests proved to give accurate results for shear bond behavior of the full slab (Abdullah and Easterling,2007). This method allowed for the construction of approximate shear bond curves for a composite

FEM analysis applied to the study of the stress transmission in the corrugated sheet slab
Master of Civil Engineering, defended by: MBOH HELBERT SHAYEH, NASPW, Yaoundé, 2019/2020

36

slab from the curves of other slabs, provided their sheets are of the same profile shape and thickness and also that the material properties are similar.

Abdullah and Samuel Easterling (2009) demonstrated, using the force equilibrium method and solving from the relation of longitudinal resistance from the m-k method, that the shear stress in the steel concrete interface of the slab depends on the sheet thickness, t, the slab depth, d, and the shear span, Ls, through the relation of equation (1.17).

$$\tau d = p \frac{td}{L_s} + s \qquad (1.17)$$

where p and s are constants whose values depend on the shape of the deck. The ratio Ls/d was called the slab slenderness and varied inversely with the longitudinal shear stress according to the above equation.

The author then suggested this method as an improved PSC and proposed that slabs of similar profile and sheet thickness may have their shear bond behavior constructed from the shear bond curves of slabs of other slenderness, reducing the number of elemental tests necessary for each slab.

Data from the elemental bending test can be used not only in the existing analytical methods but also in the numerical analysis. In the numerical analysis, the shear bond behaviour, was converted to nonlinear spring force-extension that was assigned to connector elements assigned to the steel-concrete interfacial layer as a function of the area, available in ABAQUS. A quasi-static analysis was then performed using ABAQUS/Explicit to achieve results for the force-displacement of the slab under increasing imposed loads in a set up similar to the elemental test presented in section 1.2. The concrete was modelled with Brittle cracking and the steel sheet as perfectly plastic. The details of the analysis were reported in (Abdullah, 2004). The improved PSC design procedure is found to be comparable with the m-k method (Abdullah and Easterling, 2011).

1.4.5.6 V.V. Degtyarev (2014)

This paper describes results of a study on strain and stress distribution in compact and slender composite deck slabs using nonlinear three-dimensional finite element models. The slabs were modelled as flexural members made of steel deck units and structural concrete

FEM analysis applied to the study of the stress transmission in the corrugated sheet slab
Master of Civil Engineering, defended by: MBOH HELBERT SHAYEH, NASPW, Yaoundé, 2019/2020

37

fillings interconnected at the interface with nonlinear springs representing bond between two materials. The models are capable of accounting for partial interaction between the deck and the concrete, discrete concrete cracking in the slab tension zone, and nonlinear behaviour of the materials and the interface.

The partial interaction was modelled by nonlinear springs assigned between the nodes of the sheet and the nodes of the slab bottom face. The slabs were validated against published test data and have proved to be effective in predicting load-deflection responses of composite deck slabs. The study showed that the strain and stress distributions are greatly affected by concrete cracking and slip between the deck and the concrete. The study provides information that may be useful in understanding composite slab behaviour and in developing analytical models for predicting slab strength and stiffness.

1.4.5.7 Noémi Seres and László Dunai

The subject of the ongoing research work was to analyse the composite action of the structural elements of composite floors by experimental and numerical studies with a special focus on the rolled embossments on the steel surface. The mechanical and frictional interlocks result in a complex behaviour and failure under horizontal shear. This is why the design characteristics can be determined only by standardized experiments. The aim of the current research is to determine the longitudinal shear resistance for composite floors, by applying advanced numerical model. The paper has a focus on the basic numerical models with particular considerations on the concrete model and on the numerical model of rolled embossments(Seres and Dunai, 2011) .

Conclusion

All through this chapter, the aim was to present previous studies and analyses performed on the numerical modelling of corrugated sheet slabs using the Finite Element Method. The corrugated sheet slab was reintroduced and specifics were given as to the variation of profile shapes and the participation of the slab components. Above all, the principle of composite action in the composite slab was presented, with special mention to the shear bond mechanism of slab action. Current experimental methods of composite slab design were presented to show the enormous effort required in these tests and to show those that are adopted in most national and international building codes. The basics and history of the finite element method were

FEM analysis applied to the study of the stress transmission in the corrugated sheet slab
Master of Civil Engineering, defended by: MBOH HELBERT SHAYEH, NASPW, Yaoundé, 2019/2020

38

presented, with special mention to the challenges of correct approximation of real behaviour by the FE models. This concept was extended to the field of designing corrugated sheet slabs, where early endeavours to simplify the slab design was mentioned, through semi-empirical methods and fully numerical methods. In the already existing numerical research formulated by earlier works, the special concern was found to be a good representation of the shear bond between the concrete and steel sheet in the slab. Extensive work by Abdullah and Easterling (2003,2007,2009)

FEM analysis applied to the study of the stress transmission in the corrugated sheet slab
Master of Civil Engineering, defended by: MBOH HELBERT SHAYEH, NASPW, Yaoundé, 2019/2020

39

CHAPTER 2: **METHODOLOGY**

Introduction

The aim of this chapter is to develop a FE model for a composite slab subjected to a shear bond test, like the m-k test. The method of representing the slab shear behaviour proposed by Abdullah and Easterling (2009) is implemented. As a result, a steel deck tested by Abdullah and Easterling (2007) was used in the design of a composite slab for a G+3 building according to the European norms. The building is presented in this chapter, alongside the generalities of composite slab design according to EC4 and the details of the FE model (elements, material, boundary conditions) for the composite slab. The implementations of these general guidelines will be presented in the next chapter.

2.1. **General procedure**

The steel building is presented and the actions on the structure are discussed, after which the calculations of the actions and the load combinations are detailed.

2.1.1.Presentation of the structure.

The Structure is a three-storey steel frame with composite flooring to serve as an office building. The building floor is rectangular, of length 18.9m and width 17.5m, with a total thickness of 13.0cm, The floor is a one-way floor spanning 3.5m between the steel beams as illustrated in Figure 2.2. The total height of the building is 12.5m, with a 3.5m high ground floor and 3m storey heights. It is classified as a Category B building due to its intended office use and also due to its regular structure with no elevation setbacks.
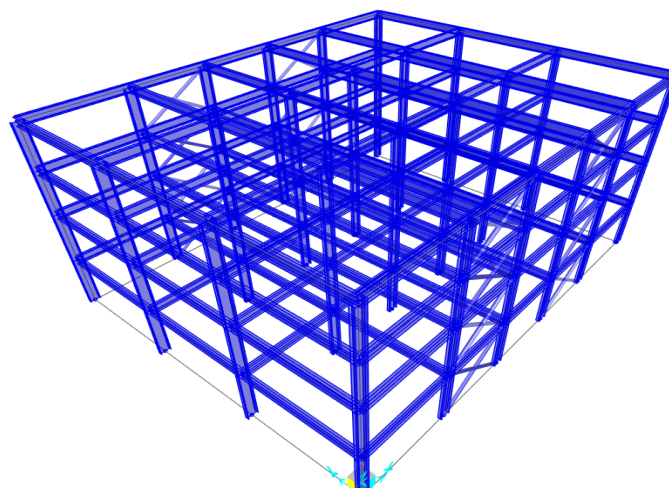
Figure 2.1. A 3D model of the building structure

FEM analysis applied to the study of the stress transmission in the corrugated sheet slab
Master of Civil Engineering, defended by: MBOH HELBERT SHAYEH, NASPW, Yaoundé, 2019/2020

40

Due to convenience with the FEM analysis to be latter done, the sheets for the composite floors are the 76mm deep VL trapezoidal profiles used by Abdullah (2004,2007) in shear bond experiments. The geometrical characteristics of these sheets, alongside the material properties for the slab concrete and the steel sheet are presented in Table 3.2 of chapter 3.

Eurocode 4 expresses several basic dimensions that are to be presented for the composite slab. They include the slab thickness, the width of the ribs, the depth of the sheet, the sheet thickness, the depth to the neutral axis of the sheet amongst other parameters illustrated in Figure 2.3 and reported in the following chapter (Table 3.1). These dimensions help in the calculation of the self-weights and resistances to moment and shear. To reduce calculation on the part of the designer, sheet manufacturers usually provide as well the resistant moment of the sheet in hogging and in sagging.
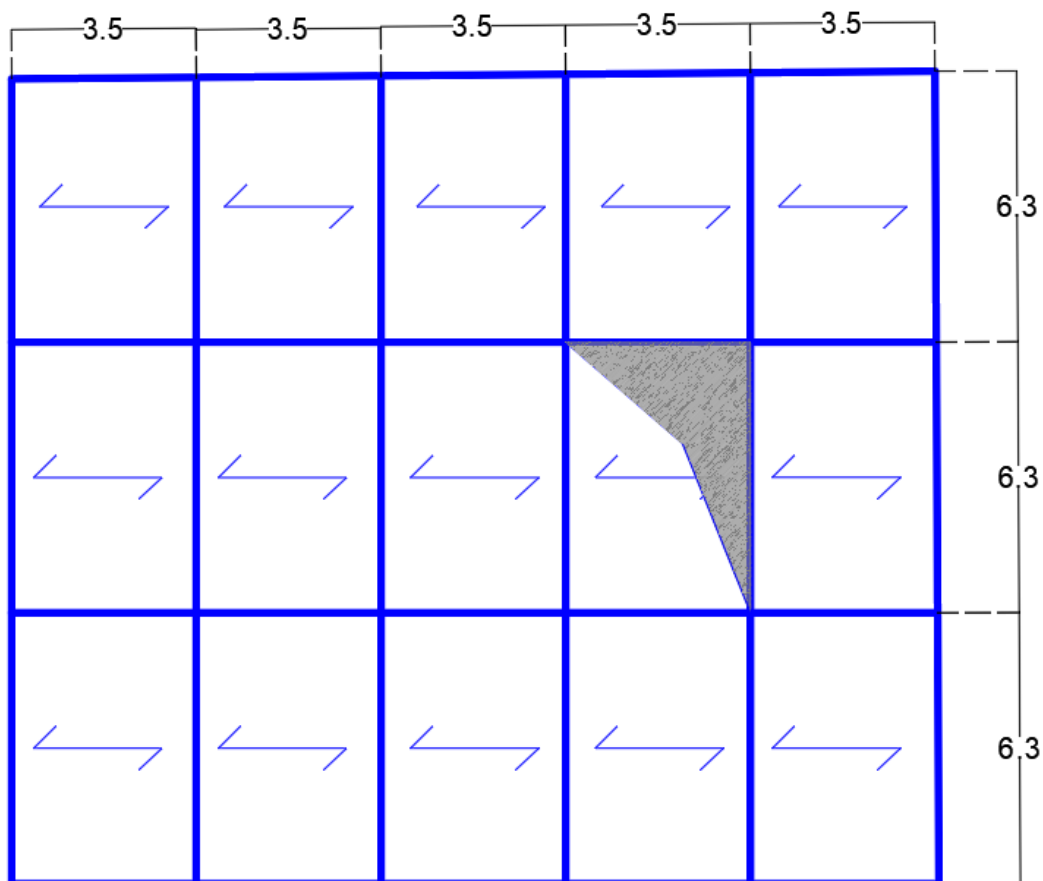
Figure 2.2. Floor plan of the structure (dimensions in m)

FEM analysis applied to the study of the stress transmission in the corrugated sheet slab
Master of Civil Engineering, defended by: MBOH HELBERT SHAYEH, NASPW, Yaoundé, 2019/2020

41

open trough profile
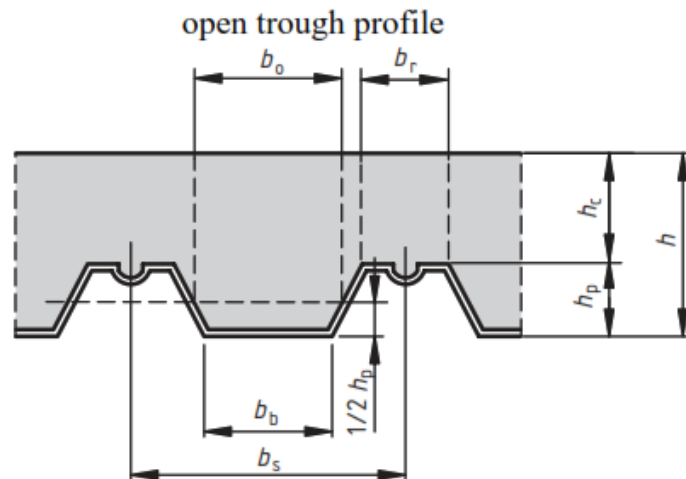
Figure 2.3. Required data for composite slab according to EC4

2.1.2. Evaluation of the actions on the building

During the nominal life of a building, the main actions that act on the building have to be considered in the building design. The European codes EN 1991 separates these actions into categories depending on their frequency: permanent actions and live actions.

2.1.2.1 Permanent actions

The structural loads (G1) are the self-weights of elements that bear the loads on the structure, while the non-structural (G2) loads are self-weights of non-resisting components. Each of these loads are discussed in this section.

a. Steel sheet self-weight

The corrugated sheet at every stage of the building design resists the loads on the slab. The self-weight of sheets is mostly contained in the manufacturer documentation as a uniformly distributed area load. For slab design, the load will be converted to a linear load after multiplying by the width of the slab portion that is to be designed.

b. Concrete self-weight

During the construction phase of the building, the concrete is considered non-structural as it has not yet achieved its strength during curing. The concrete becomes a structural component during the service stage of the building as has already achieved its full strength. The wet concrete unit weight specified by Eurocode 1 is 25 KN/m^3 while the dry concrete unit weight is 24KN/m^3. An additional 1KN/m^3 is added if the concrete is reinforced. This weight is

FEM analysis applied to the study of the stress transmission in the corrugated sheet slab
Master of Civil Engineering, defended by: MBOH HELBERT SHAYEH, NASPW, Yaoundé, 2019/2020

42

converted to a uniformly distributed linear load on the slab by multiplying by the cross-sectional area of the concrete in the design width. For the beam design, it is multiplied by the effective width of the concrete flange

c. Non-structural permanent loads

These loads include the weight of floor finishes, non-structural partition walls, ceiling installation and services. The characteristic geometry used to calculate the linear loads of all the aforementioned weights is summarized in Table 2.1.

2.1.2.2 Variable or life actions

The variable actions are not prevalent in the structure and the values assigned to them are based on good engineering practice. The variable actions for composite buildings include:

d. Construction loads

EN 1991-1-6 suggests a minimum construction load of 1.5 KN/m^2 over the slab area as for these loads.

e. Imposed loads

Imposed actions or service loads are loads due to the use of the building by occupants or related installations. EN 1991-1-1 suggests several ranges of loads to be used on the building based on its category of use. In the case of our office building (Category B), imposed loads are between 2.0 and 3.0 KN/m^2.

2.1.1. Combination of actions

The permanent and variable actions for each stage of the structure's nominal life were combined in certain specific ways as prescribed by EN1991 to obtain the loads for verifying the resistance and functionality of the structural elements according to Equation (2.1).

$$P = \gamma_g * (G_1 + G_2) + \gamma_q * \Psi_{m1} * Q_1 + \sum_{i=1}^{n} \Psi_{mi} Q_{mi} \qquad (2.1)$$

FEM analysis applied to the study of the stress transmission in the corrugated sheet slab
Master of Civil Engineering, defended by: MBOH HELBERT SHAYEH, NASPW, Yaoundé, 2019/2020

43

Table 2.1. Summary of all actions on a composite building

Action	Type	Significant characteristic geometry	Stage in nominal life
Sheet	Permanent	slab width	Both
Wet reinforced concrete		Area of cross-section	Construction
Dry reinforced concrete		Area of cross-section	Composite
Structural beam		Area of cross-section	Both
Finishes		thickness	Composite
Non-structural partition walls		Slab width	Composite
Ceiling and services		Slab width	Composite
Imposed loads	Variable	Slab width	Composite
Construction loads		Slab width	Composite

2.1.1.1 Ultimate limit state

Where G_1 and G_2 are the non-structural and structural permanent loads, Q_1 is the dominant variable load while Q_i are the non-dominant loads. γ_g and γ_q are the load combination factors, of values 1.0 and 0 in favourable conditions and 1.3 and 1.5 in unfavourable situations according to EN 19991.

2.1.1.2 Serviceability limit state

For non-reversible Serviceability Limit State (SLS), the rare combination is applied for the verifications with allowable stress method.

$$P = (G_1 + G_2) + Q_1 + \sum_{i=1}^{n} \Psi_{mi} Q_{mi} \tag{2.2}$$

2.2. **Static design methodology**

The static design is done based on the static analysis. Static analysis studies the behaviour

FEM analysis applied to the study of the stress transmission in the corrugated sheet slab
Master of Civil Engineering, defended by: MBOH HELBERT SHAYEH, NASPW, Yaoundé, 2019/2020

44

of the structure under static loads application. The analysis starts with the modelling of the slab and the beam.

2.2.1.Slab design

The composite slab was designed according to the European norms, by considering the construction (non-composite) and composite stages during and after erection of the structure according to EN 1994-1-1, EN 1992-1-1, EN 1993-1-5 and EN 1993-1-3 for the composite design, the concrete design and the steel section design respectively.

2.2.1.1 Generalities for the slab design

The ideal design of a composite slab is done as a continuous element, however clause 9.4.2(5) of EN 1994-1-1 allows that the slab be designed as a series of simply supported slabs. The design of a composite slab depends on whether it is propped or unpropped during the construction stage. The unpropped slab was chosen in this project, as it is mostly used due to the quicker construction it allows as time for placing of props is spared, although with limits to the span. The resistance of the slab to longitudinal shear forces will be calculated depending on the deck characteristics provided by its manufacturer. These values may be the m,k stresses or the percentage partial connection if the slab was designed using the m-k method or the partial connection method respectively.

The necessary geometrical and mechanical characteristics of the steel sheet are provided in Table 3.2.The resistances for the sheet and the composite slab were done according to EN 1993-1-3/5 and EN 1994-1-1 respectively. Below shall be presented the global and local resistances of the sheet and slab as calculated in accordance with the aforementioned design codes.

2.2.1.2 Corrugated sheet verifications according to EC3

Cold formed sheets have to be verified for specific load conditions, inherent with their condition of use and their geometry. The corrugated sheet slab is considered according to EN 1993-1-3/5 as a profiled sheeting with two or more unstiffened webs. Several things have to be verified for such sheets according to EN 1993-1-3/5. However, there is a precision as to the effective area of the sheet section, and the effective section modulus, necessary to calculate resistant forces and moments in the section.

FEM analysis applied to the study of the stress transmission in the corrugated sheet slab
Master of Civil Engineering, defended by: MBOH HELBERT SHAYEH, NASPW, Yaoundé, 2019/2020

45

a. Effective Area of the sheet

The effective area of a profile sheet is calculated so as to ensure that all the section undergoes axial compression, or to account whether its geometry renders some parts unresponsive to loads because they have already buckled. This can also be caused by the phenomenon known as shear lag. Shear lag occurs when some elements of the cross section are not connected, as when only one leg of an angle is bolted to a gusset plate (William , 2012).
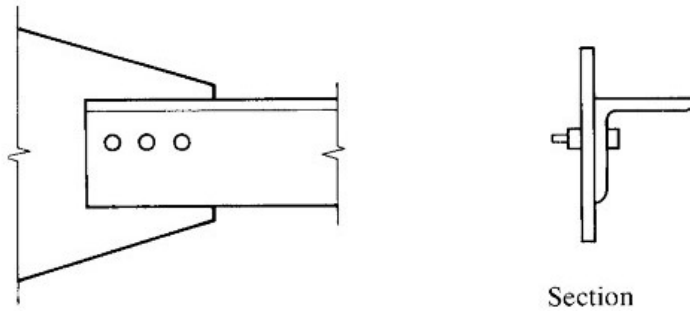
Section

Figure 2.4. Shear lag in angled sections connected at one leg

In plate elements however, shear lag is less likely than plate buckling. Hence only plate buckling is considered when calculating the characteristics of the effective section. The effective area is calculated as a coefficient of the actual area. The coefficient, ρ ,depends on the slenderness of the plate λ_p and calculated according to EN 1993-1-5 as:

$$\rho = \begin{cases} 1.0 & for\ \lambda_p \leq 0.673 \\ \dfrac{\lambda_p - 0.055(3 + \psi)}{\lambda_p{}^2} \leq 1.0 & for\ \lambda_p > 0.673 \end{cases} \qquad (2.3)$$

$$\lambda_p = \sqrt{\frac{f_y}{\sigma_{cr}}} = \frac{\frac{b}{t}}{28.4\varepsilon\sqrt{k_\sigma}} \qquad (2.4)$$

Where b is the member width (flange or web)

t   is the thickness

$\varepsilon = \sqrt{(235/f_y)}$

k_σ is the buckling factor corresponding to the stress ratio ψ and boundary conditions. ψ is usually equal to 1, making k_σ equal to 4.0 according to Table A2 of Annex A.

b. Ultimate limit state checks

FEM analysis applied to the study of the stress transmission in the corrugated sheet slab
Master of Civil Engineering, defended by: MBOH HELBERT SHAYEH, NASPW, Yaoundé, 2019/2020

46

The common ultimate limit state checks for the profiled sheet according to Eurocode 3 are described in this section.

i.   The shear resistance of the sheet

The resistance of the web to shear is calculated as recommended by EN 1993-1 in terms of the web height between the flanges (h_w), the slope, ϕ, of the web relative to the flanges, the shear buckling strength, f_{bv}, of the web and its thickness, t.

$$V_{b,rd} = \frac{\frac{hw}{sin\emptyset} * t * f_{bv}}{\gamma_{mo}} \qquad (2.5)$$

f_{bv} depends on the relative slenderness of the web λ_w and the yield strength of the steel, f_{yb}, as shown in Table A2 of Annex A. For webs with no longitudinal stiffeners, EN 1993-1-3 recommends equation (2.6) to calculate the relative slenderness in terms of the slant height, s_w of the web. The slant height is the distance between the midpoints of the corners of the flanges as demonstrated in Figure 2.5.

$$\overline{\lambda}_w = 0.346 \frac{s_w}{t} \sqrt{\frac{f_{yb}}{E}} \qquad (2.6)$$
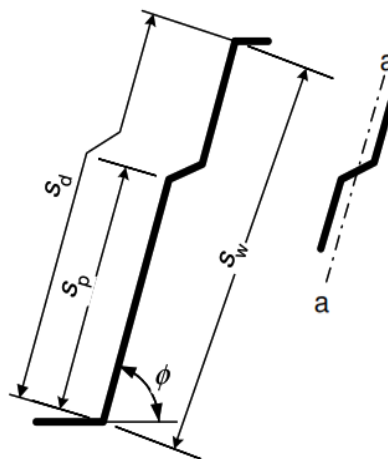
Figure 2.5. A web with a longitudinal stiffener. (EN 1993-1-3)

ii.   The local transverse resistance of the unstiffened webs

FEM analysis applied to the study of the stress transmission in the corrugated sheet slab
Master of Civil Engineering, defended by: MBOH HELBERT SHAYEH, NASPW, Yaoundé, 2019/2020

47

For sheets with 2 or more unstiffened webs, clause 6.1.7.3 of EN 1993-1-3, proposes the verification of the transverse resistance according the relation.

$$R_{w,Rd} = \frac{\alpha t^2 \sqrt{f_{yb} * E}\left(1 - 0.1\sqrt{\frac{r}{t}}\right)\left[0.5 + \sqrt{\frac{0.02 l_a}{t}}\right]\left(2.4 + \left(\frac{\emptyset}{90}\right)^2\right)}{\gamma_{M1}} \tag{2.7}$$

where: h_w is the web height between the midlines of the flanges;

   r is the internal radius of the section corners;

   ϕ is the angle of the web relative to the flanges (in degrees);

   f_{yb} is the yield strength of the steel;

   E is the Young's modulus of steel;

   l_a is the effective bearing length for the relevant category of the support;

   α is the relevant category coefficient. The relevant category (1 or 2) is based on the clear distance, e, between the local load and the nearest support, or the clear distance, c, from the support reaction or local load to a free end. The values for l_a and α according to EN 1993-1-3 are presented in Table A3 of Annex A.

iii.   Combined shear force, axial force and moment

For cross-sections subject to the combined axial force N_{Ed}, bending moment M_{Ed} and shear force V_{Ed}, the following check is required if the shear force is greater than half the shear resistance V_{rd}.

$$\frac{N_{ed}}{N_{rd}} + \frac{M_{y,ed}}{M_{y,rd}} + \left(1 - \frac{M_{f,rd}}{M_{pl,rd}}\right)\left(2\frac{V_{ed}}{V_{w,rd}} - 1\right)^2 \leq 1.0 \tag{2.8}$$

where,

N_{Rd} is the design resistance of a cross-section for uniform tension or compression;

$M_{y,Rd}$ is the design moment resistance of the cross-section provided by the manufacturer;

$V_{w,Rd}$ is the design shear resistance of the web ($V_{b,Rd}$) given in (i) above;

$M_{f,Rd}$ is the moment of resistance of a cross-section consisting of the effective area of flanges only;

$M_{pl,Rd}$ is the plastic moment of resistance of the cross-section.

FEM analysis applied to the study of the stress transmission in the corrugated sheet slab
Master of Civil Engineering, defended by: MBOH HELBERT SHAYEH, NASPW, Yaoundé, 2019/2020

48

iv. **Combined action of bending moment and a transverse force due to local load or a support reaction.**

EN 1993-1-5 proposes the following 3 verifications be made where the maximum bending moment coincides with a support reaction.

$$\left(\frac{M_{Ed}}{M_{c,rd}}\right) \leq 1 \quad , \quad \left(\frac{F_{Ed}}{R_{w,rd}}\right) \leq 1 \; and \; \left(\frac{M_{Ed}}{M_{c,rd}}\right) + \left(\frac{F_{Ed}}{R_{w,rd}}\right) \leq 1.25$$

Where $M_{c,rd}$ is the moment resistance provided by the manufacturer,

$R_{w,rd}$ is the local transverse resistance expressed in (i)au-dessus.

F_{Ed} is the support reaction. For a simply supported slab, this support reaction is equal to the vertical shear force

c. **Serviceability limit state checks**

The deck deflection is the only parameter that is verified for the serviceability limits. The deflection, δ should not exceed 1/180th the slab span expressed in equation. The slab deflection is calculated as for a simply supported slab as shown in equation (2.9) and (2.10).

$$\delta < \frac{L}{180} \tag{2.9}$$

$$\delta = \frac{qL^2}{180} \tag{2.10}$$

2.2.1.3 ULS design of the composite slab

The permanent and variable loads are calculated and combined according to the rare combination proposed by Eurocode 1

$$P_{ULS} = 1.3 * g_k + 1.5 * q_k \tag{2.11}$$

a. **The Construction stage**

In the construction stage, only the steel deck resists the loads which were pre-calculated in section 1.1.3.1. EN 1994-1-1 allows that the continuous slab be dimensioned as simply supported as long as crack reinforcement is provided above the internal supports of the slab.

FEM analysis applied to the study of the stress transmission in the corrugated sheet slab
Master of Civil Engineering, defended by: MBOH HELBERT SHAYEH, NASPW, Yaoundé, 2019/2020

49

The uniform load acting on the sheet is thus calculated by multiplying the area load with the slab width. The design moment and shear force are calculated from the actions by the expressions in (2.12).

$$M_{ed} = P_{ULS} * L2/8$$
$$V_{ed} = P_{ULS} * l/2$$

(2.12)

The moment resistance was verified by ensuring that $M_{ed} < M_{rd}$ as recommended by Eurocode 4. This is supplemented by all the local and global checks for the profiled sheet, mentioned in section 2.2.1.2.

b. The composite stage

As the name suggests, the steel-concrete composite carries the loads during the service stage of the building. The calculations to be done will entail checking for several resistances of the composite section. Wherever the stresses are tensile, only the sheet is considered to resist, as concrete has a low tensile resistance.

The loads at the composite stage of the slab are calculated as indicated in section 2.1.2 above. Clause 9.4.2(5) of EN 1994-1-1 allows the design of the slab as a simply supported span, as long as the minimum reinforcement above the internal supports is provided. This will be assured by the slab choice. The solicitations in such a case then become:

$$M_{ed} = (P_{ULS} * l^2)/8 \text{ and } V_{ed} = (P_{ULS} * l)/2$$

Several checks are then carried out to ensure that the slab will function properly under the given loads.

i. Moment resistance of the section

The design moment of the load condition is checked to be less than the section resistant moment of the composite section. The resistant moment is calculated based on the assumption that the steel yields when the stress in the concrete is at 85% of the design compressive strength.

FEM analysis applied to the study of the stress transmission in the corrugated sheet slab
Master of Civil Engineering, defended by: MBOH HELBERT SHAYEH, NASPW, Yaoundé, 2019/2020

50
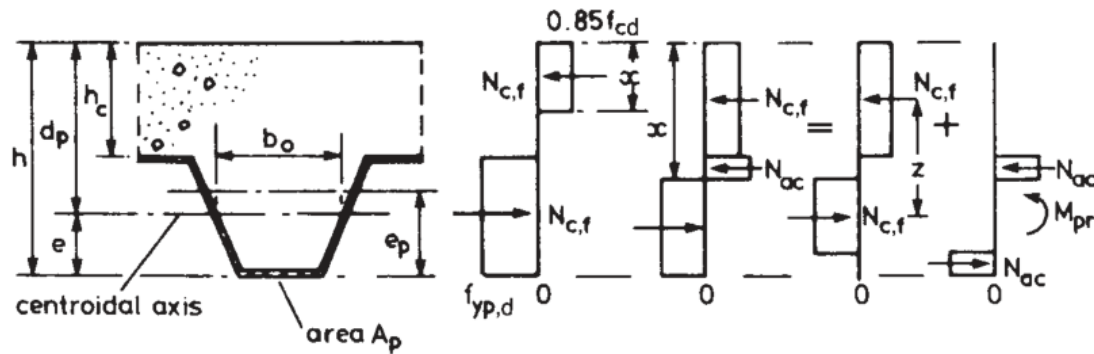
Figure 2.6. Representation of sagging moments in cross section of a loaded composite slab (R.P. Johnson)

From fig. The resistant moment will thus be calculated by the formula:

$$M_{pl,rd} = \min(N_{c,f}, N_p) * z$$

$$z = \left(d_p - \frac{x_{pl}}{2}\right)$$

Where $N_{c,f}$ and N_p are the axial forces to cause crushing in the concrete and yield in the steel; d_p and x_{pl} are the distances to the top of the steel sheet and the plastic neutral axis from the top concrete fibre. Each force is calculated as a product of the area in tension/compression and the tensile/compressive strength

$$N_{c,f} = 0.85 * f_{cd} * hc * b \qquad (2.13)$$

$$N_{p,a} = f_{yp,d} * A_{pe} \qquad (2.14)$$

x_{pl} is calculated by finding the concrete depth over which the two forces $N_{c,f}$ and N_p are equally expressed in the equation. If it is less than the concrete topping thickness, hc, then the neutral axis lies entirely within the concrete. This is usually the case of the study.

$$x_{pl} = \frac{A_{pe} * f_{yd}}{0.85 * f_{cd} * b} \qquad (2.15)$$

However, when $x_{pl} > h_c$, the lever arm for the resistant moment will be calculated by separating the forces into 2 states as shown in fig: a moment created as a result of a balancing tensile force for the compressive force $N_{c, a}$ in the sheet and a moment between the concrete compression and the remaining sheet tensile forces. The equation proposed by Eurocode for the moment resulting in balancing the sheet compressive force was adopted as

$$M_{pr} = 1.25 * M_{pa}\left(1 - \frac{N_{c,f}}{N_{pa}}\right)$$

FEM analysis applied to the study of the stress transmission in the corrugated sheet slab
Master of Civil Engineering, defended by: MBOH HELBERT SHAYEH, NASPW, Yaoundé, 2019/2020

51

This expression was used to develop an expression for the lever arm, z, for the couple between the compression in the concrete and the tension in the steel. Should Nc,f = Npa, then Mpr = 0 which is only possible if Na,c=0. This will mean there is no compression in the steel. Hence xpl = hc and $z = d_p - \frac{hc}{2} = h - e - \frac{hc}{2}$

If Nc,f is too small (weak concrete) Mpr = Mpa. Hence z = h-ep-0.5hc

Hence the linear expression for the lever arm in terms of the ratio Nc,f/Npa is :

$$z = h - 0.5h_c - e_p + \left(e_p - e\right)\frac{N_{c,f}}{N_{pa}}$$

Hence the equation for the lever arm, dependent on the depth of the plastic neutral axis can be summarized by the relation

$$z = \begin{cases} \left(d_p - \dfrac{x_{pl}}{2}\right) & if\ x_{pl} \le h_c \\ h - 0.5h_c - e_p + \left(e_p - e\right)\dfrac{N_{c,f}}{N_{pa}} & if\ xpl > h_c \end{cases} \qquad (2.16)$$

ii. Longitudinal shear resistance

In slabs where no anchoring is performed at the ends of the slab, EN 1994-1-1 demands the longitudinal shear resistance of the composite section be calculated using the m and k values of the sheet according to the equation.

$$V_{l,rd} = \frac{b * d_p}{\gamma_{vs}}\left(\frac{m * A_p}{b * L_s} + k\right) \qquad (2.17)$$

where γ_{vs} is the safety factor of value 1.25, and A_p is the slab section, L_s is the shear span of the slab, usually ¼ the centre-to-centre span of the slab.

iii. Vertical shear resistance

Eurocode 4 permits that the vertical shear design in the slab is carried out according to Eurocode 2 design for concrete beams, with the steel sheet considered as longitudinal reinforcement. The resistant shear force for a concrete beam according to EC2 is calculated by the equation (2.19).

FEM analysis applied to the study of the stress transmission in the corrugated sheet slab
Master of Civil Engineering, defended by: MBOH HELBERT SHAYEH, NASPW, Yaoundé, 2019/2020

52

$$V_{v,rd} = \left\{ C_{rd,c} * k * (1000 * \rho_1 * f_{ck})^{\frac{1}{3}} + k_1 \sigma_{cp} \right\} b_w d \tag{2.18}$$

$$V_{rd,\min} = \left\{ v_{\min} + k_1 \sigma_{cp} \right\} b_w d \tag{2.19}$$

Where $v_{\min} = 0.035 * k^{\frac{3}{2}} \sqrt{f_{ck}}$ is the minimum shear stress in the concrete

$C_{rd,c} = 0.18/\gamma_c = 0.12$

$k = 1 + \sqrt{\dfrac{200}{d}} \leq 2.0$

$k_1 = 0.15$

$\rho_1 = \dfrac{A_{sl}}{b_w d} \leq 0.02$, the effective ratio of reinforcement

A_{sl} is the area of reinforcement with its section extended over a length of $l_{bd} + d$ pf the concrete. $[A_{sl} = A_{pe}]$

b_w is the smallest width of the concrete section in tension $[b_w = \dfrac{b}{bs} * bo]$

d is the effective depth of the reinforcement in the beam $[d = d_p]$

σ_{cp} is the axial stress in the concrete $[\sigma_{cp} = 0]$

The above data was adapted for the composite slab, as the sheet can be considered as tensile reinforcement to the concrete, with the corresponding values in the square brackets. Reinforcement contributes to the resistance only where it is fully anchored beyond the cross-section considered. The sheeting is unlikely to satisfy this condition and hence only the minimum value is used (Johnson, 2004).

$$V_{ED} < V_{rd,\min} = v_{\min} * b * d_p = 0.035 * k^{\frac{3}{2}} \sqrt{f_{ck}} b * d_p \tag{2.20}$$

2.2.1.4 SLS design

The cracking in the concrete can however be verified first before specifying the verifications at the composite stage and the construction stage.

a Crack control

As the slab was designed as continuous, crack reinforcement was to be provided at internal supports. EN 1994-1-1 demands the minimum reinforcement area per meter of the slab width be 0.2% of the area for the concrete above the ribs.

$$A_s \geq A_{s,req} = \frac{0.2}{100} * b * h_c \ (in \ mm^2/m \ of \ slab \ width)$$

FEM analysis applied to the study of the stress transmission in the corrugated sheet slab
Master of Civil Engineering, defended by: MBOH HELBERT SHAYEH, NASPW, Yaoundé, 2019/2020

53

b   Deflection checks

The deflection verification of the slab may be omitted if the span to depth ratio of the slab doesn't exceed 20 for simply supported spans and 36 for continuous spans according to EN 1992-1-1. If these limits are surpassed, deflection checks must be made for the construction stage as well as the compressive stage.

i.   Construction stage deflection check

Before these calculations, the probability for the arrival of premature buckling in the sheet under the construction stage loads is checked to prevent irreversible deformation. This verification is important in regions of internal support and is calculated from the stress in the sheet under bending.

The construction load is calculated as $e_d = b * g_{sls}$, and the bending moment for the simply supported slab is calculated as $M_{ED} = \frac{e_d l^2}{8}$. The maximum compressive stress in the top flange of the sheeting is calculated as $\sigma_{comp} = \frac{M_{ED}}{I_p}(h_p - e)$ where I_y is the section moment of the sheet about its centroid, hp is the section height, and e is the height to the centroidal axis.

The buckling is then determined for the deck by checking if the section is fully effective using the method earlier explained in section a with the strain ε used in the calculation of the plate slenderness, λ_p, expressed as $\varepsilon = \sqrt{\frac{235}{\sigma_{comp}}}$.

If the section is fully effective under serviceability load conditions, then the deflection for the simply supported slab is calculated according to equation (2.21).

$$\delta_{t1} = \frac{5}{384} * \frac{(e_d * L^4)}{E_a * I_p} \tag{2.21}$$

Where L   is the slab span;

   Ea   is the material young's modulus;

   Ip is the the section second moment of area for the sheet.

The deflection was then verified if $\delta_1 < \frac{L}{180}$.

FEM analysis applied to the study of the stress transmission in the corrugated sheet slab
Master of Civil Engineering, defended by: MBOH HELBERT SHAYEH, NASPW, Yaoundé, 2019/2020

54

ii. Composite stage deflection check

The deflection in the composite stage is verified if $\delta_{tot} \leq \frac{L}{250}$, where L is the span. This deflection is calculated as the sum of the deflection due to permanent actions (δ_1) and the deflection due to variable actions (δ_2) calculated in section 2.1.1 of this work. The slab is taken as a continuous span for the composite stage. For the permanent actions are put on every span, while the variable actions are disposed to have maximum effect at one span.

a) Permanent actions   b) Variable actions

Figure 2.7. Disposition of actions for SLS deflection verifications of a slab

As a result, the deflections are calculated according to the expressions in equation (2.22).

$$\delta_1 = 0.0054 * \frac{\left(P_{SLS,g} * L^4\right)}{EI_c} \quad and \quad \delta_2 = 0.0099 * \frac{\left(P_{SLS,q} * L^4\right)}{EI_c} \tag{2.22}$$

The section moment I_c is calculated as an average of the section moments when the concrete is cracked (I_{cc}) and when the concrete is uncracked (I_{cu}). For a composite slab under positive bending moment, cracking occurs at the concrete in the ribs, so it is not considered in calculating the cracked section moment. A modular ratio for the composite section is used calculated by the expression

$$n = \frac{Ea}{E_{cm}''}$$

where E_{cm}'' is the average concrete section modulus considering creep, calculated in terms of the concrete modulus of elasticity according to the equation

$$E_{cm}'' = \frac{1}{2}\left[E_{cm} + \frac{E_{cm}}{3}\right]$$

The depth to the centroid, of the cracked and uncracked sections, xc and xu are calculated by balancing the static moment for the participating sections, by the overall equation

$$x = \frac{\sum A_i z_i}{\sum A_i}$$

FEM analysis applied to the study of the stress transmission in the corrugated sheet slab
Master of Civil Engineering, defended by: MBOH HELBERT SHAYEH, NASPW, Yaoundé, 2019/2020

55

Thus, xc and xu, in terms of the section areas and centroids, taking into consideration the different materials in the modular ratios are given by equation (2.23).

$$x_u = \frac{b \cdot h_c \left(\frac{h_c}{2}\right) + b_m \cdot h_p (h - h_p) + A_p \cdot (h - e)}{b \cdot h_c + b_m \cdot h_p + A_p}$$

$$x_c = \frac{nA_p}{b}\left(\sqrt{1 + \frac{2bd_p}{nA_p}} - 1\right)$$

(2.23)

Where Ap is the steel cross-sectional area

$b_m = \frac{b}{b_s} b'_m$ is the overall width of the concrete in the ribs;

$b'_m = \frac{(b_b + 2t + b_o)}{2}$ is the average width of one rib.

The moments of inertia for the composite section at cracked and uncracked condition were calculated as prescribed by the Eurocodes in terms of the geometric dimensions described above.

$$I_{cu} = \frac{bh_c{}^3}{12n} + \frac{bh_c}{n}\left(x_u - \frac{h_c}{2}\right)^2 + \frac{b_m h_p{}^3}{12n}$$

$$+ \frac{b_m h_p}{n}\left(h - x_u - \frac{h_p}{2}\right)^2 + A_p(d_p - x_u)^2 + I_p$$

(2.24)

$$I_{cc} = \frac{bx_c{}^3}{3n} + A_p(d_p - x_c)^2 + I_p$$
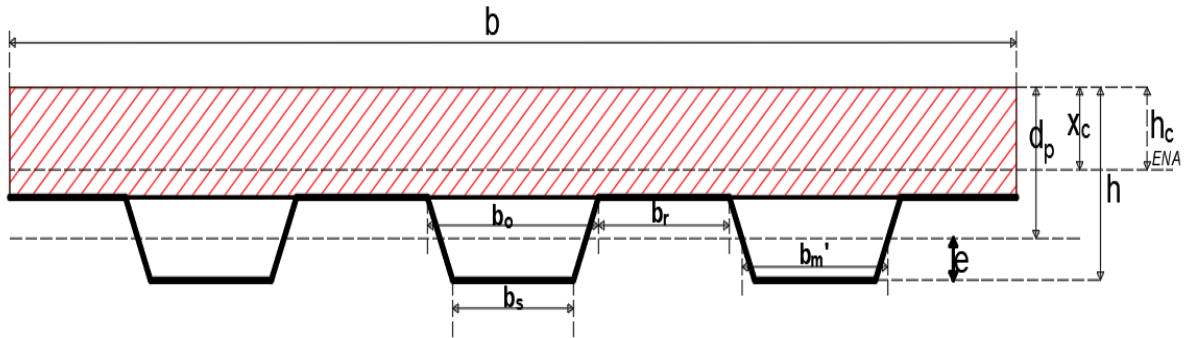
Concrete section considered in the determination of the depth of the Elastic Neutral Axis, x_c.

FEM analysis applied to the study of the stress transmission in the corrugated sheet slab
Master of Civil Engineering, defended by: MBOH HELBERT SHAYEH, NASPW, Yaoundé, 2019/2020

56

Concrete section considered in the determination of the depth of the Elastic Neutral Axis,x_u.
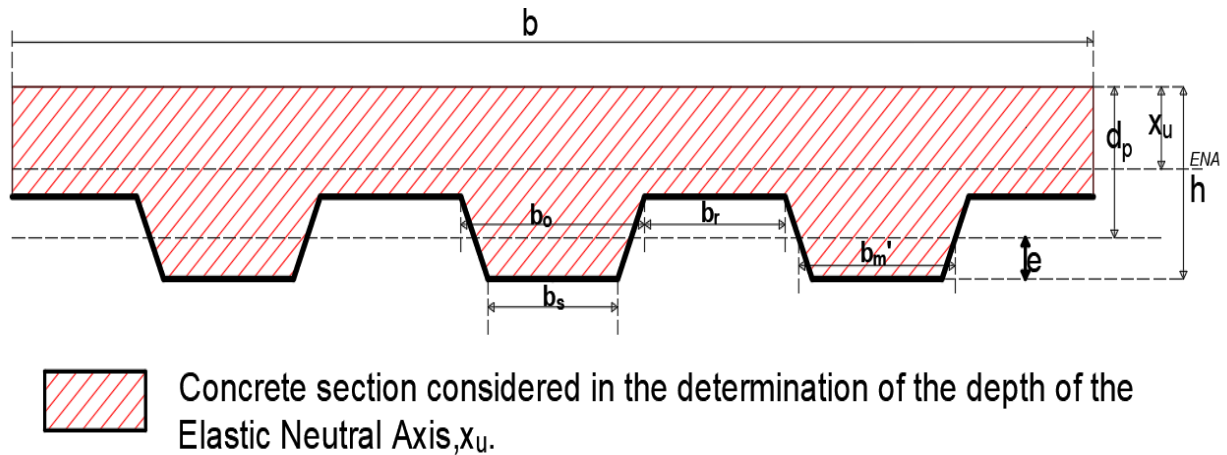
2.3. Slab detailing requirements

The detail requirements for the verified slab were done according to EC4 requirements.

2.3.1. Slab dimensions

The overall depth of the slab should be greater than 90mm

The thickness of the concrete above the main flat surface of the top of the ribs of the sheeting should be greater than 50mm

The ratio of the width of the sheet rib to the rib spacing $\frac{br}{bs}$ should be less than 0.6

2.3.2. Reinforcement requirement

The minimum area of the reinforcement in both directions of the slab should not be less than $80 mm^2/m$. This minimum area is calculated for unpropped slabs as 0.2% of the concrete topping area. The spacing of the reinforcement should also be greater than 2times the slab height.

2.4. Finite element modelling of the corrugated sheet slab

FEM analysis applied to the study of the stress transmission in the corrugated sheet slab
Master of Civil Engineering, defended by: MBOH HELBERT SHAYEH, NASPW, Yaoundé, 2019/2020

57

A finite element analysis was conducted to study the evolution of stress in the composite slab, spanning between supporting beams, subject to bending displacements in similar conditions to the shear bond test procedure. The stresses in concrete and in the sheet could then be understood, alongside the effect of cracking in the concrete on the supporting sheet and even in the mesh reinforcement, alongside predictions for the m,k values of the sheet. The representation of the concrete and sheet with proper elements and materials, the modelling of the composite slab and the boundary conditions to study only a half-span are discussed in this section.

2.4.1.Objective

The aim of this work is to show that FEM analysis, accompanied by a few small-scale tests, can be used in the design of composite slabs with good predictions as to the evolution of stress distribution, of crack propagation in the concrete and development of buckles in the sheet. Each phenomenon could then be cross-examined to see the accuracy of the above technique.

The specimen of the dimensioned slab comprised of a bottom flange, the webs and half the width of the top flanges as shown in figure 2.8. It was loaded by line loads a quarter span away from the supports, in a simply supported configuration to emulate the m-k experimental design. The supporting beam and shear connectors were omitted to simplify the model, while concrete rebar was introduced to better show the slab resistance. The modelling of every component is discussed in this section, while the model parameters are presented in section 3.5.
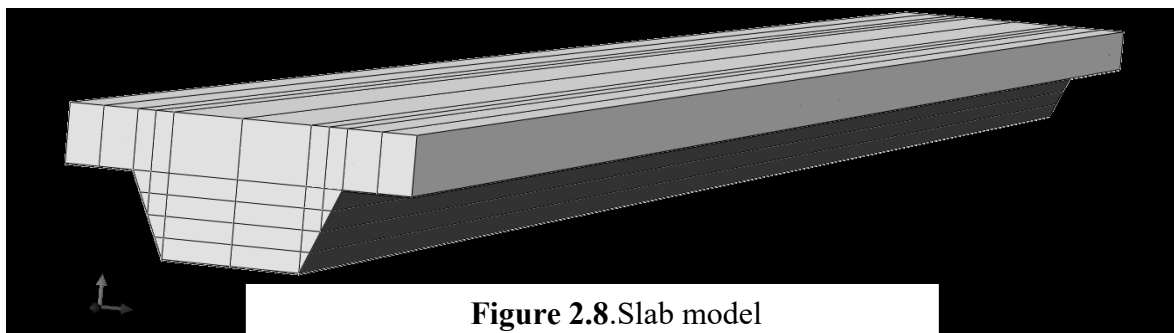
Figure 2.8.Slab model

2.4.2.Elements

The concrete was modelled with 8-node hexagonal C3D8R 3D solid elements with reduced integration, which are capable of plastic deformations, cracking in tension, and crushing in compression. Quadratic reduced-integration elements are not susceptible to shear

FEM analysis applied to the study of the stress transmission in the corrugated sheet slab
Master of Civil Engineering, defended by: MBOH HELBERT SHAYEH, NASPW, Yaoundé, 2019/2020

58

locking, even when subjected to complicated states of stress. Therefore, these elements are generally the best choice for most general stress/displacement simulations, except in large-displacement simulations involving very large strains and in some types of contact analyses (ABAQUS manual,2002). The steel sheet is modelled with 4-node S4R shell elements capable of plastic deformation in the plane of the elements. The reinforcement bars for the mesh reinforcement are modelled with 2-node 3D Truss elements (T3D2) which are able to undergo deformations and submit to axial loading.

2.4.3.Material modelling

The behaviour of concrete and steel are to be nonlinear so as to approximate real behaviour. The material models used for the concrete and steel elements were the Concrete Damaged Plasticity model and the steel material plasticity.

2.4.3.1 Concrete damaged Plasticity

The concrete was modelled as nonlinear elastoplastic, using the concrete damaged plasticity model according to Lubliner et al. The compressive behavior of the concrete is linear elastic until about half the compressive strength, beyond which the plastic behavior is explained by continuum damage mechanics and the application of scalar damaged elasticity in combination with isotropic tensile and compressive plasticity developed in concrete damaged plasticity (Lubliner et al,1989).

According to this model, the yield surface of the concrete depends on the effective stress and plastic strain according to equation (2.25).

$$F(\bar{\sigma}, \tilde{\varepsilon}^{pl}) = \frac{1}{1-\alpha}\left[\bar{q} - 3\alpha\bar{p} + \beta\tilde{\varepsilon}^{pl}\langle\widehat{\bar{\sigma}}_{max}\rangle - \gamma\langle-\widehat{\bar{\sigma}}_{max}\rangle\right] \qquad (2.25)$$

Where $\bar{p}$ is the effective hydrostatic pressure stress tensor which are used by the yield surface and plastic flow potential function (Lubliner et al ,1989). $\widehat{\bar{\sigma}}_{max}$ is the algebraically maximum eigenvalue of the deviatory part of the effective stress tensor (σ). The parameters α, β and γ are dimensionless material constants. Further details on how these parameters affect the damage plasticity model have been outlined by Lubliner et al (1989). The function β is defined according to equation (2.26)

FEM analysis applied to the study of the stress transmission in the corrugated sheet slab
Master of Civil Engineering, defended by: MBOH HELBERT SHAYEH, NASPW, Yaoundé, 2019/2020

59

$$\beta(\bar{\varepsilon}^{pl}) = \frac{\bar{\sigma}_{co}(\tilde{\varepsilon}_c^{pl})}{\bar{\sigma}_{to}(\tilde{\varepsilon}_t^{pl})} (1 - \alpha) - (1 + \alpha) \qquad (2.26)$$

Where $\bar{\sigma}_{co}$ and $\bar{\sigma}_{to}$ are the ultimate uniaxial compressive and tensile yield stresses respectively. In conditions of biaxial compression with the maximum principal effective stress equal to zero ($\hat{\bar{\sigma}}_{max} = 0$) the yield or failure surface reduces to the Drucker-Prager yield condition in which α becomes the only parameter needed to define the failure surface. The parameter α is obtained by a comparison between the initial equibiaxial and uniaxial compressive yield stresses σ_{b0} and σ_{c0} as shown in equation (2.27).

$$\alpha = ((\bar{\sigma}_{co}/\bar{\sigma}_{bo}) - 1)/(2(\bar{\sigma}_{co}/\bar{\sigma}_{bo}) - 1) \qquad (2.27)$$

According to Lubliner et al (1989), typical values of the ratio for concrete $\left(\frac{\bar{\sigma}_{co}}{\bar{\sigma}_{bo}}\right)$ based on experimental results are reported in the range from 1.10 to 1.16, yielding values of α between 0.08 and 0.12. The third parameter γ determines the shape of the yield surface in the plasticity model. It is present in the yield function only for triaxial compression stress state, when ($\hat{\bar{\sigma}}_{max} < 0$). It can be obtained by comparing the yield conditions along the tensile and compressive meridians according to equation (2.28).

$$\gamma = \frac{3(1 - K_c)}{2K_c - 1} \qquad (2.28)$$

Kc is the ratio of the hydrostatic effective stress in the tensile meridian to that on the compressive meridian when the maximum principal stress is negative. Kc defines the shape of the yield surface in the deviatory plane. The value of Kc is assumed to be 0.6 as result of the triaxial test results.

These fundamental notions of concrete damaged plasticity allow the user to easily model the material by entering the required parameters in the CDP model of ABAQUS/CAE as described in the material modelling.

Concrete material modelling

The uniaxial response of concrete under compressive loading is linear up to initial yield stress, σc0. Then, the material response becomes plastic with stress hardening and followed by strain softening beyond the peak compressive stress σcu as shown in Figure 2.9. When the

FEM analysis applied to the study of the stress transmission in the corrugated sheet slab
Master of Civil Engineering, defended by: MBOH HELBERT SHAYEH, NASPW, Yaoundé, 2019/2020

60

concrete specimen is unloaded at any point on the softening branch of the stress–strain curve, the elastic stiffness of the material becomes degraded and is characterized by the compressive damage variable, dc. The zero value of compressive damage variable represents undamaged material and value equal to one denotes total loss of the compressive strength. The compressive stress–strain curve and elastic stiffness were determined as per BS EN 1992–1–1 provision. If E_0 is the elastic stiffness of the undamaged material, εc is the total compressive strain and $\tilde{\varepsilon}_c^{pl}$ is the compressive equivalent plastic strain, the compressive damage variable, dc is calculated as expressed in equation (2.29).

$$d_c = 1 - \frac{\sigma_c}{E_0\left(\varepsilon_c - \varepsilon_c^{pl}\right)} \tag{2.29}$$

The compressive inelastic (or crushing) strain $\tilde{\varepsilon}_c^{in}$ is also required for CDP model which is calculated from as suggested in ABAQUS manual.

Figure 2.9 also shows the uniaxial stress-strain behavior of concrete in tension. This behavior comprises two parts the first of which is a linear elastic behavior and the second part initiates together with crack occurrence and its propagation in concrete material under tension. This is demonstrated by the descending branch of the uniaxial tensile stress-strain diagram. The damage parameter is also calculated by equation (2.30)
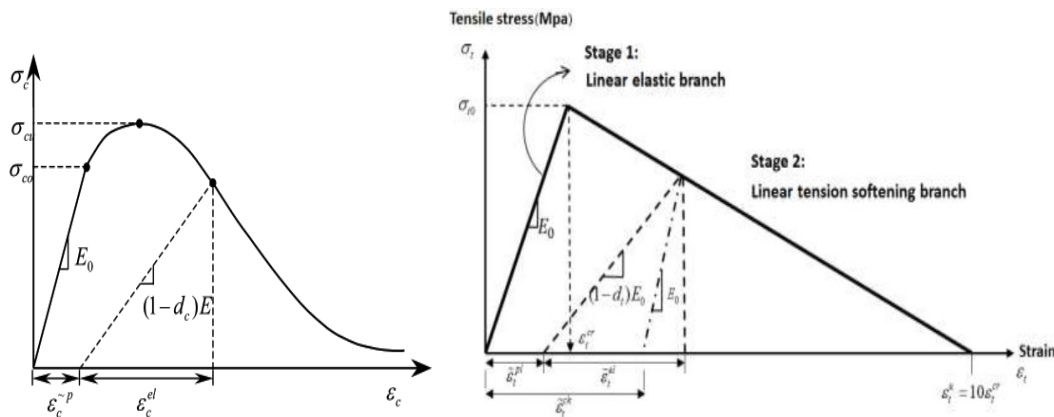
Figure 2.9. Compressive and tensile stress-strain relationship for ABAQUS

$$d_t = 1 - \frac{\sigma_t}{E_0\left(\varepsilon_t - \varepsilon_t^{pl}\right)} \tag{2.30}$$

All these equations were used in Microsoft Excel to prepare the data for the concrete damaged plasticity in ABAQUS reported in section 3.5.1.

FEM analysis applied to the study of the stress transmission in the corrugated sheet slab
Master of Civil Engineering, defended by: MBOH HELBERT SHAYEH, NASPW, Yaoundé, 2019/2020

61

2.4.3.2 Steel plasticity

The steel material for the corrugated deck was modelled as elastic perfectly plastic. This ensures that the stress strain behaviour is linear until the elastic limit, beyond which the material deforms at the same stress, redistributing stresses to non-yielded portions of the surface. The same plasticity model is used for the concrete reinforcement.

2.4.4. Interactions

The main interactions between the system components include the shear bond between the sheet and the concrete, the contact between the sheet and concrete and the shear bond between the reinforcement and the surrounding concrete. Each will be explained here.

2.4.4.1 Steel- concrete interaction

The shear bond between the concrete slab and the steel deck is responsible for the composite behavior of the assembly and hence for the slab resistance. The transfer of shear stress was modelled by taking data form small-scale bending tests and deriving a good approximate for the shear-slip curve for the dimensioned slab.

a. Partial connection experimental behavior

Abdullah provided shear bond curves for slabs of different slenderness with 1.2mm sheets obtained through bending tests, and displayed in figure 2.10 for with similar profiles to the deck of our project. The points for the shear bond curve for the project slab were interpolated, beginning with the point of ultimate stress. A way was proposed to determine the shear stress in a composite slat in terms of the slenderness and the thickness, as given in equation (2.31).

$$\tau d = p\frac{td}{L_s} + s \qquad (2.31)$$

From this relation:
- The coefficients p and s were calculated using the ultimate stresses and slenderness for two slabs of slenderness greater and less than the slenderness of the project slab.

- The slenderness $(\frac{L_s}{d})$ of the project slab was then used to calculate the corresponding ultimate stress the above equation. The corresponding slip to this shear stress was calculated by interpolating the line joining the two maxima of the stress-slip curves of the standard slabs, and finding the corresponding slip using equation (2.32).

FEM analysis applied to the study of the stress transmission in the corrugated sheet slab
Master of Civil Engineering, defended by: MBOH HELBERT SHAYEH, NASPW, Yaoundé, 2019/2020

62

$$s_p = \frac{\tau_p - (\tau_2 - ms_2)}{m} \qquad (2.32)$$

Where s_p and τ_p are the slip and shear stress for the project slab, while m is the slope of the line joining the maxima of the standard slabs, calculated according to equation

$$m = \frac{\tau_1 - \tau_2}{s_1 - s_2} \qquad (2.33)$$

Where τ_1 and τ_2 and s_1 and s_2 are the shear stresses for both slabs and their corresponding slips.

- Further points for the shear bond curve are found by holding the ratio of their distance to corresponding points of the standard curves the same as for the maximum point. This is illustrated in figure 2.10.

FEM analysis applied to the study of the stress transmission in the corrugated sheet slab
Master of Civil Engineering, defended by: MBOH HELBERT SHAYEH, NASPW, Yaoundé, 2019/2020

63
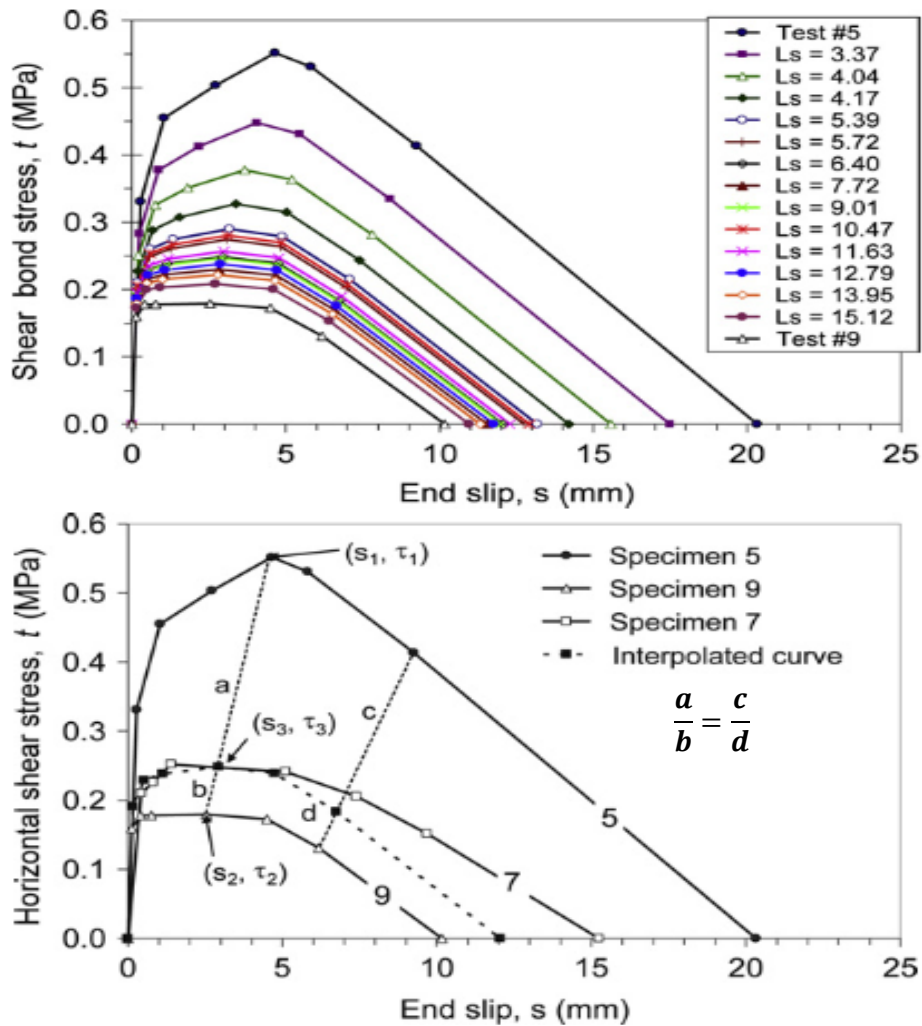
Figure 2.10. Shear bond behaviour for slabs with 76mm deep and 1.21mm thick sheets Method of interpolation of shear bond stress for slab of intermediate slenderness. (Abdullah and Easterling,2009)

b. Adaptation to FEM model

The shear behavior of the slab was assigned to CONN3D2 elements available in ABAQUS, in the Radial-Thrust configuration. The Radial-thrust elements (figure 2.11) are made of 2 perpendicular springs whose behavior can be independently configured. The connector elements were placed between nodes of the concrete bottom face and the sheet along the span at the middle of the flange and at the intersection between the sheet web and the flanges labelled as 'foldlines' in this report.

The radial spring was assigned a nonlinear force-displacement behavior calculated from the stress-slip curve, while the thrust spring was not assigned any property. The spring force

FEM analysis applied to the study of the stress transmission in the corrugated sheet slab
Master of Civil Engineering, defended by: MBOH HELBERT SHAYEH, NASPW, Yaoundé, 2019/2020

64

for each connector was e obtained by multiplying the shear stress τ by the related area, A, and dividing by the number of shear connectors along the line as summarized in equation (2.34). The connector displacements were taken as the corresponding slips to the shear forces.

$$F = \frac{\tau * A}{n_s} = \frac{\tau * L * b}{n_s} \qquad (2.34)$$

With L being the slab span and b the influence width to be supported by the shear connector depending on its position:

$For\ midflange\ connector, b = \frac{b_f}{2}$

$For\ fold\ line\ connector, \quad b = \frac{b_f}{4} + \frac{b_w}{2}.$

Where bf and bw are the widths of the flange and the web. With the help of the mesh created for the sheet and the concrete in the CAE model, the node numbers at the 'foldline' and the 'midflange' positions were obtained and the pairs were prepared and integrated into the model input file.
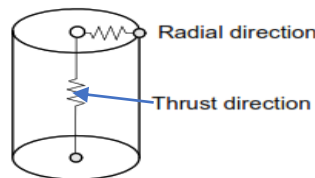
Figure 2.11. Radial-thrust connector elements (Abaqus manual, 2012)
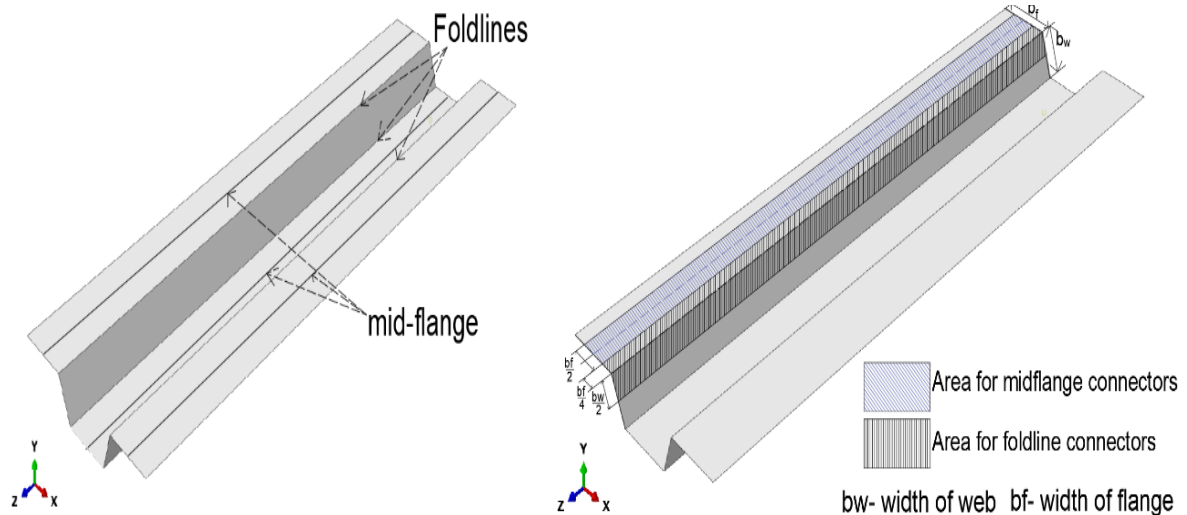
Figure 2.12. Foldline and mid flange positions(a) for connector elements and their respective shear areas(b).

FEM analysis applied to the study of the stress transmission in the corrugated sheet slab
Master of Civil Engineering, defended by: MBOH HELBERT SHAYEH, NASPW, Yaoundé, 2019/2020

65

2.4.4.2 Contact between materials

The contact between the concrete and the sheet was modelled by creating a surface-to-surface contact interaction between the bottom face of the concrete slab and the sheet deck flanges and webs. The interactions were assigned a "hard" contact in the normal direction with NO SEPARATION so as to ensure that the surfaces do not overlap. Since the tangential behavior was already being modelled by the CONN3D2 elements, it was set to frictionless.

The concrete-reinforcement shear bond was modelled by assigning an Embedment constraint between them. This allows the reinforcement to deform with the concrete and to have total shear bond with the concrete.

2.4.5. Boundary conditions

In an initial step, the boundary conditions to model the supports and the continuity of the slab along the width were assigned. For the support, a line of nodes on the bottom flange of the sheet 2 elements away from one end were restricted form translation in any direction, permitting only rotation, while on the other end, the roller support was modelled by restricting translation in the direction parallel to the slab depth. The concrete nodes at ends of the top flanges were restricted from translation in the direction parallel to the slab width, while a symmetry along this direction was assigned to the nodes of the steel sheet at the middle of the top flanges (XSYMM(U1=UR2=UR3=0).

In a second step, 2 nodes on the concrete top face, located a shear span away from the support nodes on both ends were assigned an imposed displacement of 100mm in the negative Y-direction. This displacement was applied incrementally at a linear rate, so as to capture the moments of crack formation and propagation and was sufficiently high to cause total failure in the slab. A couple constraint was then applied to all nodes on the concrete top face a shear span away from both supports, to keep their vertical displacement equal throughout the analysis. This thus simulated the linear load on the slab.

The second step was an ABAQUS/Explicit dynamic step which is normally used for dynamic analysis. However, if the loading is slowed down enough, the analysis will become near static, often called quasi static. This is adopted by assigning a time period to the step that is 5 to 10 times the natural period of the model, hence reducing the frequency of the dynamic

FEM analysis applied to the study of the stress transmission in the corrugated sheet slab
Master of Civil Engineering, defended by: MBOH HELBERT SHAYEH, NASPW, Yaoundé, 2019/2020

66

analysis. The natural frequency was found by first carrying out a frequency analysis. A smooth amplitude was also assigned to the imposed displacement.

Conclusion

After introducing the important concepts and state of art in composite slab academia as far as experimentation and Finite Element Analysis are concerned, the design of the composite slab for a regular G+3 steel building for office use was carried out to explain the decisions taken in design and detailing according to Eurocode 4 and related codes. The Finite Element approach was used to model the slab components and the slab composite action and the technique of shear interaction adapted to the composite slab shear bond was explained, in an effort to study the evolution of stresses in the slab under full and partial connection.

FEM analysis applied to the study of the stress transmission in the corrugated sheet slab
Master of Civil Engineering, defended by: MBOH HELBERT SHAYEH, NASPW, Yaoundé, 2019/2020

67

CHAPTER 3: **STATIC ANALYSIS RESULTS AND FINITE ELEMENT ANALYSIS**

3.1. **Introduction**

This section will concretely report the design of the composite slab according to Eurocode 4, by appealing to the sheet and slab information and then report the calculated resistances that ensured a verified composite slab. The finite element model for the analysis is also presented so as to give a view of all the necessary information that was provided, in accord with the precedent chapter.

3.2. **Preliminary analysis of the members and choices of materials**

A 76.2mm trapezoidal sheet was chosen for the composite slab, with a steel grade of 350MPa. In order that the detailing may be in line with EC4 predictions, the sheet is covered with a concrete topping of 53.8mm, with concrete of class C30. The dimensions of the slab and trapezoidal sheet as described in section 2.1.1 are presented in Tables 3.1 and 3.2.

Table 3.1. Geometric properties for the composite slab.

Geometry	Symbol	value	
Slab length	l	3.5	m
Slab thickness	h	130.00	mm
Slab width	b	1000.00	mm
Height of concrete	hc	53.8	mm
Height to centroidal axis of sheet	e	37.74	mm
Effective depth of the sheet	dp	87.26	mm
Height to PNA	ep	39.50	mm
Elastic modular ratio	n	6.40	
Cracked modular ratio	nc	9.59	
Shear span	Ls	1000.00	mm
	γvs	1.25	
Provided reinforcement per m width of sheet	As	193.00	mm²/m

FEM analysis applied to the study of the stress transmission in the corrugated sheet slab
Master of Civil Engineering, defended by: MBOH HELBERT SHAYEH, NASPW, Yaoundé, 2019/2020

68

Table 3.2. Geometric and material characteristics of the corrugated sheet

Dimension	Symbol [unit]	Value
Characteristic yield strength of steel material	F_{yp} [N/mm2]	350
Partial safety factor of resistance for cold-formed steel,γ_M		1
Design yield strength for the steel	$F_{yp,d}$ [N/mm2]	350
Sheet thickness	t [mm]	1.21
Height of sheet flange	hp [mm]	76
Height to centroidal axes	e [mm]	37.74
Center-to-Centre distance between flanges	b_s[mm]	305
Distance between neighboring bottom flanges	b_1[mm]	164
Bottom flange width	b_b[mm]	141
Top flange width	b_r[mm]	135
Distance between neighboring top flanges	b_o[mm]	170
Angle between webs and flanges	ϕ[°]	79.198
Area of sheet per m slab width	Ap =Ape [mm2/m]	1800
Second moment of area of sheet	Ip [mm4]	1813851
Young modulus of sheet	Ep = Ea [N/mm2]	210000
Poisson ratio	ν	0.3
Sheet sagging resistance moment (provided by manufacturer)	Mrd,s [KNm/m]	16.072
Sheet hogging resistance moment (provided by manufacturer)	$M_{rd,h}$[KNm/m]	16.2085
Empirical factors from m-k test (provided by manufacturer)	m [N/mm2]	184
	k [N/mm2]	0.053

Concrete of strength class C30/37 was preliminary chosen for the slab design. The mechanical properties of the concrete as per calculation based on Eurocode 2 are summarized in Table 3.3.

Table 3.3. Concrete C30/37 mechanical properties (EC2)

Characteristic	Symbol		
Characteristic compressive strength	f_{ck}	30	N/mm2
Partial safety factor of resistance	γ	1.5	
Design compressive strength	f_{cd}	20	N/mm2
Mean compressive strength	f_{cm}	38	N/mm2
Mean modulus of elasticity	E_{cm}	32836.6	N/mm2

FEM analysis applied to the study of the stress transmission in the corrugated sheet slab
Master of Civil Engineering, defended by: MBOH HELBERT SHAYEH, NASPW, Yaoundé, 2019/2020

69

3.3. **Actions on the building**

The permanent and life actions on the building as explained in section 2.1.2.1 are reported in the following section. They are all converted to linear loads for the slab design.

3.3.1.1 Permanent actions

Prior to calculating the permanent actions due to structural and non-structural self-weights, the total weight of the floor finishes will be calculated by considering all the details of the floor covering, and is reported in Table 3.4 . The linear loads per metre width of the slab for each self-weight was calculated as explained in section 2.1.2.1.

Table 3.4. Calculation of linear load for floor finishes

Component	Unit weight (KN/m^3)	Thickness m	Surface load KN/m^2
Ceramic tiles	22	0.02	0.44
Mortar	20	0.02	0.4
Sand layer	18	0.02	0.36
Plaster	10	0.02	0.2
Total load for floor finishes			**1.4**

With the surface loads for the finishes calculated, all the permanent actions on the building could then be calculated. The actions were summed for those which acted in the construction stage and for those acting during the service stage of the building's nominal life. They are reported in Table 3.5 and Table 3.6.

Table 3.5. Permanent actions due to self-weights on the building.

Structure	Self-weight	Unit	Geometric characteristic	Unit	Linear load (KN/m)
Sheet	0.1443	KN/m^2	b=1	m	0.136
Wet concrete	25	(KN/m^3)	0.09189	m2	2.389
Dry concrete	26	(KN/m^3)	0.09189	m2	2.297
Finishes	1.4	KN/m^2	1	m	1.4
Partition walls	1.3	KN/m^2	1	m	1.3
Ceiling and services	1	KN/m^2	1	m	1

FEM analysis applied to the study of the stress transmission in the corrugated sheet slab
Master of Civil Engineering, defended by: MBOH HELBERT SHAYEH, NASPW, Yaoundé, 2019/2020

70

Table 3.6. Total permanent loads at the construction and composite stage

Construction stage			Composite stage		
Component	Linear load		Component	Linear load	
Sheet	0.136	KN/m	Sheet	0.14	KN/m
Wet concrete	2.389	KN/m	Dry concrete	2.30	KN/m
			Finishes	1.40	KN/m
			Non-structural partition walls	1.30	KN/m
			Ceiling and services	1.00	KN/m
Total, g_{k1} =	**2.525**	**KN/m**	$g_{k,2}$=	**6.13**	**KN/m**

3.3.1.2 Variable actions

The linear loads over the slab were calculated as the product of the uniform surface loads for the variable actions and the width of the slab to be dimensioned.

Table 3.7. Variable actions on the building

Description	Value (KN/m²)	Slab width	Unit	Linear load (KN/m)	Stage
Construction load	1.5	1	m	1.5	Construction (qk1)
Imposed loads	2.5	1	m	2.5	Composite (qk2)

3.4. Composite slab design

The composite slab design was done at the construction and composite stage, respecting the Eurocode 4 design requirements presented in section 2.2.1.

3.4.1. Construction stage

The construction stage loads calculated according to section 2.1.2.

3.4.1.1 Ultimate limit state design

The total permanent and variable actions calculated for the construction stage above were used to calculate the total ultimate load combination according to equation (2.2).

$$P_{ULS,1} = 1.3 * (2.525) + 1.5 * (1.5) = \frac{5.533 KN}{m}$$

FEM analysis applied to the study of the stress transmission in the corrugated sheet slab
Master of Civil Engineering, defended by: MBOH HELBERT SHAYEH, NASPW, Yaoundé, 2019/2020

71

As a consequence, the design moment and shear forces were calculated respectively as $M_{ed,1} = 8.471 KN/m$ and $V_{ed,1} = 9.68 KN$. The resistances of the sheet to actions were calculated and compared to these actions. All parameters necessary for calculating the local and global resistances of the sheet were summarized in the table below.

Slab characteristic and parameter	Symbol	Equation	Value	
web height between the flanges	hw	h − t	73.78	mm
slant height of the web	sw	hw/sinϕ	96.05	mm
Design yield strength	f_{yb}	F_{yp}/γ_{vs}	280	MPa
Relative slenderness of the web	λω	Equation (2.6)	1.01	
Shear buckling strength	fbv	Table A2	134.02	MPa
Number of webs per width	nw	b/bs	6	
Relevant category	α	Table A3	0.075	
Effective bearing length	la	Table A3	10	mm
Internal radius of the section corners	r	sharp corners	0	mm

From the above parameters, the sheet was verified to the construction load by ensuring that the resistance surpasses the solicitation (R>S)

Resistance Parameter (R)	Symbol	Equation	Value	S	(S<R)?
Sheet sagging moment resistance	$M_{s,rd}$		14.48KNm/m	**Med**	OK
Shear resistance of the web	$V_{b,rd}$	Equation(2.5)	8.99KN/m per web	**Med**	OK
Total shear resistance		$n_w * V_{b,rd}$	59.00KN/m	**Ved**	OK
local transverse resistance of one web	Rw,rd	Equation(2.7)	1.8404KN/m per web	-	-
Total transverse resistance		$n_w * R_{w,rd}$	11.04KN/m	**Ved**	OK
Half the shear resistance		$0.5 * V_{b,rd}$	29.5KN/m	**Ved**	OK
Combined moment, axial force and shear	Verification not required since $V_{ed} < 0.5 * V_{b,rd}$ as explained in section iii				

FEM analysis applied to the study of the stress transmission in the corrugated sheet slab
Master of Civil Engineering, defended by: MBOH HELBERT SHAYEH, NASPW, Yaoundé, 2019/2020

72

3.4.1.2 Serviceability limit state design

The characteristic combination of actions for irreversible loads is used for this combination according to equation (2.1) in section 2.1.1.

$$P_{SLS} = 1.0(2.525) + 1.0 * (1.5) = 5.533 KN/m$$

Premature buckling is first verified in the sheet flange as explained in section 1.The calculated variables are summarized in Table 3.8 below.

Table 3.8. Verification of premature vuckling in the sheet section

Slab characteristic/ parameter	Symbol	Equation	Value
Compressional stress on top flange	σcomp	$\frac{M_{ED}}{I_p}(h_p - e)$	79.01MPa
Strain	ε	$\sqrt{(235/\sigma_{comp})}$	17.72
stress ratio	ψ	see Table A1	1
Buckling factor	kσ	see Table A1	4
Plate slenderness	λp	Equation (2.4)	1.02
Coefficient of effective area	ρ	Equation (2.3)	0.77 Not all the section is effective

The entire section is not effective; hence some has already buckled, this will be handled by adding props to the slab during the construction stage. The verification for deflection is summarized in the table below.

Parameter	symbol	Equation	Value
Deflection	δ_1	Equation(2.10)	13.75mm
Limit		L/180	19.44mm
Verification			**OK**

.

3.4.2.Composite stage

The concrete and the steel work together at the composite stage to resist all the actions on the building. The combinations for ultimate and serviceability limit states presented below follow the recommendations for Eurocode 4 and Eurocode 2 and were presented in section 3.4.

FEM analysis applied to the study of the stress transmission in the corrugated sheet slab
Master of Civil Engineering, defended by: MBOH HELBERT SHAYEH, NASPW, Yaoundé, 2019/2020

73

Table 3.9. Characteristics of the project slab

Parameter	symbol	Magnitude
Slab length	l	3.5m
Slab thickness	h	130mm
Slab width	b	1000mm
Center-to-center distance between flanges	bs	304.8mm
Height of concrete	hc	53.8mm
Height to centroidal axis of sheet	e	41.27mm
Depth to neutral axis of sheet	dp	88.73mm
Height to PNA	ep	41.27mm
Elastic modular ratio	n	6.40
Cracked modular ratio	nc	9.60
Shear span	Ls	875mm
safety factor for longitudinal shear	γvs	1.25
Empirical factors from m-k test (provided by manufacturer)	m	184MPa
	k	0.053MPa
Area of sheet	Ap	1666mm2/m
Area of concrete	Ac	91890mm2/m
Area of provided reinforcement per m width of slab	As	193mm2/m

3.4.2.1 Ultimate limit state design

The combined load from the permanent and variable actions for ultimate load design according to is $P_{ULS,2} = 1.3 * (6.13) + 1.5 * (2.5) = 11.72 KN/m$

The calculated bending moment M_{ed} and shear force V_{ed} due the ultimate load per metre slab width, following recommended equations for simply supported spans are 17.95KN/m/m and 20.52KN/m respectively.

FEM analysis applied to the study of the stress transmission in the corrugated sheet slab
Master of Civil Engineering, defended by: MBOH HELBERT SHAYEH, NASPW, Yaoundé, 2019/2020

74

Table 3.10. Summary of the ULS verifications

Description (R)	Symbol	Equation	Value
Axial force in the concrete	N_c,f	Equation(2.13)	914.6KN/m
Axial force in the sheet	Npa	Equation(2.14)	583.1KN/m
Depth of neutral axis	xpl	Equation(2.15)	34.30mm
Lever arm	z	Equation (2.16)	71.58
Composite bending resistance	M_{rd}	$\min\left(N_{c,f}, N_p\right) * z$	**41.74KNm/m**
			>M$_{ED}$ Verified
Longitudinal shear resistance	$V_{l,rd}$	$\dfrac{b * d_p}{\gamma_{vs}}\left(\dfrac{m * A_p}{b * L_s} + k\right)$	**28.63KN/m**
			>V$_{ED}$ Verified
Compressional axial stress	σcp	Ned/A	0
EC2 coefficients for vertical shear resistance	k	$1 + \sqrt{(200/d)} \leq 2.0$	2
	k$_1$	0.15	0.15
	ρ$_1$	$A_{sl}/(b_w * d_p) \leq 0.02$	0.020
	C$_{rdc}$	0.18/γ$_c$	0.12
Average width of concrete web in ribs	bw	$b/bs * bo$	604.3mm
Minimum shear stress	v_{min}	$0.035 * k^{\frac{3}{2}}\sqrt{f_{ck}}$	
Resistance of concrete strut	$V_{c,rd}$	Equation(2.18)	50.38KN/m
Minimum resistance of concrete strut	$V_{c,rd,min}$	Equation(2.19)	29.08KN/m
Design resistance of concrete strut		$\min\left(V_{c,rd}, V_{c,rd,min}\right)$	**29.08KN/m>V$_{ED}$** **OK**

With satisfactory verifications for the composite slab at both the construction and the composite stage under ultimate loads, the serviceability checks will be made for the steel deck and the composite slab at construction and composite stages respectively.

3.4.2.2 Serviceability limit state design

FEM analysis applied to the study of the stress transmission in the corrugated sheet slab
Master of Civil Engineering, defended by: MBOH HELBERT SHAYEH, NASPW, Yaoundé, 2019/2020

75

The frequent combination was used for this analysis as proposed in section 2.1.1. Due to different load dispositions for the deflection calculation, the loads were separately calculated. The calculated parameters and the eventual loads are summarized in that follows;

Permanent load	Psls,g	G1	6.13KN/m
Frequent combination variable load factor	ψ		0.7
Design variable load	Psls,q	ψ*Q	1.75 KN/m

For crack control, a A193 mesh fabric assuring a 193mm2 per meter of slab width is used. The required mesh area is

$$\frac{0.2}{100} * A_c = \frac{0.2 * 91890}{100} mm^2/m = 183.78 mm^2/m < 193 mm^2/m \ (Verified)$$

The necessity for deflection was noticed by the span effective depth ratio:

$$\frac{l}{d_p} = \frac{3500}{88.73} = 39.445 > 20 (limit \ for \ simply \ supported \ span)$$

The deflection check for the composite slab will need to be carried out. The parameters calculated and the final verifications done followed section ii and are summarized in the table that follows.

Equivalent width of rib	b'm		151.24	mm
Total width of rib in the slab strip	bm		496.19	mm
Depth to neutral axis in the uncracked phase	xu	Equation (2.23)	58.93	mm
Depth to neutral axis in the cracked phase	xc	Equation (2.23)	39.62	mm
Moment of inertia for the uncracked section	Icu	Equation (2.24)	16485926.08	mm4/m
Moment of inertia for the racked section	Icc	Equation (2.24)	7887731.26	mm4/m
Average moment of inertia	Ic	0.5*(Icc+Icu)	12186828.67	mm4/m

The calculated deflections and the verification are presented in the table below. The slab was seen to stay within the deflection limits.

FEM analysis applied to the study of the stress transmission in the corrugated sheet slab
Master of Civil Engineering, defended by: MBOH HELBERT SHAYEH, NASPW, Yaoundé, 2019/2020

76

Deflection under permanent loads	$\delta 1$	Equation(2.22)	1.94	mm
Deflection under live loads (frequent combination)	$\delta 2$	Equation(2.22)	1.016	mm
Total slab deflection	**δ**	**$\delta 1 + \delta 2$**	**2.96**	**mm**
Limit deflection	**δ_l**	**L/250**	**14**	**mm**
Verification		**$\delta < \delta_l$?**	**OK**	

3.4.3. Slab details

The detail checks according to EC4 for the slab detail discussed in section 2.3 are summarized here.

3.4.3.1 Slab dimension

- The total depth of the slab is $h = 130 > 90mm \ (OK)$

- The ratio br/bs of the project slab is $\frac{b_r}{b_s} = \frac{120.7}{305} \approx 0{,}395 < 0.6 (OK)$

- The thickness of the concrete $h_c = h - h_p = 130 - 76.2 = 53{,}8mm > 50mm (OK)$

3.4.3.2 Reinforcement requirement

- The minimum reinforcement for a slab is 80mm2/m in any direction

  For an unpropped slab, the minimum area is $A_{s,min} = 0.002 \cdot b \cdot hc = 147mm^2/m$

  With the A193 mesh, 5 bars of 7mm diameter are disposed at an interspacing of 200mm;

$$A_s = 5 \cdot \pi \cdot \frac{7^2}{4} = \frac{245 \cdot \pi}{4} \approx 192{,}4226 > 147 > 80mm^2/m(OK)$$

- The 200m bar spacing for the reinforcement is less than the limit spacing of 350mm (OK)

FEM analysis applied to the study of the stress transmission in the corrugated sheet slab
Master of Civil Engineering, defended by: MBOH HELBERT SHAYEH, NASPW, Yaoundé, 2019/2020

77

a. <u>Cross sectional view</u>

b. <u>View along span</u>
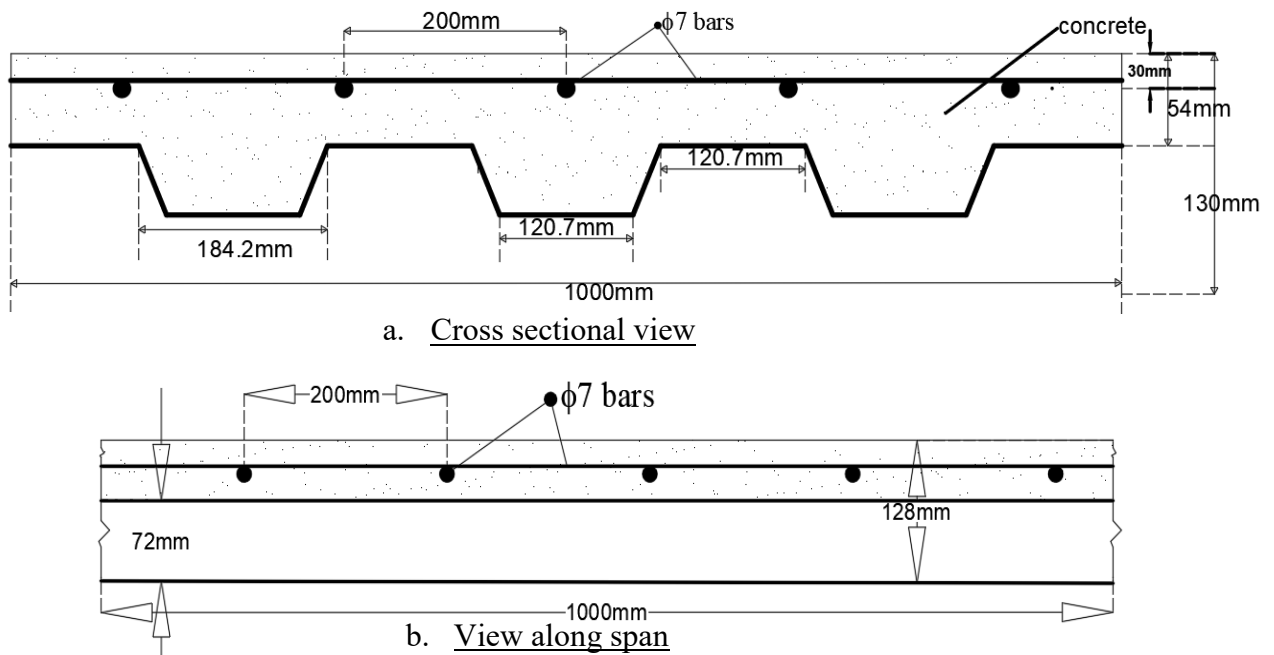
Figure 3.1. Final slab detail

3.5. **Finite Element Analysis of composite slabs**

The model for the composite slab was done with ABAQUS by having recourse the CAE interface and the input file interface as the CONN3D2 elements were more easily assigned using this interface.

3.5.1.Elements

The solid elements for the concrete, the shell elements for the sheet and the Truss elements for the reinforcement are shown in Figure 3.2.

FEM analysis applied to the study of the stress transmission in the corrugated sheet slab
Master of Civil Engineering, defended by: MBOH HELBERT SHAYEH, NASPW, Yaoundé, 2019/2020

78

The mesh size for the concrete was 35mm along the slab direction, while the sheet mesh size was 17.5mm. A smaller mesh size was chosen for the sheet to ease the analysis calculation of the contact interaction, since the Abaqus manual recommends a finer mesh for the slave surface.

3.5.2.Materials

The data used to configure the CDP model for C30/37 concrete and the steel plasticity for the steel components are summarized in this section.

3.5.2.1 Concrete damaged plasticity
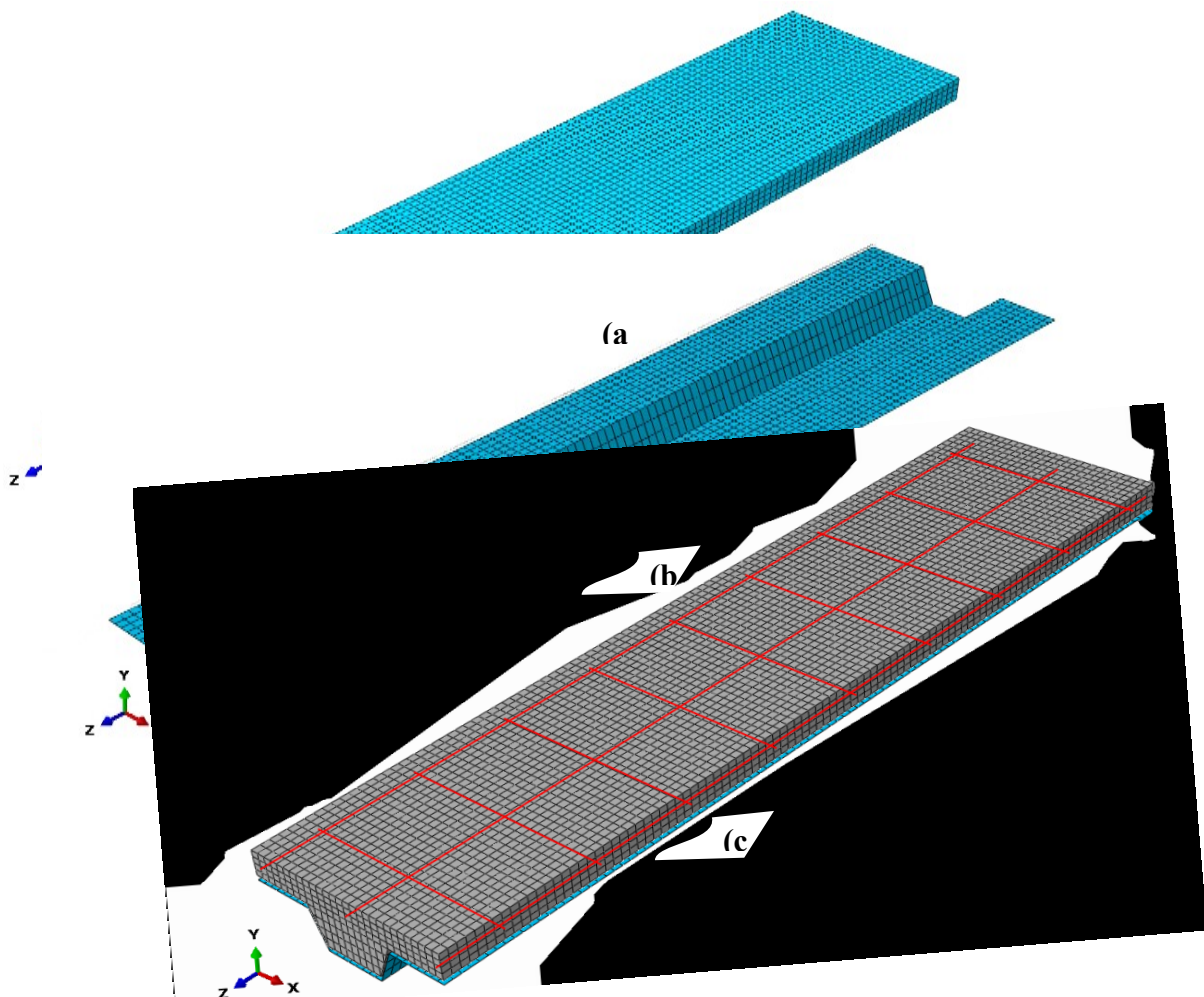
Figure 3.2. Elements for concrete slab, for steel deck and for the wires

FEM analysis applied to the study of the stress transmission in the corrugated sheet slab
Master of Civil Engineering, defended by: MBOH HELBERT SHAYEH, NASPW, Yaoundé, 2019/2020

79

The concrete damaged plasticity model is presented in Table 3.11 below. The plasticity parameters for the calculation of the yield surface were assigned their default values as presented in section 2.4.3.1 , while the damage parameters were calculated using equations (2.29) and (2.30) reported earlier.

Table 3.11. Summary of CDP data for C30/37 concrete

Concrete class	C30/37	Plasticity parameters	
		Dilation angle	31
Concrete Elasticity		Eccentricity	0.1
E (GPa)	26.6	fc0/fb0	1.16
Poisson ratio, v	0.2	K	0.67
		Viscosity parameter	0
Concrete compressive behaviour		Concrete compression damage	
Yield stress (MPa)	Inelastic strain	Damage parameter	Inelastic strain
15.3	0	0	0
22.5	0.000119844	0	0.000119844
25.2	0.000214786	0	0.000214786
27.3	0.000333074	0	0.000333074
28.8	0.000474708	0	0.000474708
29.7	0.000639689	0	0.000639689
30	0.000828016	0	0.000828016
28.8	0.001274708	0.04	0.001274708
27.3	0.001533074	0.09	0.001533074
22.5	0.002119844	0.25	0.002119844
19.2	0.002448249	0.36	0.002448249
15.3	0.0028	0.49	0.0028
10.8	0.003175097	0.64	0.003175097
5.7	0.003573541	0.81	0.003573541
Concrete tensile behaviour		Concrete tension damage	
Yield stress (MPa)	Cracking strain	Damage parameter	Cracking strain
3	0	0	0
0.03	0.001167315	0.99	0.001167315

FEM analysis applied to the study of the stress transmission in the corrugated sheet slab
Master of Civil Engineering, defended by: MBOH HELBERT SHAYEH, NASPW, Yaoundé, 2019/2020

80

3.5.2.2 Steel material properties

The properties for the steel material used to model the concrete reinforcement and the steel decking is reported in Table 3.12.

Table 3.12. Steel material properties

Property	Value
Steel elastic modulus, Es	210 000 [N/mm^2]
Steel Poisson ratio, v	0.3
Yield stress (profiled sheet), fyk	350 [N/mm^2]
Yield stress (mesh reinforcement), fyk	343.1[N/mm^2]

3.5.3.Steel-concrete interaction

The calculated values for the slab slenderness, the coefficients for the shear bond curve interpolation equation (2.31) are shown in Table 3.13 while the approximate shear – end slip behaviour, obtained by interpolation is graphically represented in Figure 3.3.

Table 3.13. Calculation of slab slenderness and corresponding ultimate stresses

Description	Symbol	Value
Slab span between supports	L	3500mm
Shear span	Ls (L/4)	875mm
effective depth	dp	88.73mm
Slenderness of project slab	Ls/dp	9.87
Standard slab 1 (Abdullah, 2009)	Slenderness	12.04
	τ_{max}	0.2728MPa
Standard slab 2 (Abdullah, 2009)	Slenderness	4.51
	τ_{max}	0.1447MPa
Coefficients for interpolation equation (2.31)	p	-0.362
	s	1.9704

FEM analysis applied to the study of the stress transmission in the corrugated sheet slab
Master of Civil Engineering, defended by: MBOH HELBERT SHAYEH, NASPW, Yaoundé, 2019/2020

81
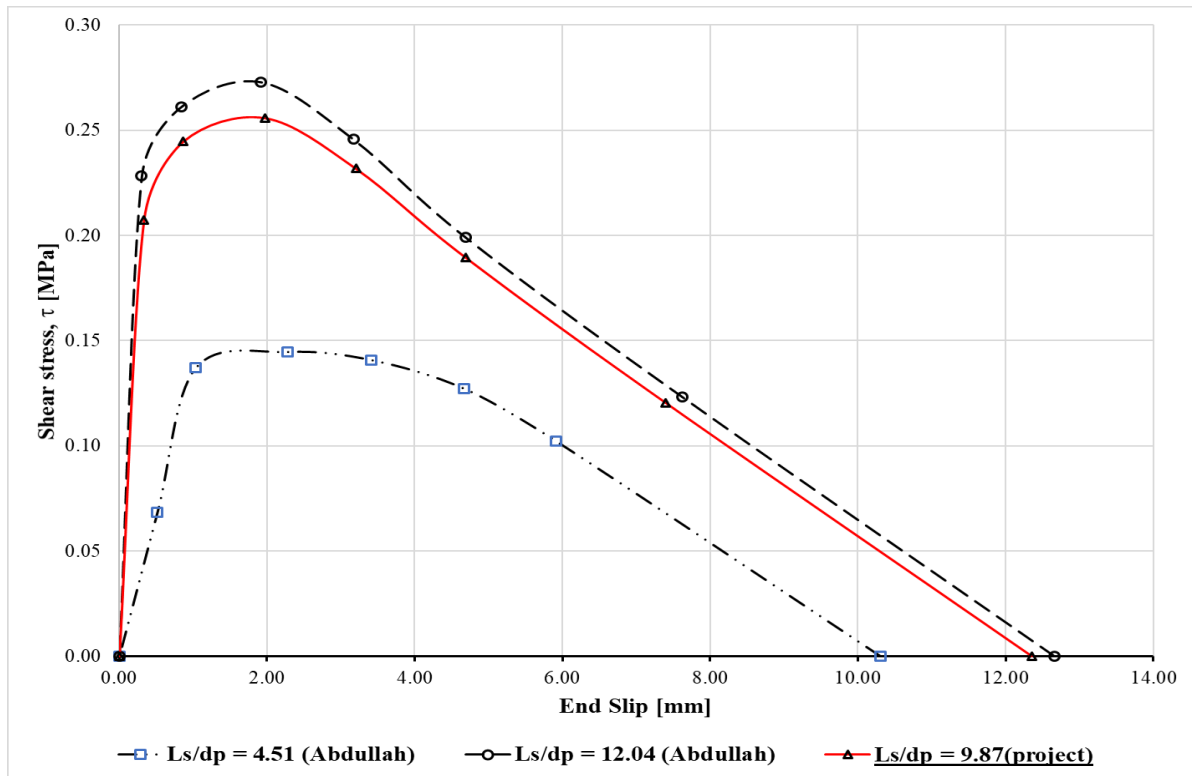
Figure 3.3. Interpolated shear bond curve for project slab.

The spring behaviour calculated according to equation (2.34) for the 'mid-flange' and 'foldline' connector positions are presented in Table 3.14. The nonlinear elastic behaviours are assigned to the radial direction of the connector elements which is parallel to the longitudinal direction of the slabs. This direction is the x-direction for the coordinate system of the connector elements as shown in Figure 3.4 and Figure 3.5.

Table 3.14. Shear bond and connector spring behaviour for the slab.

Shear bond		Spring behaviour at mid-flange		Spring behaviour at foldlines	
τ [MPa]	slip [mm]	Force [N]	displacement [mm]	Force [N]	displacement [mm]
0.0000	0.0000	0.0000	0.0000	0.0000	0.0000
0.2236	0.3105	214.5346	0.3105	254.0541	0.3105
0.2574	0.8479	253.3788	0.8479	300.0539	0.8479
0.2689	1.9342	264.8528	1.9342	313.6415	1.9342
0.2424	3.1780	239.8872	3.1780	284.0770	3.1780
0.1968	4.6890	196.1814	4.6890	232.3200	4.6890
0.1226	7.5670	124.7623	7.5670	147.7448	7.5670
0	12.5908	0.0000	12.5908	0.0000	12.5908

FEM analysis applied to the study of the stress transmission in the corrugated sheet slab
Master of Civil Engineering, defended by: MBOH HELBERT SHAYEH, NASPW, Yaoundé, 2019/2020

82
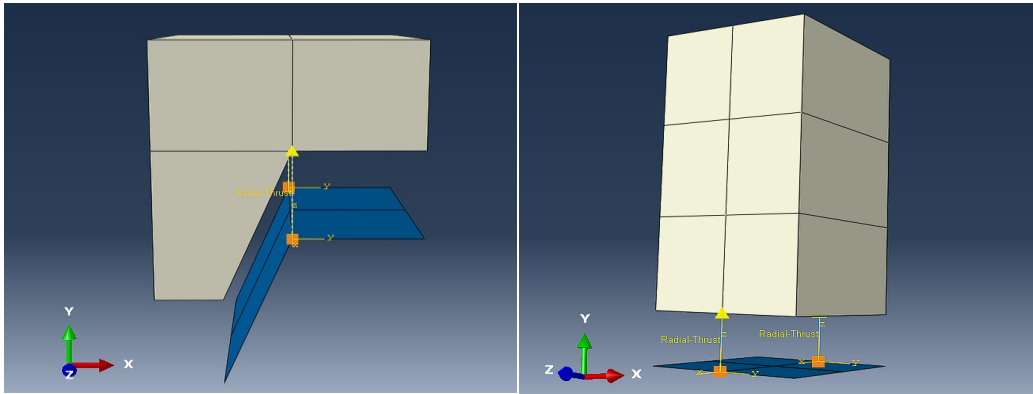
Figure 3.4. Individual radial-thrust connector elements at 'foldline' (left) and 'midflange'(right) positions
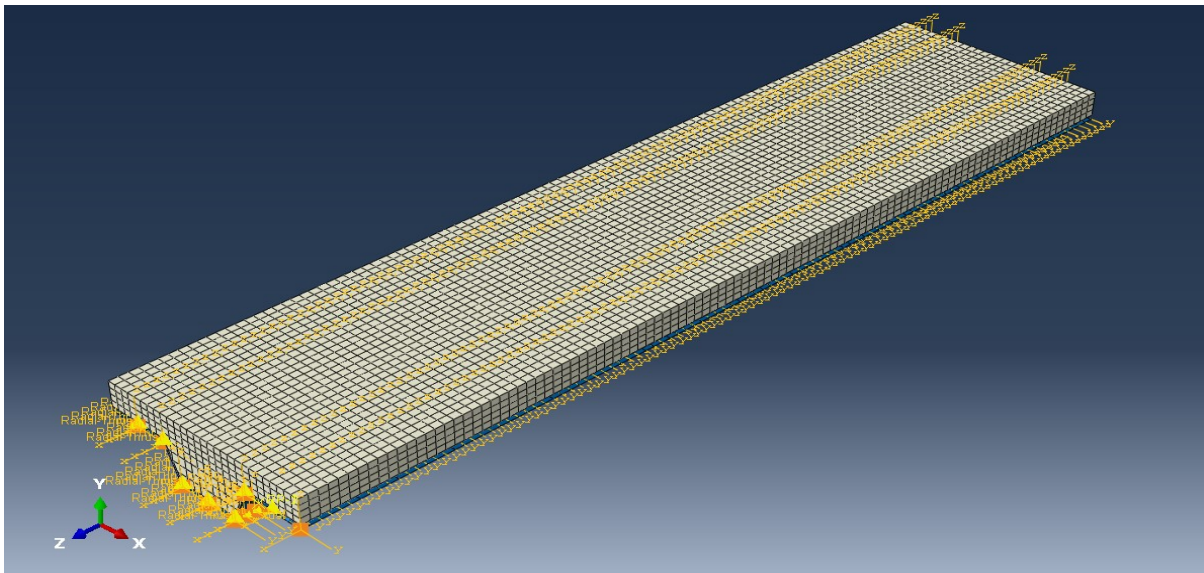
Figure 3.5. Positions of connector elements along slab length

3.5.4. Interactions and boundary conditions

The interactions applied for the contact interaction are summarized in Table 3.15 . The boundary conditions assigned as explained in section 2.4.5 are illustrated in Figure 3.6.

Table 3.15.Contact interactions

Master Surface	Slave surface	Contact property	
		Tangential behaviour	Normal behaviour
Concrete bottom face	Sheet top flanges	• Frictionless	• "Hard" contact • NO separation after contact
	Sheet webs		
	Sheet bottom flange		

FEM analysis applied to the study of the stress transmission in the corrugated sheet slab
Master of Civil Engineering, defended by: MBOH HELBERT SHAYEH, NASPW, Yaoundé, 2019/2020
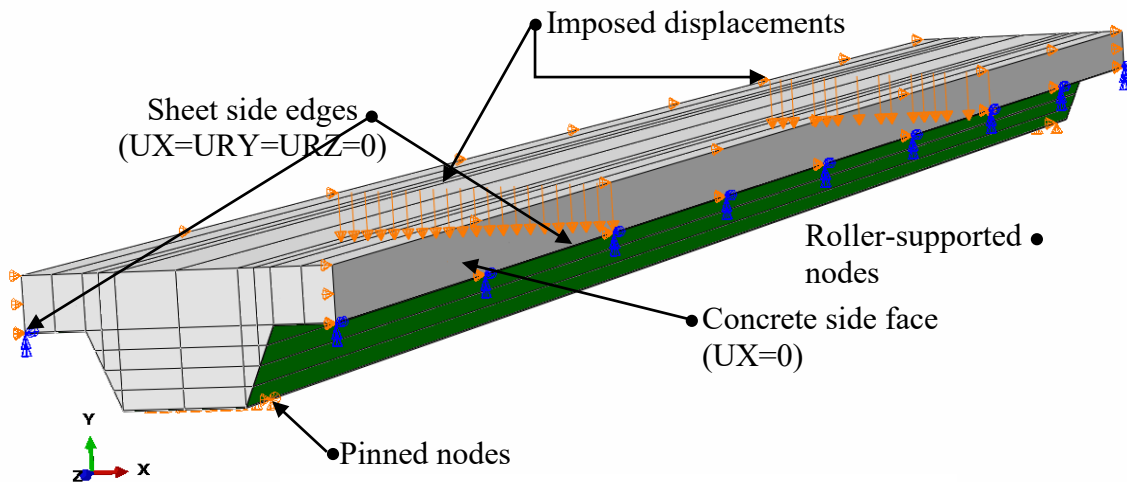
83

Figure 3.6. Boundary conditions for the model

3.5.5. Model verification and study

With all the established parameters of the model in place, the model was then verified to see if its results were within acceptable limits to experimental behaviour. This verification was done by observation of crack propagation and by in-depth comparison of characteristic curves.

The load displacement curve and the load-slip curve of the analysis were compared with the corresponding curves for compact and slender slabs obtained from experiments carried out by Abdullah et al (2004,2007,2009) and Degtyarev (2014). The load for this finite element study is taken as the sum of the reaction force for the nodes that were assigned the roller support constraint, while the displacement was measured from the midspan displacement. The end slip was measured as the difference between the longitudinal displacement of the concrete node and the sheet node at the slab end.

With the model properly verified, the stress distribution in the slab was studied, alongside the buckling development in the sheet. The study each of these mechanical phenomena is explained in this section

3.5.5.1 Crack propagation

With the help of the concrete damaged plasticity model, Abaqus/CAE can provide the user with visual representations on the evolution of cracks in the concrete elements as the load was continually increased. This feature was used to observe the 3D crack propagation in the

FEM analysis applied to the study of the stress transmission in the corrugated sheet slab
Master of Civil Engineering, defended by: MBOH HELBERT SHAYEH, NASPW, Yaoundé, 2019/2020

84

concrete, and to see if the behaviour of the model is concurrent with experimental observations on crack development and propagation.

3.5.5.2 Stress distribution

The stress in the slab was observed at 4 main stages of loading evolution: the ultimate load stage, the serviceability load stage, and 2 other stages before and after cracking. The ultimate stage was taken as the time when the maximum reaction force was reached, while the serviceable stage was taken as the time when 60% of the maximum reaction force was achieved. The stress was then observed along the slab length at 3 main positions: the concrete bottom face, the concrete top face and the sheet bottom flange. In each case, the stresses were averaged across the width, i.e. across the slab width for the concrete top face stresses, and across the width of the rib for the sheet bottom flange and for the concrete bottom face. Due to symmetry of the stresses along the span, the stresses were displayed only for the half-span. The length along the slab was normalized against the slab length to make the tables more presentable. The stresses were also normalized against the concrete tensile stress for the concrete bottom flange, against the concrete compressive strength for the concrete top face and against the yield strength of steel for the steel flange, making it easier to identify areas that have already reached failure.

3.5.5.3 Buckling development

Buckling in the sheet was studied by simply observing the deformed configuration of the sheet at the ultimate load stage and the serviceable load stage, paying special attention to the top flanges and the webs.

Conclusion

With all the static actions taken into account, a complete design and detailing of the corrugated sheet slab was carried out and a finite element model was established with shear bond behaviour approximated from elemental bending tests of similar profiles. The boundary conditions of the model were to emulate the m-k design experimental setup so as to be able to compare the accuracy of the proposed method.

FEM analysis applied to the study of the stress transmission in the corrugated sheet slab
Master of Civil Engineering, defended by: MBOH HELBERT SHAYEH, NASPW, Yaoundé, 2019/2020

85

CHAPTER 4: **FINITE ELEMENT ANALYSIS RESULTS AND INTERPRETATION**

Introduction

The results of the FEM model described in the previous chapter are presented and discussed in this section. They are preceded by a verification of the model characteristic curves and crack pattern, followed by a study on the evolution of stress distribution in the slab and on the development of buckling in the sheet.

4.1. **Model verification**

The model verification constitutes comparing the general observations in the analysis as it pertains to crack propagation and in seeing whether the load displacement curve and the load slip curve will follow conventional slab behaviour.

4.1.1. Crack propagation

The concrete cracking commenced very early in the analysis. The concrete elements in the rib below the line of loading began first to crack. More cracks appeared in the rib concrete, in the zone between the two major cracks and these minor cracks grew in magnitude with loading, until newer cracks were observed beyond the load lines as illustrated in Figure 4.1.
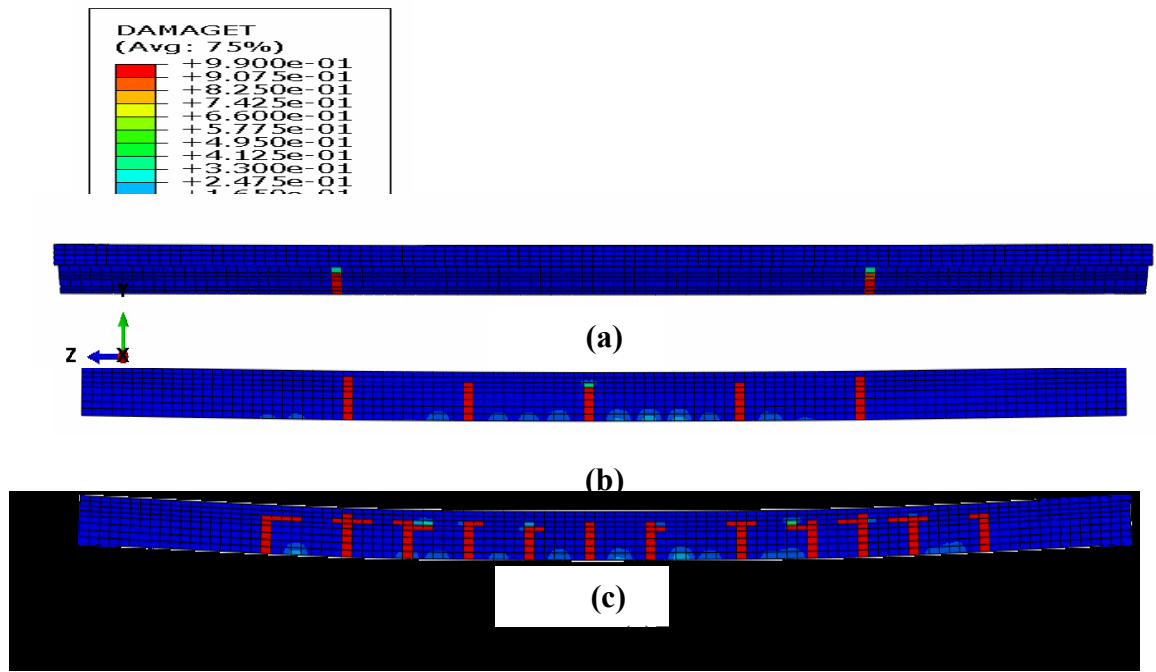
(b)Development of major and minor cracks in the constant moment region (c)More cracks beyond the constant moment region

FEM analysis applied to the study of the stress transmission in the corrugated sheet slab
Master of Civil Engineering, defended by: MBOH HELBERT SHAYEH, NASPW, Yaoundé, 2019/2020

86

The permeance of cracks below the load lines corresponded to observations to the experiments on full scale slabs carried out by Abdullah (2004), while the appearance of cracks firstly in the constant moment region corresponded with the FE model observation by Degtyarev (2014). It was also observed that the cracking propagation direction at failure due to slip was very similar to that observed by Abdullah (2004).
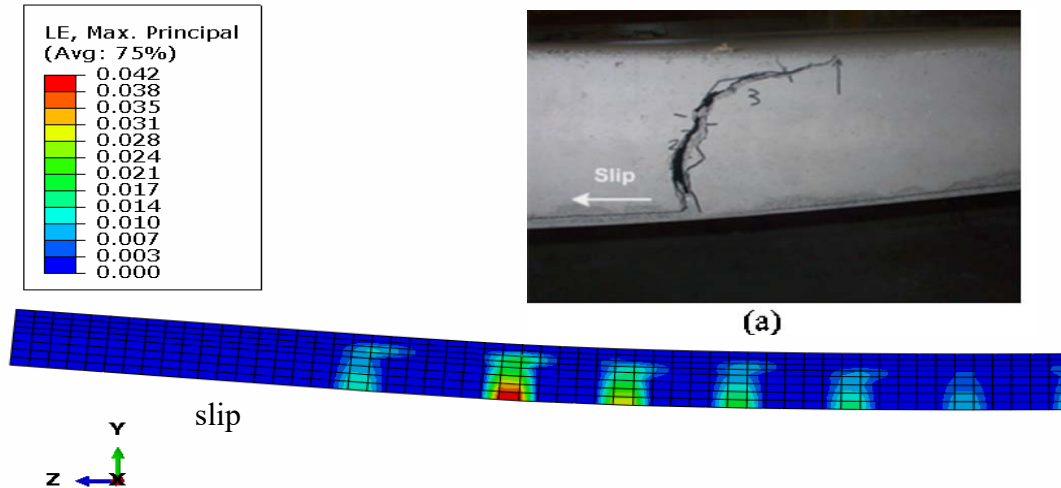
Figure 4.2. Longitudinal strain in the rib of the concrete compared to experimental result(a)

The above observations were favourable to the FE model but are not totally sufficient for proving its validity. The model validity was totally verified through the load-displacement curve and the load-end slip curve reported in the following sections.

4.1.2. Load displacement curve

The total reaction force at the support nodes of one side were plotted against the average displacement of the nodes at the bottom of the sheet in Figure 4.3.

As the displacement was increasingly applied, the support reaction increased linearly, until the material behaviour became nonlinear, at which point the reaction force increased in nonlinear fashion. The ultimate reaction force was eventually obtained, beyond which the stress transfer ability of the slab was increasingly compromised, leading to a steady reduction in the reaction force at the support.

FEM analysis applied to the study of the stress transmission in the corrugated sheet slab
Master of Civil Engineering, defended by: MBOH HELBERT SHAYEH, NASPW, Yaoundé, 2019/2020

87
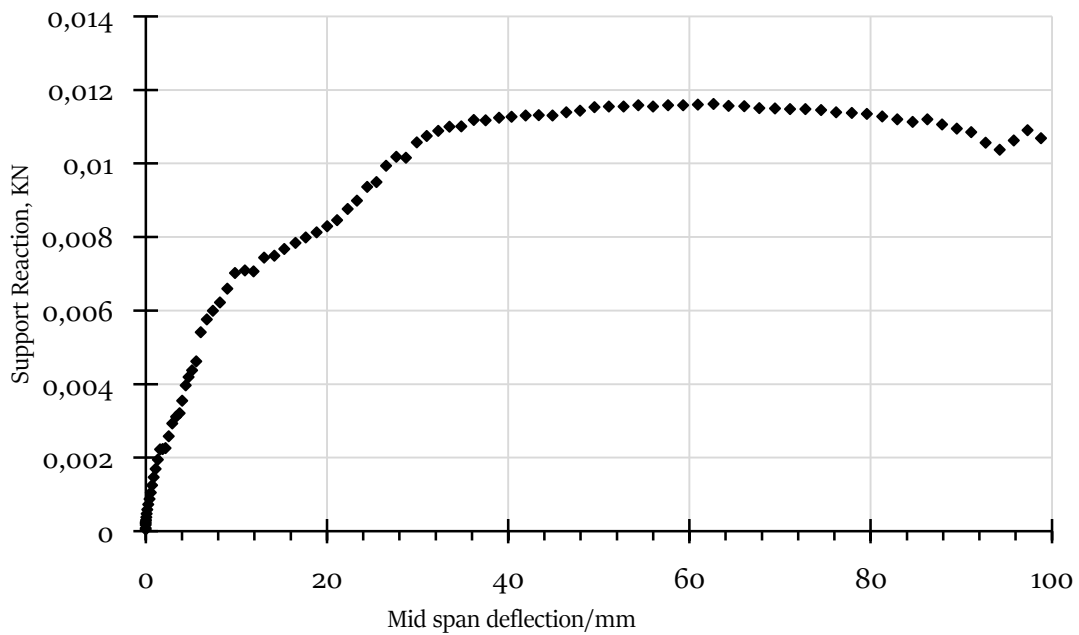
Figure 4.3. Load-displacement curve for the model

This is observed by the decrease in reaction force after the ultimate reaction force of 11.62KN and this behaviour is consistent with that of experimental results observed by Abdullah (2009) compact and slender slabs of similar sheet profile as illustrated in Figure 4.4. From the curve of Figure 4.4, it can be seen that the model slab behaves more like a compact slab than a slender one.
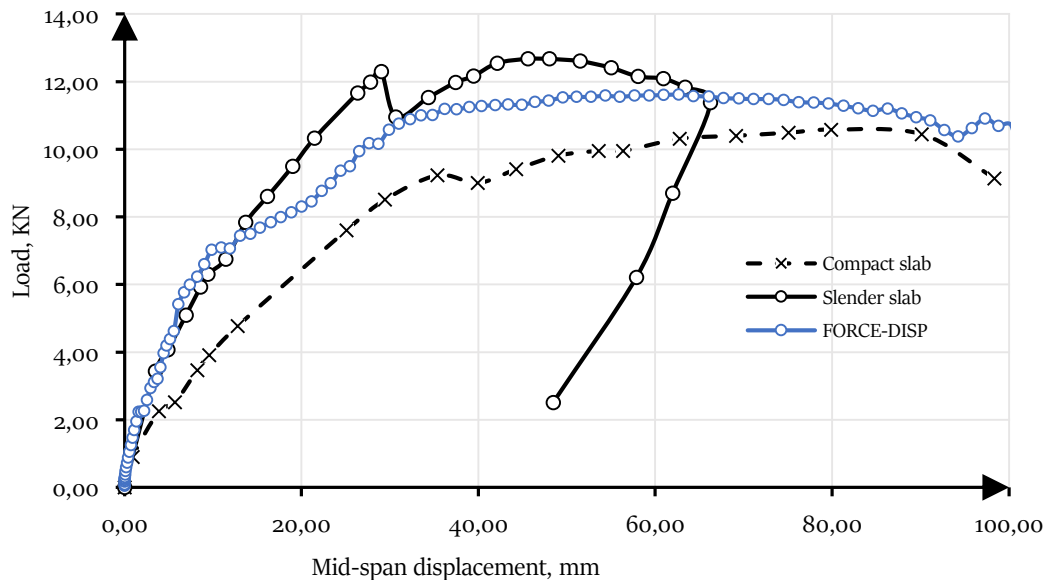
Figure 4.4. Comparison of load-span curve for model with expermiantal results for slabs of similar profiles.

FEM analysis applied to the study of the stress transmission in the corrugated sheet slab
Master of Civil Engineering, defended by: MBOH HELBERT SHAYEH, NASPW, Yaoundé, 2019/2020

88

4.1.3.Load-slip curve

The load slip curve obtained as explained in section 3.5.5 is plotted alongside the corresponding curves obtained from full scale tests carried out by Abdullah (2004) in Figure 4.5. The load slip curve for the model again coherent with expected behaviour of full-scale tests.
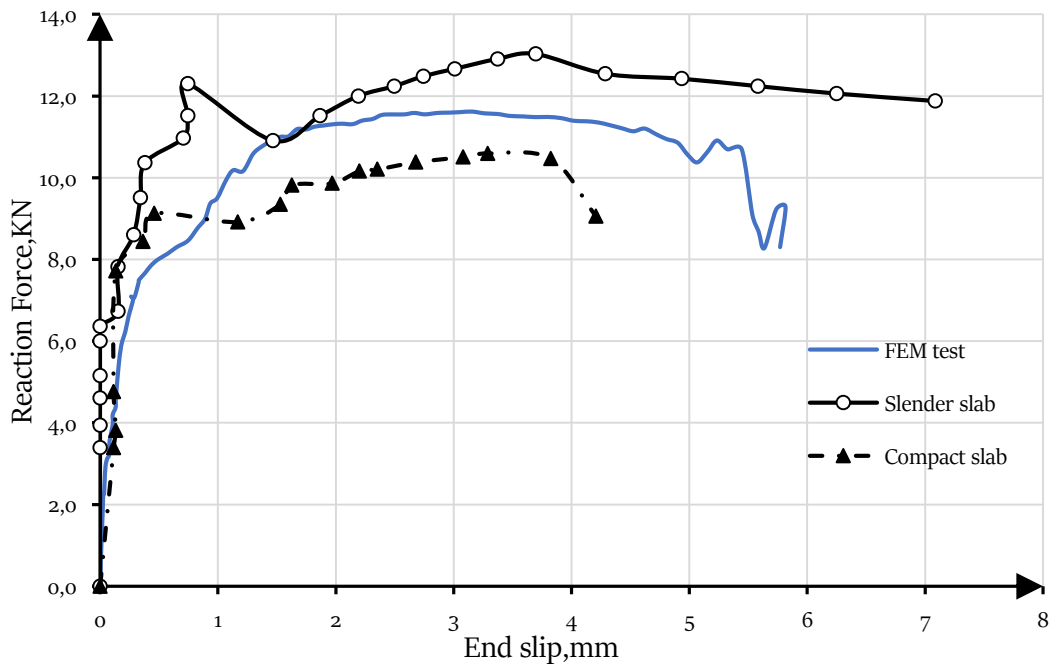
Figure 4.5. Load slip curve

With the model now verified from general observation and from the characteristic curves plotted against full-scale experimental results, the stress distribution and the crack propagation in the slab can now be studied.

4.2. **Stress distribution**

The evolution of stress in the model before and after cracking, and at SLS and ULS are presented in this section. Due to symmetry of results about the span, the stresses are shown for only half the slab span, where the distance is normalized with the slab span. Also presented are the distribution of stress in the sheet at Ultimate limit state. The stresses in each component of the slab is also detailed at the end of this section

FEM analysis applied to the study of the stress transmission in the corrugated sheet slab
Master of Civil Engineering, defended by: MBOH HELBERT SHAYEH, NASPW, Yaoundé, 2019/2020

89

4.2.1.Before and after cracking

The stress distribution along the slab length before and after cracking are shown for the concrete top face, the concrete bottom face and the steel bottom flange in Figure 4.6, where negative stresses indicate compression. As noticed in all the curves of the figure, most of the load was resisted by the sheet bottom flange.

The decrease in stress at the concrete bottom face below the cracking stress of 3MPa indicates the appearance of cracking. This is further evidenced by the sharp increase in compressive stress at the concrete top face and the increased tensile stress at the sheet bottom around the position of load application. This increase in stresses is due to the fall in the depth of the neutral axis as a result of the concrete cracking equally observed by Degtyarev (2014).

FEM analysis applied to the study of the stress transmission in the corrugated sheet slab
Master of Civil Engineering, defended by: MBOH HELBERT SHAYEH, NASPW, Yaoundé, 2019/2020

90

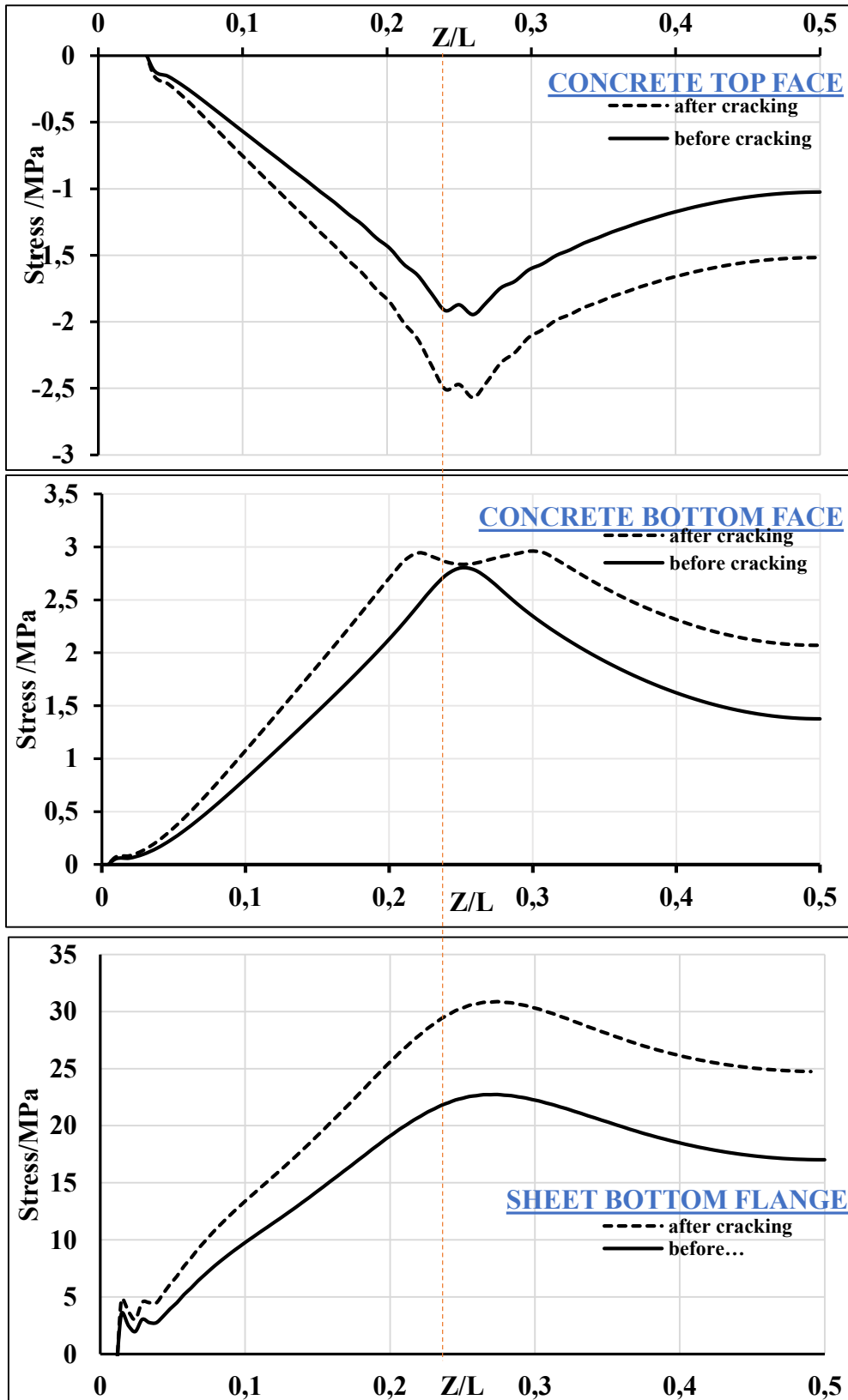**Figure 4.6.** Stress distribution along composite slab before and after cracking. The dashed red line indicates the position of loading in the slab

FEM analysis applied to the study of the stress transmission in the corrugated sheet slab
Master of Civil Engineering, defended by: MBOH HELBERT SHAYEH, NASPW, Yaoundé, 2019/2020

91

4.2.2. Limit states

The stress distribution at the ultimate and serviceability limit states along slab span is presented in Figure 4.7, at the same positions as in the previous section. With the knowledge acquired on stress changes on the advent of cracks in each position, a proper understanding of the cracking in the slab can be made for each state.

At the serviceability state, the concrete top face has 2 stress maxima: one at the load position and the other a distance away. Both spikes in compressive stress indicate the presence of major cracks in the concrete, evidenced by the deep troughs in the stress curves for the concrete bottom face and the crests at the same positions for the sheet flange. The smaller troughs visible in the serviceability state curve for the concrete bottom flange indicate the presence of minor cracks, although there seems to be no abrupt increases in stress at the top face or at the sheet flange. Hence there are 4 major cracks and 6 minor cracks between the two load positions in the concrete bottom, due to symmetry.

At the ultimate load state, the steel flange has yielded at the entire constant moment section due to the increased loading and the growth in cracks and increase in crack width for already present cracks. The plastic neutral axis must now be very high up the concrete. Cracks also develop beyond the constant moment zone as evidenced by the presence of minima out of this zone in the curve for the concrete bottom flange.

FEM analysis applied to the study of the stress transmission in the corrugated sheet slab
Master of Civil Engineering, defended by: MBOH HELBERT SHAYEH, NASPW, Yaoundé, 2019/2020

92
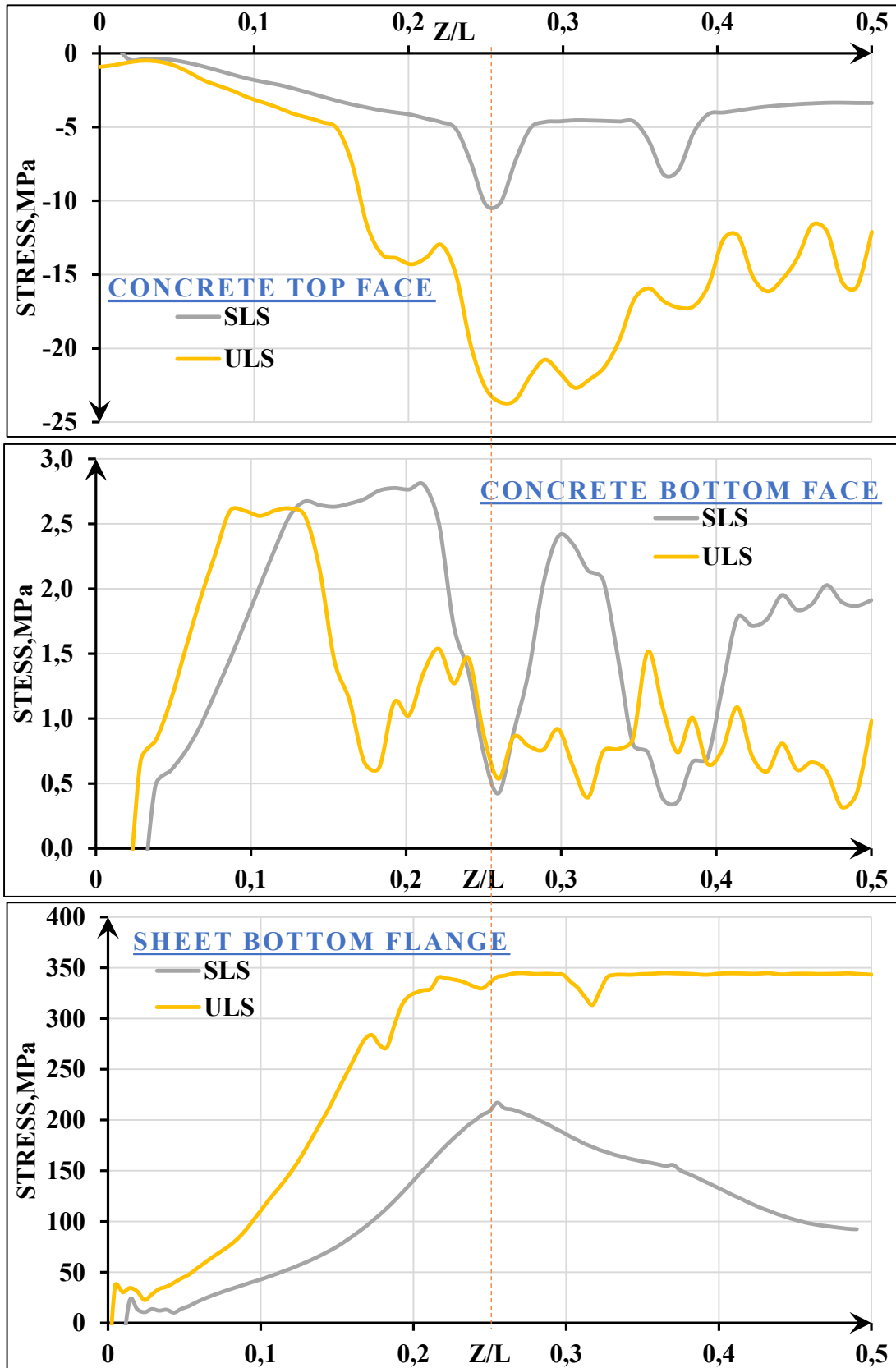
Figure 4.7. Stress distribution in the composite slab model at ULS and SLS

FEM analysis applied to the study of the stress transmission in the corrugated sheet slab
Master of Civil Engineering, defended by: MBOH HELBERT SHAYEH, NASPW, Yaoundé, 2019/2020

93

4.2.3. Stresses in the slab components

The stresses in the slab component of the model are presented and explained in this section.

4.2.3.1 Stresses in the Concrete

The stress obtained at the concrete critical section are discussed, followed by the tensile and compressive stress in all the concrete.

a. Stresses in the critical section

The ULS stress shows that the concrete bottom is already cracked and has lost all its ability to resist. The entire concrete bottom is cracked, all the way to the top, with the exception of a few areas, supported by the concrete reinforcement and the top which bears the compressive loads. It is also noticed the largest compression is achieved above the top flange of the concrete.

Figure 4.8. Stress distribution in the slab critical section

b. Tension in the concrete

The overall tensile stresses at ULS are presented only for half the span due to symmetry of results. The maximum tensile stresses occur at the bottom face of the concrete top flanges. This is likely due to the loss of stress resistance at these locations owing to buckling in the top flange.

FEM analysis applied to the study of the stress transmission in the corrugated sheet slab
Master of Civil Engineering, defended by: MBOH HELBERT SHAYEH, NASPW, Yaoundé, 2019/2020
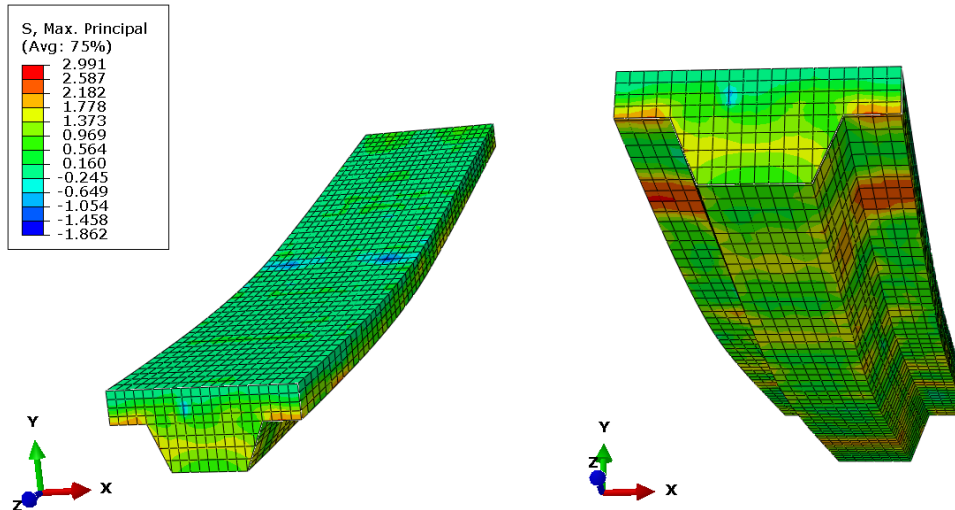
94

Figure 4.9. Tensile stresses in the concrete at ULS

c. Compression in the concrete

The overall tensile stresses at ULS are presented for half the span due to symmetry of results. The maximum compressive forces are located at the zones where the imposed displacement was applied.
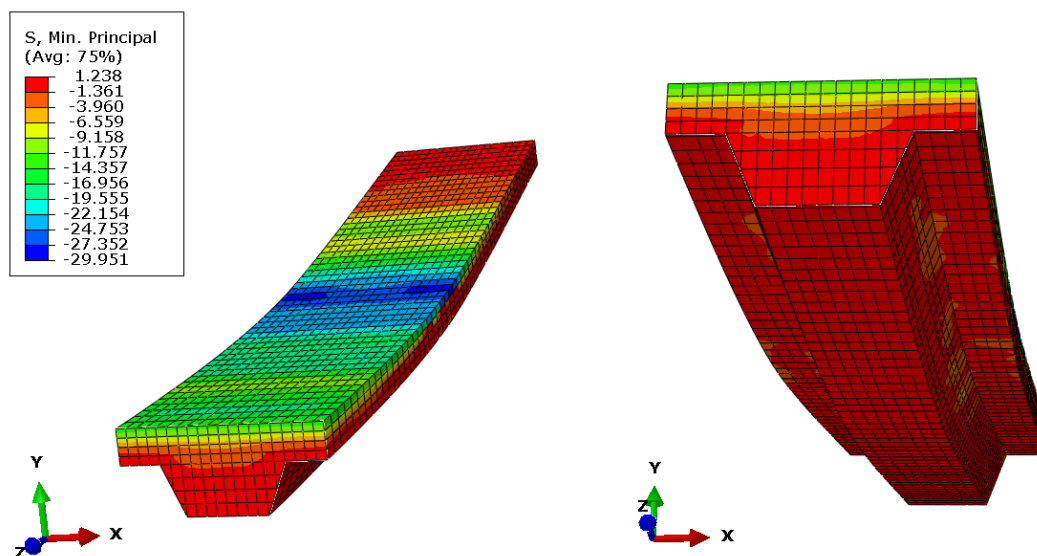

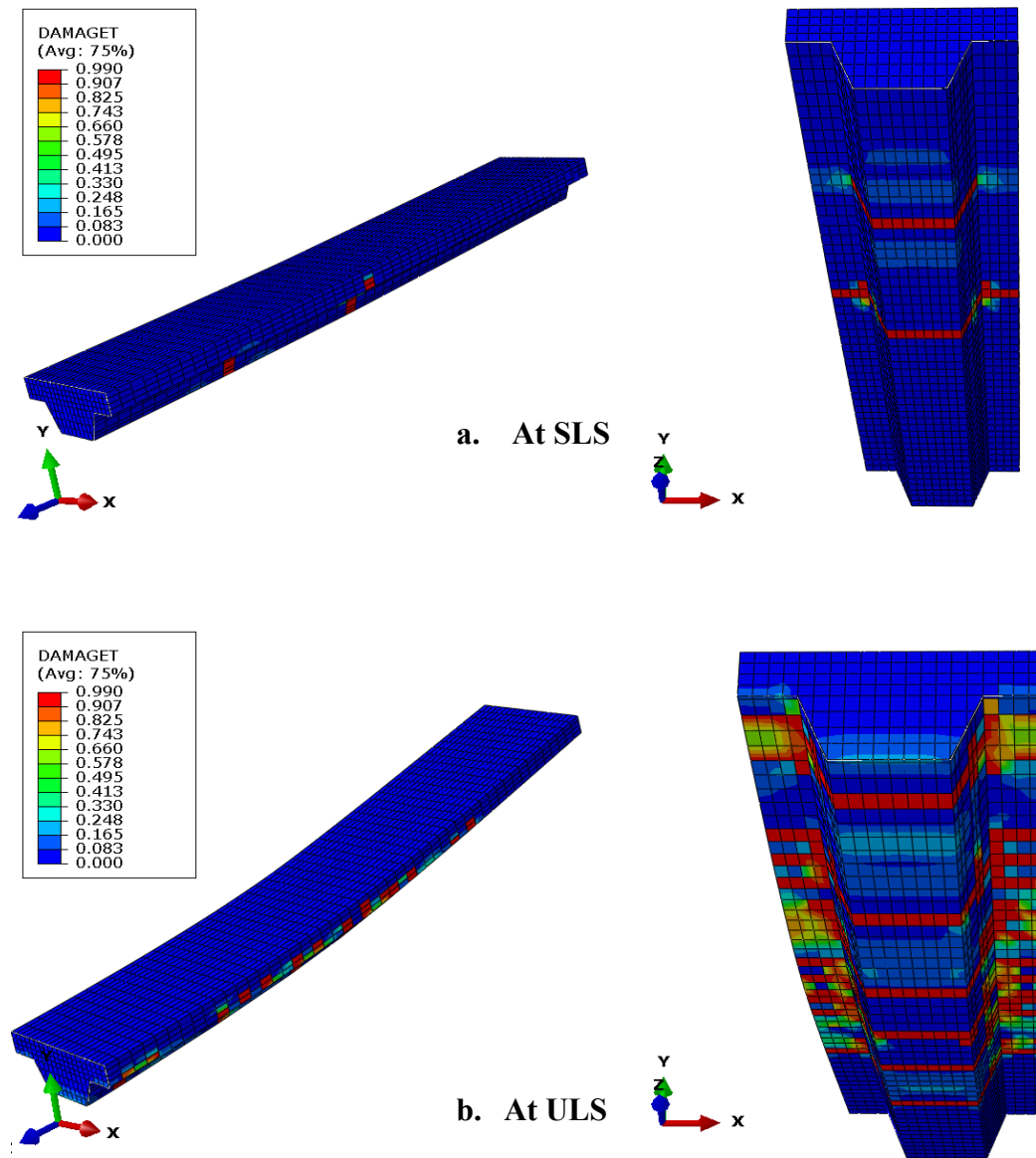**Figure 4.10.** Concrete compressive stresses at ULS (half-span for better view)

FEM analysis applied to the study of the stress transmission in the corrugated sheet slab
Master of Civil Engineering, defended by: MBOH HELBERT SHAYEH, NASPW, Yaoundé, 2019/2020

95

d. Crack pattern in the concrete

The crack pattern along the in the concrete is presented in the figures below. Figure 4.11 shows the crack pattern in the concrete at serviceability limit state and at ultimate limit state for the half span. The evolution of cracking from the bottom of the concrete unto the concrete at the flanges is observed, followed by a longitudinal propagation of the cracks along the slab width. The cracks for the full span at ULS are shown in for the entire slab and in the ribs in Figure 4.12.

a. At SLS

b. At ULS

Figure 4.11. Crack pattern in the concrete(half-span)

FEM analysis applied to the study of the stress transmission in the corrugated sheet slab
Master of Civil Engineering, defended by: MBOH HELBERT SHAYEH, NASPW, Yaoundé, 2019/2020
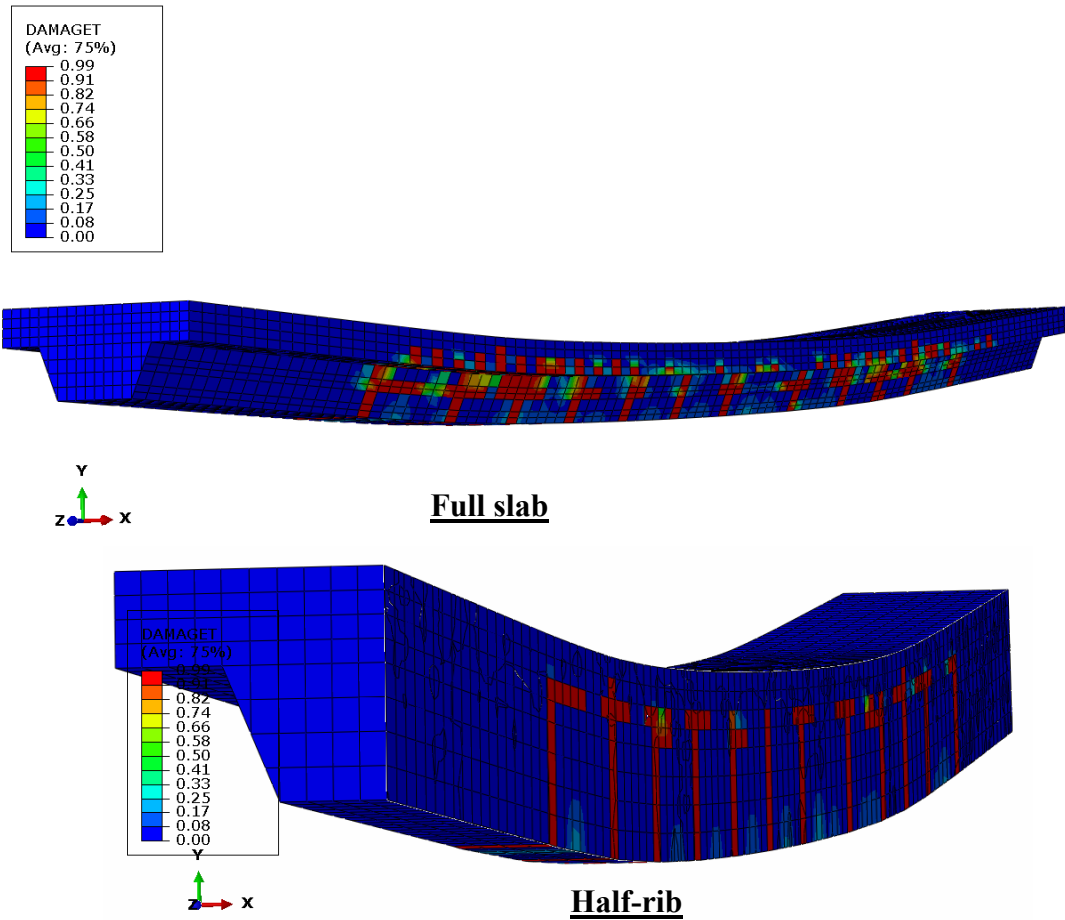
96

Figure 4.12. Crack pattern along in the concrete for the full-span

4.2.3.2 Concrete reinforcement

The presence of the concrete reinforcement is widely responsible for the subtle differences that have been noticed over the course of the model. The presence of the reinforcement is widely responsible for the non-uniformity of stress in the slab over the constant moment region of the span. The stresses in the reinforcement are discussed below.

a. Tensile stresses

The tensile stresses in the concrete reinforcement are shown in Figure 4.13. As can be seen, the stresses are highest around the regions where the imposed displacements were assigned. At ULS, the bottom concrete at these positions had already crack with sufficient opening widths, leading to a neutral axis higher up the reinforcement depth. As a result, the concrete

FEM analysis applied to the study of the stress transmission in the corrugated sheet slab
Master of Civil Engineering, defended by: MBOH HELBERT SHAYEH, NASPW, Yaoundé, 2019/2020

97

reinforcement together with the steel sheet act as tensile reinforcement at all locations of major cracked sections.
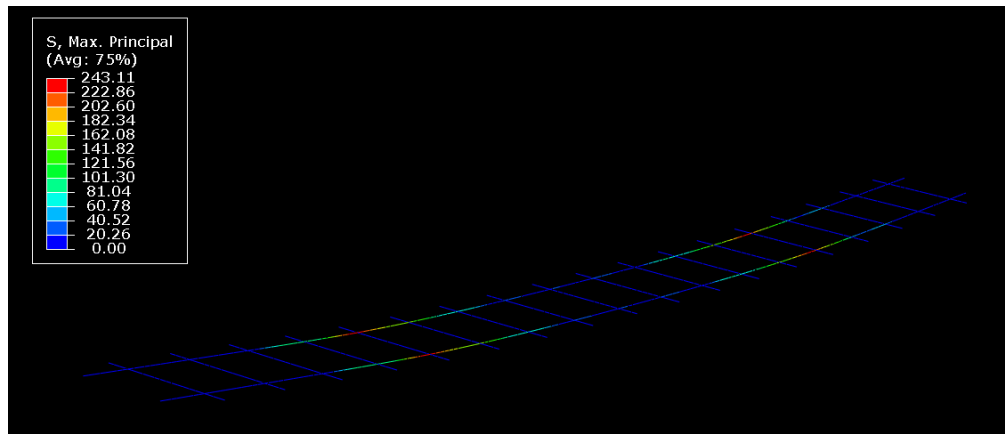

Figure 4.13. Tensile stresses in the concrete mesh

b. Compressive stresses

Figure 4.14 shows the compresses stresses in the reinforcement at ULS. With the many cracks now present in and around the constant moment region, the maximum tensile stress in the concrete bottom shifts to the end position, resulting in an increase in the depth of the neutral axis here. The concrete reinforcement at the ends thus assist as compressive reinforcement due the many cracks developed in the section.

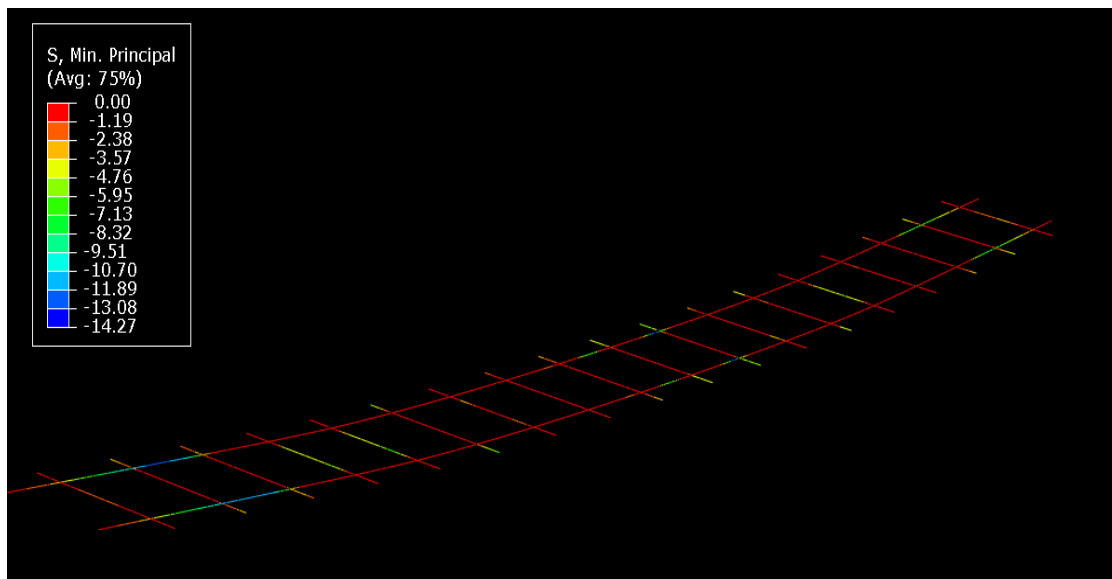**Figure 4.14.** Compressive stresses in the concrete reinforcement

FEM analysis applied to the study of the stress transmission in the corrugated sheet slab
Master of Civil Engineering, defended by: MBOH HELBERT SHAYEH, NASPW, Yaoundé, 2019/2020

98

4.2.3.3 Stresses in the corrugated sheet

The stresses obtained in the corrugated sheet at ULS are discussed, alongside the evolution of buckling in parts of the sheet.

a. Tensile stresses

The tensile stresses in the corrugated profile are presented in Figure 4.15 uniquely at ultimate load phase for the analysis. Most of the bottom flange is already yielded especially in the constant moment zone. Most of the web in the span is under tension due to the low depth of the plastic neutral axis at these positions owing to cracking in the concrete bottom. Positive moments are noticed in the top flange due to the existence of buckles.
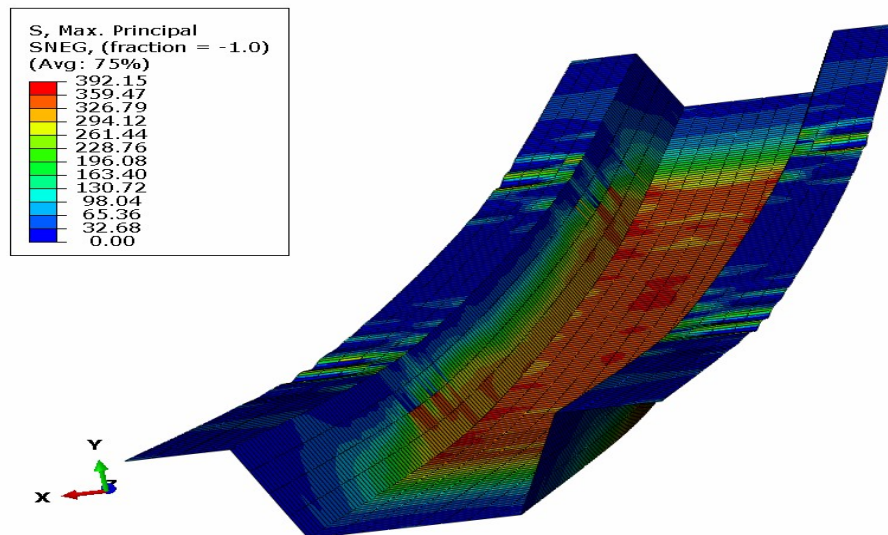

Figure 4.15. Tensile stresses in the corrugateed sheet

b. Compressive stresses

The compressive stresses in the steel sheet are shown in Figure 4.16.

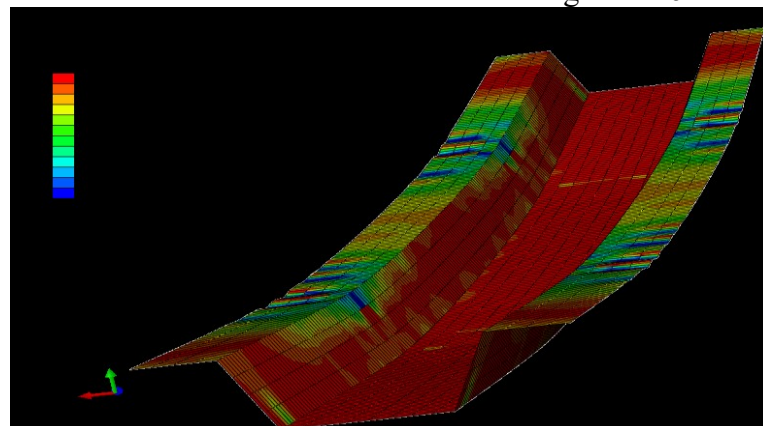**Figure 4.16.** Compression in the corrugated steel sheet

FEM analysis applied to the study of the stress transmission in the corrugated sheet slab
Master of Civil Engineering, defended by: MBOH HELBERT SHAYEH, NASPW, Yaoundé, 2019/2020

99

4.2.3.4 Plastic deformations in the sheet

The plastic deformations in the sheet indicated the zones that have already yielded. As can be seen from F, the zones of load application are very much yielded at ULS, especially due to the tensile stresses at the bottom flange. The yielding at the top flanges are principally due to the buckling in the sheet which will be discussed in the next section.
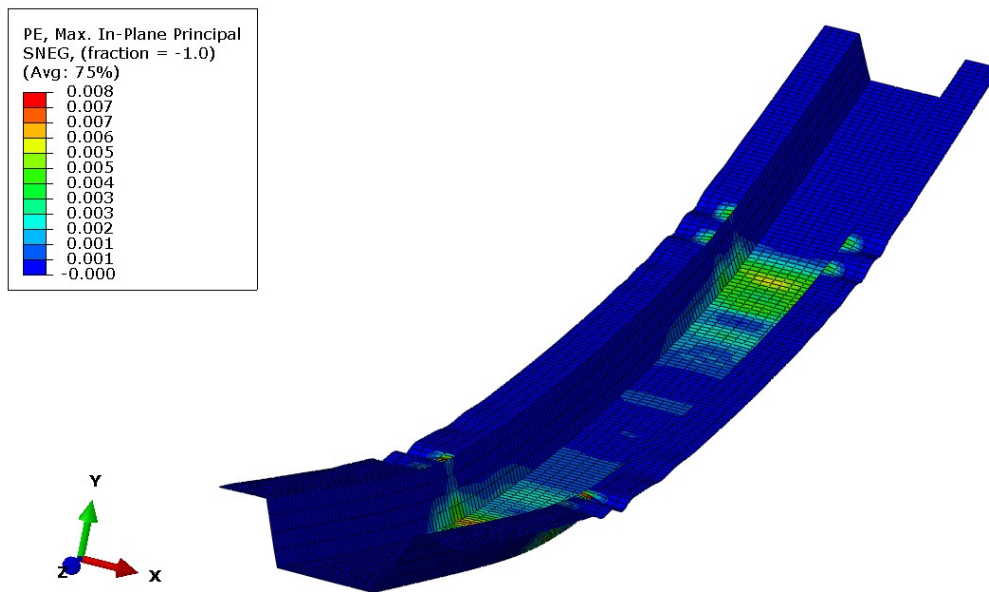

Figure 4.17. Plastic deformations in the corrugated sheet

4.3. **Buckling**

The buckling in the sheet was observed at the top flanges, exactly below the points of load application on either side of the slab before reaching the ultimate state. The deformation is confirmed to be a buckle because the steel had not yet yielded at the flanges at this moment. The buckles grew in magnitude and in number about the sheet section before ultimate state was reached and kept increasing before the slab totally failed as observed by Crisinel and Marimon (2004).

A generally large buckle was observed at the slab breakdown, represented in Figure 4.20 which is coherent with the full-scale experiments from Abdullah (2004). The depth of the buckle was measured to be about 5cm. Web buckling was also observed at the slab breakdown state as evidenced by the deformation peaks in the web of Figure 4.21.

FEM analysis applied to the study of the stress transmission in the corrugated sheet slab
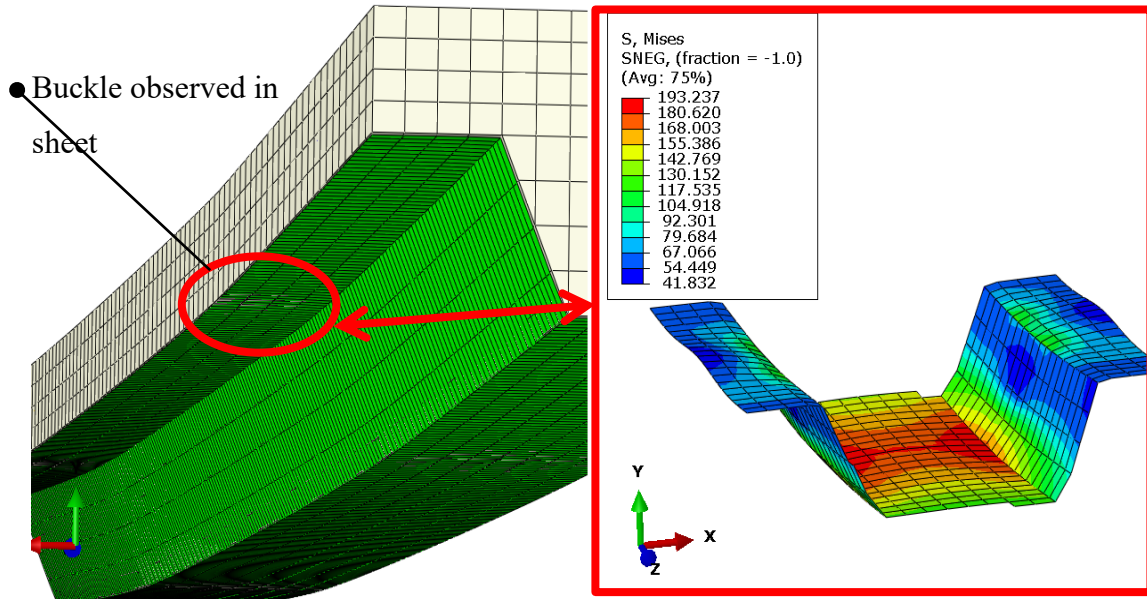Master of Civil Engineering, defended by: MBOH HELBERT SHAYEH, NASPW, Yaoundé, 2019/2020

100

Figure 4.18. Early buckling in sheet before ULS.
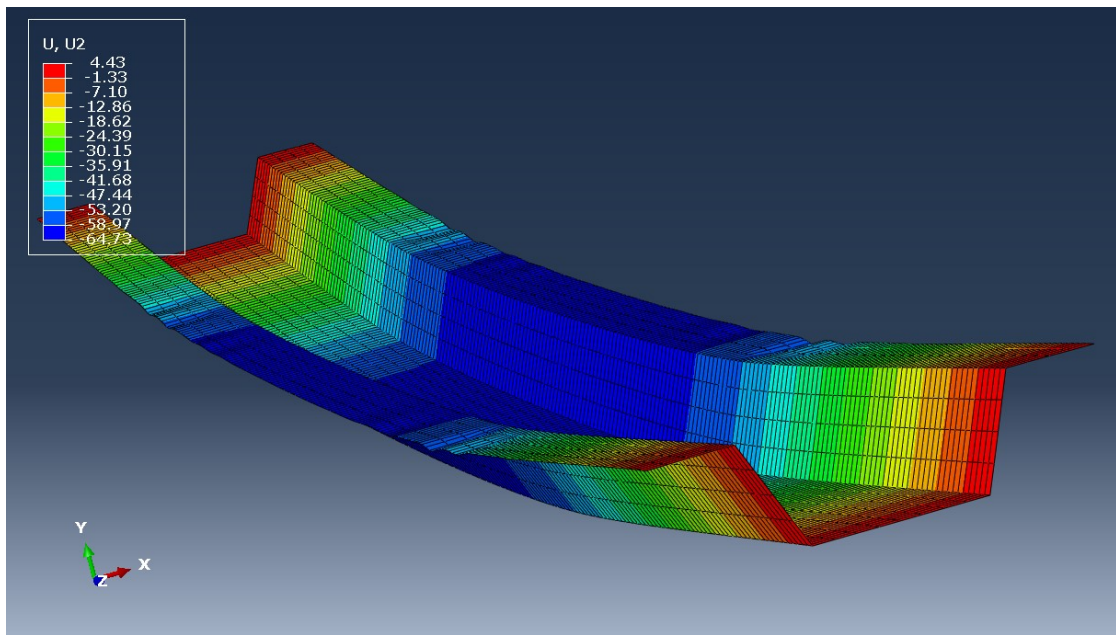
Figure 4.19. Buckling in sheet at ULS

FEM analysis applied to the study of the stress transmission in the corrugated sheet slab
Master of Civil Engineering, defended by: MBOH HELBERT SHAYEH, NASPW, Yaoundé, 2019/2020

101
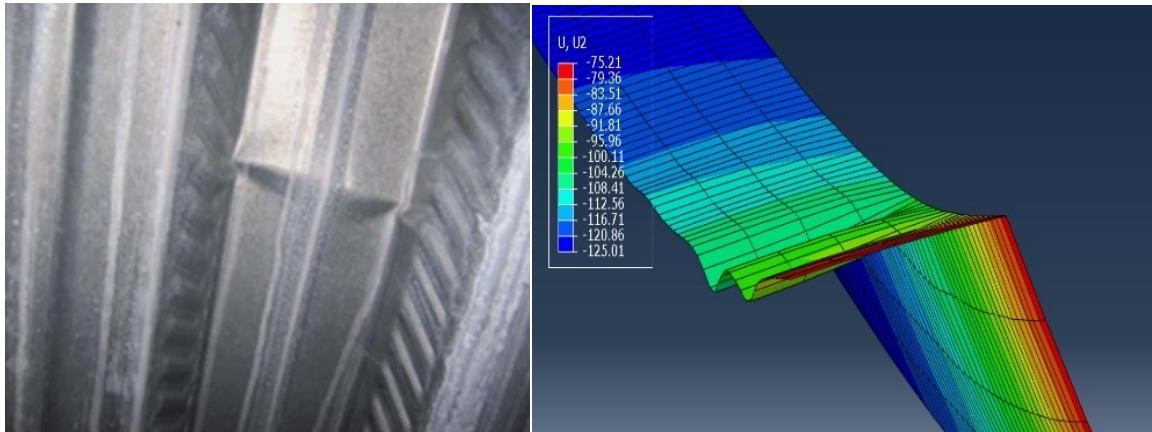
Figure 4.20. Buckling in the top flange of the sheet observed by Abdullah (2009) in experiment and the model at the slab failure
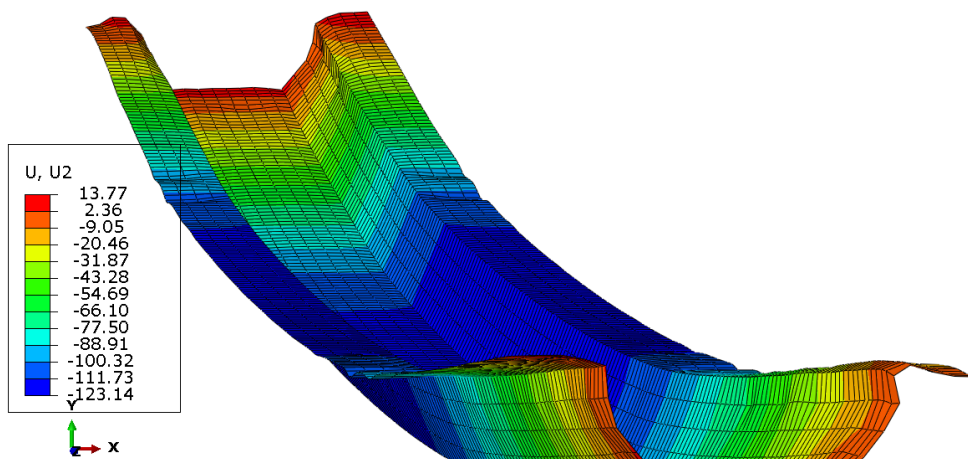
Figure 4.21. Top flange buckling at slab failure
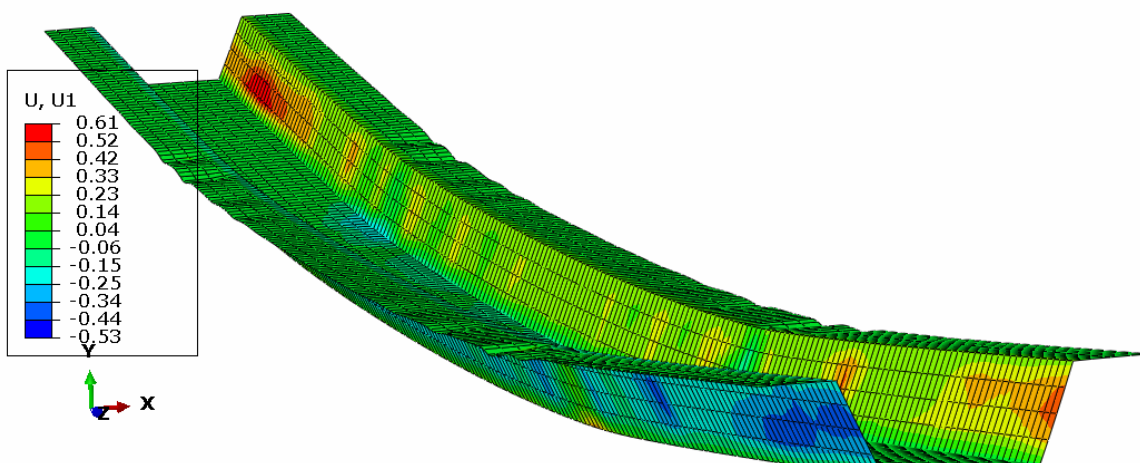
Figure 4.22. Web buckling at slab failure

FEM analysis applied to the study of the stress transmission in the corrugated sheet slab
Master of Civil Engineering, defended by: MBOH HELBERT SHAYEH, NASPW, Yaoundé, 2019/2020

102

4.4. **Connector element results**

The longitudinal forces and displacements in the connector elements from the analysis at the ultimate limit state are presented in Figure 4.23 and Figure 4.24. The longitudinal displacement of the connector elements is equivalent to the slip between the concrete and the sheet From Figure 4.24, the slip in the slab could be seen to be maximum at the ends of the slab, and minimum at the midspan as noticed by Abdullah (2004). The longitudinal force-displacement graph for the element at the end of the span in Figure 4.25 reveals similar behaviour to the shear stress-end slip curve used to configure the shear bond in the connectors.

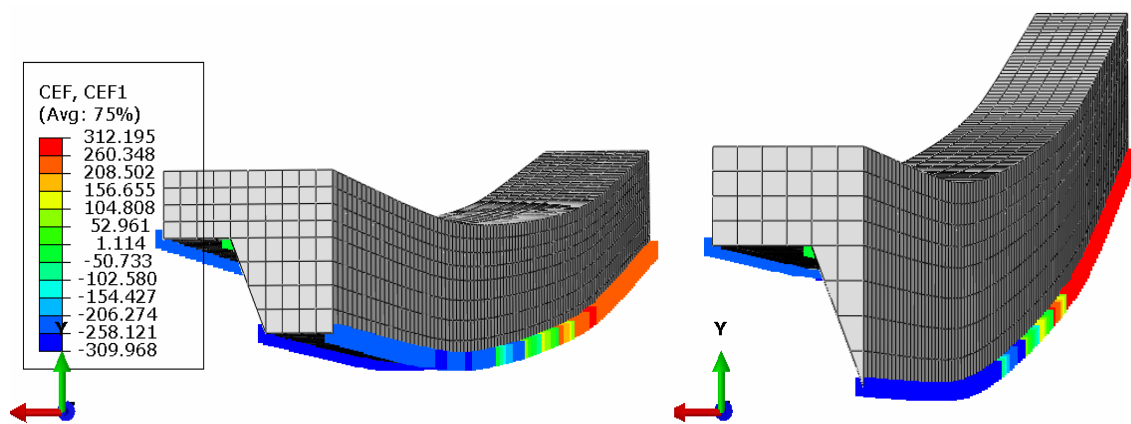**Figure 4.23.** Connector forces in the longitudinal direction at ULS. At the midflange (left) and at the foldline positions

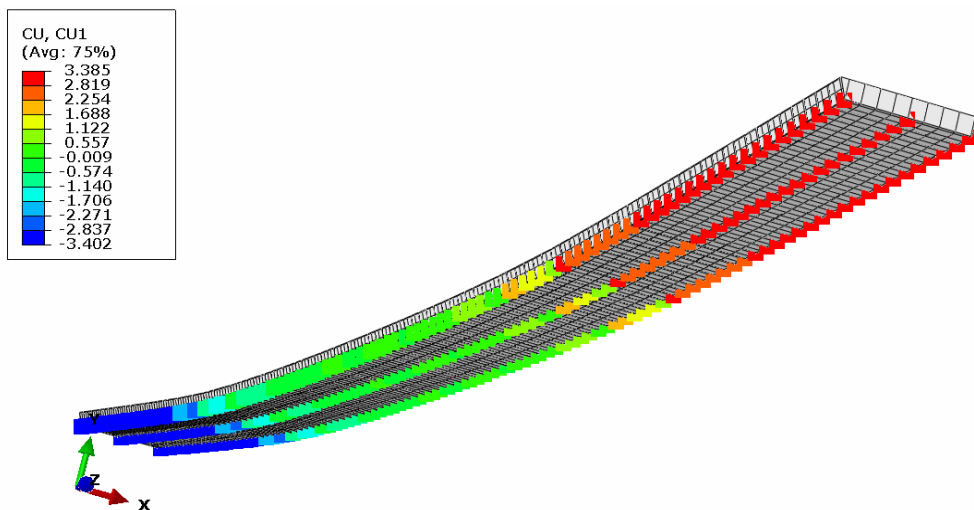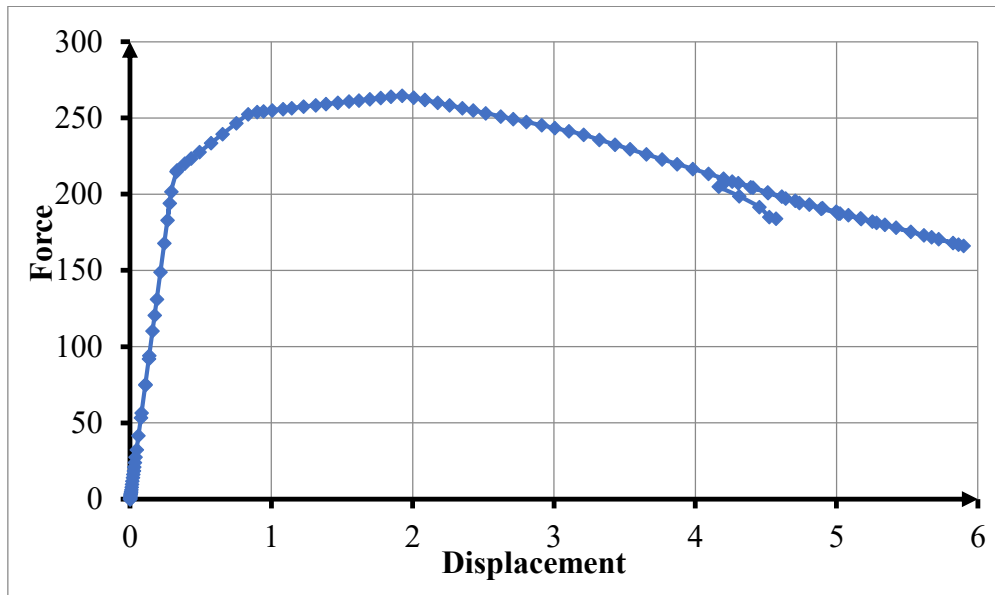**Figure 4.24.** Connector longitudinal displacement along the bottom flange

FEM analysis applied to the study of the stress transmission in the corrugated sheet slab
Master of Civil Engineering, defended by: MBOH HELBERT SHAYEH, NASPW, Yaoundé, 2019/2020

103

Figure 4.25. Force-displacement curve for connector element at the slab end

Conclusion

The analysis results of this study have endeavoured to present the finite element analysis of the numerical model of the slab designed in the previous chapter, subjected to similar boundary conditions as in the m-k experimental test of slab design. A nonlinear finite analysis of the composite slab was performed first to judge the accuracy of a FEM test and then to capture the stress distribution in each component of the slab and to see the cracking and buckling behaviours in the slab. Comparing the FEM results with experimental results verified the mechanical behaviour of the model. Concrete damage plasticity material model is applied to the numerical procedure as a distributed plasticity over the whole geometry of the specimens to appropriately simulate material nonlinearity. The results obtained for the slab showed that the cracking in the concrete bottom leads to the beginning of many nonlinear effects and when prolonged engages high displacements of the neutral axis, leading to the contribution of the antic crack reinforcement and yielding in the steel sheet. While the objective of the work was obtained, more is recommended for the FEM to be decisive in slab design. As a first resort, more accuracy is obtainable if the elemental bending tests are carried out for many sheet profiles, so as to not have to approximate for each section. Also, full scale models incorporating the supporting beams are recommended to take into account the effects of end anchorage as well as buckling and post-buckling analyses to understand the role of buckles in the weakening of the sheet.

FEM analysis applied to the study of the stress transmission in the corrugated sheet slab
Master of Civil Engineering, defended by: MBOH HELBERT SHAYEH, NASPW, Yaoundé, 2019/2020

104

GENERAL CONCLUSION

Composite slabs are a confident solution to building and bridge decking, due to the structural consistency of the steel sheets that can be laid on the supporting frame and the concrete cast without the necessity of propping. Considering the high cost and difficulty of designing composite slabs by current experimental design procedures, a FE model was proposed based on research findings that determined the shear bond behaviour by carrying out small scale bending tests. The model unlike the full-scale tests incorporated the slab reinforcement at the design concrete cover. Geometrical and material nonlinearity was applied for each component of the model in a quasi-static analysis carried out on a designed slab using ABAQUS/Explicit. The shear bond behaviour was modelled by assigning nonlinear spring properties to connector elements assigned between the nodes of the concrete bottom face and the sheet flanges. The connector properties were approximated from shear bond curves of a slender and compact slab of the same sheet profile, obtained via elemental bending tests. The validation of the model with a large number of test results showed agreement between experimental and numerical results. The load-displacement curve and the load-slip curve of the models agreed with load-displacement curves obtained in experiments and other numerical tests. The stresses (mises, tensile, compressive) were studied in the concrete, the sheet and the reinforcement. The arrival of cracks in the concrete was seen to be decisive in leading to non-linearity in the section and for the contribution of the reinforcement to deformation. Buckling in the flange was found to not overly disturb the resistance of the slab until a high proportion of buckles were developed in the section. The results of the study performed in this work demonstrated that the finite element model suggested in this work adequately simulates composite slabs under the conditions of the shear bond experimental tests. The work recommended full-scale numerical models incorporating the supporting steel beam to model the experimental conditions without neglecting end anchorage. Alongside this, more elemental bending tests need to be carried out for different sheet profiles, to ease the work of designers who will simply need to approximate the shear bond behaviour for their slab section.

FEM analysis applied to the study of the stress transmission in the corrugated sheet slab
Master of Civil Engineering, defended by: MBOH HELBERT SHAYEH, NASPW, Yaoundé, 2019/2020

105

BIBLIOGRAPHY

Abdullah, R. (2004) Experimental Evaluation and Analytical Modeling of Shear Bond in Composite Slabs.

Abdullah, R. and Samuel Easterling, W. (2009) "New evaluation and modeling procedure for horizontal shear bond in composite slabs," Journal of Constructional Steel Research, 65(4). doi: 10.1016/j.jcsr.2008.10.009.

American Society of Civil Engineers (1994) Standard for the Structural Design of Composite Slabs: ANSI/ASCE 3-91, ANSI Approved December 11, 1992 ; Standard Practice for Construction and Inspection of Composite Slabs : ANSI/ASCE 9-91, ANSI Approved December 11, 1992. American Society of Civil Engineers (ANSI/ASCE).

An Li (1993) (1993). "Load Bearing Capacity and Behaviour of Composite Slabs with Profiled Steel Sheet,"

Bathe, K.-J. (2006) Finite Element Procedures.

Crisinel, M. and Marimon, F. (2004) "A new simplified method for the design of composite slabs," Journal of Constructional Steel Research, 60(3–5), pp. 481–491. doi: 10.1016/S0143-974X(03)00125-1.

Eurocode 4 (2004) Design of composite steel and concrete structures, Part 1.1: General rules and rules for buildings, Brussels, Belgium: European Committee for Standardization. .

F. C. Filippou (2015) "Mechanics and Materials Finite Element Analysis of Reinforced Concrete Structures."

Johnson, R. P. (2008) Composite Structures of Steel and Concrete: Beams, Slabs, Columns, and Frames for Buildings. Wiley. Available at: https://books.google.cm/books?id=DGH9PwbFpOgC.

Lawson, R. et al. (1999) "Slimflor and slimdek construction: European developments," in.

FEM analysis applied to the study of the stress transmission in the corrugated sheet slab
Master of Civil Engineering, defended by: MBOH HELBERT SHAYEH, NASPW, Yaoundé, 2019/2020

106

Li An and Krister Cederwall (1994) Slip and Separation At Interface of Composite Slabs. Saint Louis, Missouri.

Noor, A. K. and Peters, J. M. (1991) "Strategies for large scale structural problems on high-performance computers," Communications in Applied Numerical Methods, 7(6). doi: 10.1002/cnm.1630070607.

Patrick, M. and Bridge, R. Q. (1992) "Design of Composite Slabs for Vertical Shear," in Engineering Foundation Conference on Composite Construction in Steel and Concrete II. New York: American Society of Civil Engineers, pp. 304–322.

Porter, M. L. et al. (1976) ""Shear-Bond Analysis of Steel-Deck-Reinforced Slabs," Journal of the Structural Division, 102(ST12).

Qureshi, J., Lam, D. and Ye, J. (2011) "The influence of profiled sheeting thickness and shear connector's position on strength and ductility of headed shear connector," Engineering Structures, 33(5), pp. 1643–1656. doi: 10.1016/j.engstruct.2011.01.035.

Rackham, J. W. et al. (2009a) Composite slabs and beams using steel decking: best practice for design and construction. Metal Cladding & Roofing Manufacturers Association in partnership with the Steel Construction Institute.

Rackham, J. W. et al. (2009b) Composite slabs and beams using steel decking: best practice for design and construction. Metal Cladding & Roofing Manufacturers Association in partnership with the Steel Construction Institute.

Rackham, J W et al. (2009) Composite slabs and beams using steel decking: best practice for design and construction. doi: 10.13140/RG.2.2.15921.17767.

Samuel Easterling, W. and Young, C. S. (1992) "Strength of Composite Slabs," Journal of Structural Engineering, 118(9). doi: 10.1061/(ASCE)0733-9445(1992)118:9(2370).

Schuster, R. M. (1970) Strength and behavior of cold-rolled steel-deck-reinforced concrete floor slabs. doi: 10.31274/rtd-180813-4472.

FEM analysis applied to the study of the stress transmission in the corrugated sheet slab
Master of Civil Engineering, defended by: MBOH HELBERT SHAYEH, NASPW, Yaoundé, 2019/2020

107

Seres, N. and Dunai, L. (2011) "Modelling aspects of interface interlock in composite floors," Periodica Polytechnica Civil Engineering, 55(2). doi: 10.3311/pp.ci.2011-2.07.

Veljkovic, M. (1996) Behaviour and resistance of composite slabs.

Yu, W.-W. and LaBoube, R. A. (2010) Cold-Formed Steel Design. Hoboken, NJ, USA: John Wiley & Sons, Inc. doi: 10.1002/9780470949825.

Zienkiewicz, O. C., Taylor, R. and Zhu, J. (2005) The Finite Element Method: Its Basis and Fundamentals, The Finite Element Method: its Basis and Fundamentals: Seventh Edition.

FEM analysis applied to the study of the stress transmission in the corrugated sheet slab
Master of Civil Engineering, defended by: MBOH HELBERT SHAYEH, NASPW, Yaoundé, 2019/2020

108

ANNEX

ANNEX A: Tables for the methodology

Table A1. Calculating the stress ratio and buckling factor of profile sheet top flange

Stress distribution (compression positive)	Effective[p] width b_{eff}
σ_1 ▨▨▨▨ σ_2 b_{e1} $\bar{b}$ b_{e2}	$\underline{\psi = 1:}$ $b_{eff} = \rho\ \bar{b}$ $b_{e1} = 0,5\ b_{eff}$ $b_{e2} = 0,5\ b_{eff}$
σ_1 ▨▨ σ_2 b_{e1} $\bar{b}$ b_{e2}	$\underline{1 > \psi \geq 0:}$ $b_{eff} = \rho\ \bar{b}$ $b_{e1} = \dfrac{2}{5-\psi}b_{eff}$ $b_{e2} = b_{eff} - b_{e1}$
b_c b_t σ_1 ▨ σ_2 b_{e1} b_{e2} $\bar{b}$	$\underline{\psi < 0:}$ $b_{eff} = \rho\ b_c = \rho\ \bar{b}\,/\,(1-\psi)$ $b_{e1} = 0,4\ b_{eff}$ $b_{e2} = 0,6\ b_{eff}$

$\psi = \sigma_2/\sigma_1$	1	$1 > \psi > 0$	0	$0 > \psi > -1$	-1	$-1 > \psi > -3$
Buckling factor k_σ	4,0	$8,2\,/\,(1,05 + \psi)$	7,81	$7,81 - 6,29\psi + 9,78\psi^2$	23,9	$5,98\,(1 - \psi)^2$

Table A2. Shear buckling strength (source: section (1) of EN 1993-1-3a.

Relative web slenderness	Web without stiffening at the support	Web with stiffening at the support [1)
$\bar{\lambda}_w \leq 0,83$	$0,58\,f_{yb}$	$0,58\,f_{yb}$
$0,83 < \bar{\lambda}_w < 1,40$	$0,48\,f_{yb}\,/\bar{\lambda}_w$	$0,48\,f_{yb}\big/\bar{\lambda}_w$
$\bar{\lambda}_w \geq 1,40$	$0,67 f_{yb}\big/\bar{\lambda}_w^2$	$0,48\,f_{yb}\big/\bar{\lambda}_w$

[1)] Stiffening at the support, such as cleats, arranged to prevent distortion of the web and designed to resist the support reaction.

Table A3. Table for derivation of the effective bearing length and relevant category coefficient for a web (EN 1993-1-3)

Relevant category	l_a [mm]	α [−]
1	10	0.075 (for sheeting profiles)
		0.057 (for liner trays or for hat sections)
2	$s_s \leq l_a \geq 10$	0.075 (for sheeting profiles)
		0.057 (for liner trays or for hat sections)

FEM analysis applied to the study of the stress transmission in the corrugated sheet slab
Master of Civil Engineering, defended by: MBOH HELBERT SHAYEH, NASPW, Yaoundé, 2019/2020

109